

*Russian Academy of Sciences*

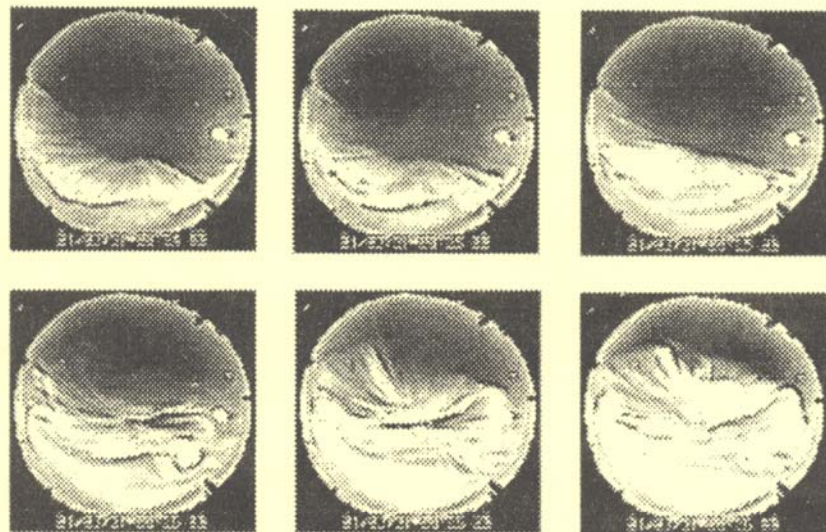
PGI -09-01-125

## PHYSICS OF AURORAL PHENOMENA

32<sup>nd</sup> Annual Seminar

3 – 6 March 2009

### Abstracts



Apatity

2009

*Russian Academy of Sciences*  
KOLA SCIENCE CENTER  
Polar Geophysical Institute

**PGI -09-01-125**

**PHYSICS OF AURORAL PHENOMENA**

32<sup>nd</sup> Annual Seminar

Abstracts

3 – 6 March 2009

Apatity

2009

The seminar is supported by the  
*Russian Foundation for Basic Research*  
grant 09-05-06008 г

The organizing committee:

Alexander Yahnin (chair)  
Boris Kozelov  
Michael Beloglazov  
Nadezhda Semenova

Addresses:

**Apatity department**  
Fersman str., 14  
Apatity, 184209  
Murmansk region  
Russia

**Murmansk department**  
Khalturina str., 15  
Murmansk, 183010  
Russia

The editorial board:

A.G. Yahnin  
N.V. Semenova

E-mail: [seminar@pgia.ru](mailto:seminar@pgia.ru)  
<http://pgia.ru/seminar>

© Kola Science Center  
Russian Academy of Science, 2009

## CONTENTS

### SESSION 1. GEOMAGNETIC STORMS AND SUBSTORMS

E.E. Antonova, I.P. Kirpichev, K.G. Orlova, I.L. Ovchinnikov, S.S. Pulinets, S.S. Rossolenko, M.V. Stepanova, V.V. Vovchenko	Features of high latitude magnetospheric topology, magnetospheric substorms and storms	15
O.M. Barkhatova, P.A. Bespalov, A.E. Levitin	Relationship between space-time variations of the ground geomagnetic field and plasmasphere at the recovery phase of geomagnetic storm	15
L.P. Borovkov	Some temporal characteristics of the auroral proton precipitations from groundbase spectroscopic measurements	16
I.V. Despirak, A.A. Lubchich, V. Guineva	Development of substorm bulges during storms of different interplanetary origins	16
E. Gordeev, M. Shukhtina, V. Sergeev, A. DeJong	Comparison of different methods of tail magnetic flux calculation	16
Yu. Katkalov, Ya. Sakharov	Data mining in for geophysical tasks	17
N.G. Kleimenova, O.V. Kozyreva	Magnetic superstorm “Bastille Day Event” (July 15-17, 2000): ULF- pulsations and substorms	17
M.V. Klimenko, V.V. Klimenko	Simulation of main ionospheric trough, light ion trough and polar cap patches during substorms	17
I.A. Kornilov, T.A. Kornilova	Study of magnetospheric substorm by auroral TV and THEMIS spacecraft data	18
I.A. Kornilov, T.A. Kornilova	Weak auroral activations and THEMIS measurements of electric and magnetic fields, energetic particles and plasma flows.	18
T.A. Kornilova, I.A. Kornilov	Auroral dynamics at different stages of storm recovery phase versus the strength of the main phase	18
O.V. Kozyreva, N.G. Kleimenova	ULF-index variations during strong magnetic storms	19
A.E. Levitin, L.A. Dremukhina, L.I. Gromova, N.G. Ptitsyna	Model of magnetic disturbances during the historic extreme magnetic storm of 1-2 September 1859	19
V.V. Pchelkin, O.I. Akhmetov	Simultaneous analysis of daily variations in the overshoots of the magnetic field background in the SHR frequency range and in the atmospheric electric field	19
Y.A. Sakharov, N.V. Kudryashova, A.N. Danilin, S.N. Saranskiy	Geomagnetic disturbances and railway automatic failures at Oktybrskaya railway	20
Ya.A. Sakharov, A.N. Danilin, V.N. Selivanov, R.M. Ostafiychuk, Yu.V. Katkalov, N.V. Kudryashova	Geomagnetically induced currents in power systems of the Kola peninsula	20

S.I. Solovyev, R.N. Boroyev, A.V. Moiseyev	Evolution of geomagnetic perturbations and aurora dynamics during the strong magnetic storms events	20
O. Troshichev and A. Janzhura	Bay-like magnetic disturbances occurring in the auroral zone during periods of intense and long-duration magnetic activity: Inconsistency with behavior of aurora	21
M.A. Volkov	The effect of electric field increasing on the substorm currents formation	21
V.L. Zverev, Ya.I. Feldstein, V.G. Vorobjev	Visual luminosity equatorwards of the auroral oval during magnetic storms	21

## SESSION 2. FIELDS, CURRENTS, PARTICLES IN THE MAGNETOSPHERE

M. Foerster, Y.I. Feldstein, S.E. Haaland, L.A. Dremukhina, L.I. Gromova, A.E. Levitin	Ionospheric convection from Cluster EDI measurements: Comparison with the ground-based IZMEM ionospheric convection model	25
I.V. Golovchanskaya	Interpretation of wavelet spectra of high-latitude low-frequency electric field fluctuations	25
E.E. Grigorenko, L.M. Zelenyi, M. Hoshino, J.-A. Sauvaud	Two regimes of ion non-adiabatic acceleration in the Earth magnetotail. Geotail and Cluster observations	25
A.E. Levitin, L.A. Dremukhina, L.I. Gromova, E.G. Avdeeva	The contribution of the external geomagnetic field to the average amplitude of the Earth's magnetic field recorded by a magnetic observatory	26
T.V. Kozelova, L.L. Lazutin, B.V. Kozelov	Ion energy spectra at $L \sim 3.6 - 6.7$ during disturbed geomagnetic conditions	26
O. Kozyreva, I. Myagkova, N. Kleimenova	Energetic electron precipitation measured by CORONAS-F satellite and polar magnetic disturbances	27
I.N. Myagkova, E.E. Antonova, M.O. Riazantseva, B. V. Marjin	Energetic electron flux precipitations near the outer ERB's boundary and auroral oval position	27
A. Nikolaev, V. Sergeev, N. Tsyanenko, V. Angelopoulos, H. Singer	Comparison between substorm current wedges and dipolarizations during 2008 THEMIS tail season	27
A.V. Petlenko, Yu.A. Kopytenko	Small-base gradient analysis of high-latitude magnetic pulsations field by usage virtual stations of BEAR network	28
A.A. Petrukovich	Origins of plasma sheet By magnetic field	28
V.C. Roldugin	Comparison of saw-teeth oscillations at GOES and GEOTAIL satellites	28
A.A. Samsonov	Propagation of oblique interplanetary shocks through the magnetosheath	28
A.A. Samsonov, D.G. Sibeck	Generation of the field-aligned currents associated with the geomagnetic sudden impulse	29
V. Sergeev, V. Angelopoulos, T. Sugak, S. Apatenkov, I. Kornilov, T. Kornilova, J. McFadden, D. Larson, J. Bonnell, M. Fillingim	Themis observations of dipolarizations and plasma injections associated with substorm current wedge	29

V.G. Vorobjev, O.I. Yagodkina	Seasonal effect in the latitudinal position of night - and dayside precipitation boundaries	29
V.G. Vorobjev, V.L. Zverev, O.I. Yagodkina	The response of midday aurorae to sharp changes of solar wind dynamic pressure under southward and northward Bz IMF conditions	30
V. V. Vovchenko, E.E. Antonova	Magnetic field distortion in the process of plasma convection in the magnetosphere of the Earth: Preliminary results of modeling	30
O.I. Yagodkina, I.V. Despirak, V. Guineva	Spatial distribution of the auroral precipitations zones depending on different solar wind streams	31
O.I. Yagodkina, V.G. Vorobjev, V.B. Belakhovsky	Dayside aurorae and geomagnetic variations associated with negative and positive solar wind dynamic pressure impulses: Case study	31
A.N. Zaitsev, V.A. Shilimov	Internet as the media for coordinated polar geophysical research	31
Б.В. Козелов	Мультифрактальные характеристики магнитосферной активности как отклик на стохастическое воздействие солнечного ветра	32
О.В. Мингалев, И.В. Мингалев, Х.В. Малова, Л.М. Зеленый	Влияние анизотропии источников плазмы на структуру тонкого токового слоя в хвосте магнитосферы	32

### SESSION 3. WAVES, WAVE-PARTICLE INTERACTION

V.B. Belakhovsky	On existence of the shock wave inside the magnetosphere	35
V.B. Belakhovsky, V.A. Pilipenko	Generation of Pc5 pulsations under fluctuations of the solar wind dynamic pressure	35
V.B. Belakhovsky, V.A. Pilipenko	Generation of magnetic and particle Pc5 pulsations at the recovery phase of strong magnetic storm	35
A.A. Bespalov, A.G. Demekhov	Generalization of the linear theory of absolute instability of whistler-mode waves in the Earth's magnetosphere	36
A.G. Demekhov	Nonlinear dynamics of a magnetospheric VLF backward-wave oscillator: Possible influence of bounce oscillations of energetic electrons	36
A.G. Demekhov, A.V. Bashinov, and V.Yu. Trakhtengerts	Self-consistent model for cyclotron acceleration of radiation belt electrons by noise-like whistler-mode wave emissions	36
A.V. Moiseyev, V.A. Mullayarov, S.N. Samsonov, S.I. Solovyev	Peculiarities of sudden commencement manifestation in geophysical phenomena on subauroral and auroral latitudes	37
A.A. Ostapenko, E.E. Titova, T. Turunen, J. Manninen, T. Rajta	Spectrum of VLF signals from lightning in far-field region	37
V. Pilipenko, O. Chugunova, M. Engebretson, T. Yeoman, M. Vellante	Mechanisms of the cusp-related Pc3-4 waves	37
T.A. Popova, A.G. Yahnin, H.U. Frey	Solar wind dynamic pressure pulses, subauroral proton flashes, and Pc1 bursts	38

V.C. Roldugin, A.V. Roldugin	Connection between geomagnetic Pc4 –5 and auroral pulsations in Barentsburg observatory	38
N.V. Yagova, V.A. Pilipenko	Parameters of auroral Pc5/Pi3 pulsations and geostationary electron flux at relativistic and keV energies	39
T.A. Yahnina, A.G. Yahnin, H.U. Frey, J. Manninen	Statistical study of properties of Intervals of Pulsations of Diminishing Periods (IPDP) and their relation to subauroral proton arcs	39
В.В. Клименко	Распределение по небесной сфере интенсивности синхротронного радиоизлучения релятивистских электронов, захваченных в дипольном магнитном поле Земли	39
В.А. Пархомов, Г.Н. Застенкер, М.О. Рязанцева, Б. Цэгмэд, Т.А. Попова	Закономерности магнитосферного отклика на большие и резкие скачки потока солнечного ветра в геомагнитных пульсациях частотного диапазона 0.2 - 5 Гц	40

#### SESSION 4. THE SUN, SOLAR WIND, COSMIC RAYS

Yu.V. Balabin, E.V. Vashenyuk, B.B. Gvozdevsky	Real-time forecast of radiation-hazardous fluxes of solar cosmic rays on the data of the neutron monitor network	43
Yu. V. Balabin, I. M. Podgorny, A. I. Podgorny, E. V. Vashenyuk	Numerical simulation of solar cosmic ray acceleration during a flare	43
I.V. Despirak, Zh.V. Dashkevich, V. Guineva	Variations of aurora emissions during substorms connected with different solar wind streams	43
A.V. Germanenko, Yu.V. Balabin, E.V. Vashenyuk, B.B. Gvozdevsky, L.I. Schur	Monitoring of various kinds of cosmic radiation for environmental studies	44
N.A. Glotova, M.A. Shukhtina	Solar wind dynamic pressure jumps characteristics and their magnetospheric effects	44
B.B. Gvozdevsky, Yu.V. Katkalov, E.V. Vashenyuk	Participation of the Apatity neutron monitor in the international Neutron Monitor Data Base	45
I.M. Ivanova, N.P. Dmitrieva	The magnetosphere time response to the IMF Bz turning	45
E.A. Kalinina, N.A. Barkhatov, A.E. Levitin	The short-term forecast of Solar wind magnetic cloud parameters reaching vicinity of the Earth	45
I.N. Myagkova, A.V. Bogomolov	Solar wind parameters and relativistic electron flux variations (2001-2005 years) correlations studies	46
V. V. Pchelkin	Effect of substorm in the propagation of the galactic cosmic rays.	46
A. I. Podgorny	The method of search for possible solar flare positions in the corona	46
I. M. Podgorny, A. I. Podgorny	Solar flare model – comparison with complex space crafts observation	47
T.E. Val'chuk	The beginning of new 24-th cycle in solar and geomagnetic activity generation	47
М.С. Калинин, М.Б. Крайнев	Коэффициенты транспортного уравнения для ГКЛ в гелиосфере с токовым слоем конечной толщины	48

М.С. Калинин, М.Б. Крайнев	Модель гелиосферного токового слоя конечной толщины	48
А.А. Любич, И.В. Дэспирак	Взаимодействие падающей гидродинамической волны с ударной волной: сравнение между аналитическим решением для идеальной среды и численными расчетами для вязкой среды	48

## SESSION 5. IONOSPHERE AND UPPER ATMOSPHERE

T. Bösinger, A. G. Demekhov, and C. Haldoupis	Appearance and interpretation of a Broadband Spectral Maximum (BSM) in low latitude ULF magnetic noise observations: Effect of a MHD cavity in the ionospheric E-F1 valley	51
O.M. Barkhatova, N.A. Barkhatov, G.I. Grigor'ev	Display of magnetogravitation waves caused by auroral electrojet dynamics in traveling ionospheric disturbances	51
M. I. Beloglazov, G. F. Remenets	VLF characteristics of magnetic cutoff in the cases of ultra relativistic electron precipitations	52
M.I. Beloglazov, M.V. Kukovyakin, G.F. Remenets	About solving ability of the self-consistent method relative to the VLF inverse problem in nonstationary conditions	53
E.N. Doronina, A.A. Namgaladze	Equatorial neutral temperature and total mass density minima as effect of the thermosphere-ionosphere coupling	54
E.N. Ermakova, D.S. Kotik	Theoretical investigations of the diurnal variations of the spectral resonance structure parameters in background magnetic noise at high latitudes	54
A.V. Frank-Kamenetsky, L.N. Makarova, V.N. Morozov, A.V. Shirochkov, G. Burns	On the connection between intensity of atmospheric electric field as measured at ground surface and ionospheric electric field in the Central Antarctica	55
N.M. Gavrilov	Global structure of gravity wave excitation from CHAMP satellite observations and its impact on general circulation of the upper atmosphere	55
V. Guineva, I. Despirak, R. Werner, E. Trondsen, S. Marple, K. Dahle, P. Stauning	The auroral emissions and the electron precipitation under different geomagnetic conditions	55
Ya. Ignatovich, S. Chernouss, A. Roldugin	High-speed spectrograph in visible spectral range for nightglow and aurora observations	56
A.S. Kirillov	Singlet and triplet molecular nitrogen in auroral ionosphere	56
A.S. Kirillov	Electronically excited molecular oxygen in the region of the nightglow of the atmosphere	56
M.V. Klimenko, V.V. Klimenko	Numerical modeling of the ionosphere effects of 01 August 2008 solar eclipse	56
M.V. Klimenko, V.V. Klimenko	Numerical modeling of the ionospheric precursors of high-latitude earthquakes	57
M.V. Klimenko, V.V. Klimenko	Numerical modeling of ionospheric parameters during sequence of geomagnetic storms on September, 9-14th, 2005	57

M.A. Knyazeva, A.A. Namgaladze	Effectivity of the plasmasphere as a source of the maintenance of the night-time ionospheric F2-layer	58
M.A. Knyazeva, A.A. Namgaladze	A model study of the 3D-topology of the enhanced electron density regions in the night-time ionospheric F2-layer	58
D.S. Kotik	Properties of the low frequency waves in the multi-component ionospheric plasma	59
V. Maklakov, S. Chernouss, N. Kalitenkov, O. Antonenko, A. Kalitenkov	GPS deviations dependence on geophysical and atmospheric disturbances	59
G.I. Mingaleva, V.S. Mingalev	Model simulation of the large-scale mid-latitude F-layer modification by powerful HF waves with different powers in the daytime	59
A.A. Mochalov, A.B. Pashin, T. Yeoman	Excitation of the artificial magnetic pulsations by SPEAR: A case study	60
E.A. Mareev, V.V. Klimenko, S.A. Yashunin	Transient luminous events: challenge for theory and ground-based/space-borne observations	60
S.V. Pilgaev, O.M. Lebed and Yu.V. Fedorenko	Preliminary results of ELF amplitude and phase measurements at Apatity and Barentsburg	60
Yu.V. Platov	Condensation of combustion products and optical phenomena in the upper atmosphere, connected with rocket engines operation	61
G.F. Remenets	“Fock Diffraction Wave” and ultra high relativistic electron precipitations into polar middle atmosphere (Devoted to the 110 birthday anniversary of academician V.A. Fock)	61
V.C. Roldugin, A.N. Vasiljev	Polarization ellipse variations of Schumann resonance in horizontal and vertical planes according to observations in Barentsburg and Lovozero	62
V.V. Safargaleev, D.N. Shibaeva, T. Sergienko, I. Sandahl, U. Brändström	Features of pulsating arcs inferred from ALIS triangulation measurements	62
N.G. Sergeeva, O.F. Ogloblina, B.E. Vasiljev, S.M. Chernyakov	Responses to the earthquakes in the lower high-latitude ionosphere	62
D.N. Shibaeva, V.V. Safargaleev, T.I. Sergienko, I.A. Kornilov	On the problem of correct collocation of ground based (optical) and high-altitude satellite measurements	63
G.M. Shved, N.V. Karpova, P.P. Ammosov, G.A. Gavril'yeva	Nightglow observations of short-period global atmospheric waves	63
V.D. Tereshchenko	Thomson scattering of electromagnetic waves in the polar mesosphere containing the charged dust	64
V.D. Tereshchenko, E.B. Vasiljev, V.A. Tereshchenko, O.F. Ogloblina, S.M. Chernyakov	About behavior of the polar lower ionosphere during a solar eclipse on August, 1, 2008	64

M.V. Uspensky, A.V., Koustov and P. Janhunen	Backscatter volume cross sections and amplitudes of electrostatic electrojet fluctuations inferred from joint STARE and EISCAT measurements	64
V.I. Zakharov, V.E. Kunitsyn, Ya.A. Ilyushin	Impact of the ionospheric perturbations on the radio occultation meteorological sounding of the Arctic atmosphere	65
O.V. Zolotov, A.A. Namgaladze, O.V. Martynenko, B.E. Prokhorov	Numerical simulations of the ionospheric TEC disturbances associated with the New Zealand earthquake of Nov. 22, 2004	65
Yu.V. Zubova, A.A. Namgaladze	Sensitivity of the Upper Atmosphere Model results to the input parameters specification for geomagnetic storms modelling	66
Е.Н. Ермакова, С.В.Поляков, Ю.В. Шлюгаев, А.В. Щенников	Экспериментальные исследования спектральных структур в фоновом низкочастотном шуме методом разнесенного приема	66
Н. Калитёнков, С. Черноус, А. Калитёнков	GPS позиционирование и авроральные возмущения	66
Н. Калитёнков, С. Черноус, А. Калитёнков, О. Антоненко, М. Иванюгин	Полярные сияния как индикатор возмущенности среды распространения навигационных радиосигналов	67
Н.В. Калитёнков, А.Н. Калитёнков, В.И. Милкин, А.В. Гурин, А.Н. Кучура	Ионосферные антенны КВ диапазона	68
Ю.А. Суковатов, А.Т. Карпачев, В.А. Телегин	F-рассеяние в дневной ионосфере средних широт, связанное с крупномасштабными неоднородностями концентрации ионосферной плазмы, выделенным по данным Интеркосмос-19	68

## SESSION 6. LOW ATMOSPHERE, OZONE

O.I. Akhmetov	Features of cosmic rays influence on ionization in a troposphere of high latitudes	71
O.I. Akhmetov	Spectral characteristics of an atmospheric current density and atmospheric pressure in high latitude atmosphere	71
M.I. Beloglazov, O.I. Akhmetov and A.N. Vasiljev	Global thunderstorm activity during 2001 and 2007 according to observations of the Schumann resonance intensity in the Arctic	71
V.V. Bertsev, L.A. Petrunkin, D.N Glebovsky	Optical quantum amplifiers simple realization	72
V.I. Demin	Altitude distribution of air temperature in the Khibiny massif and mesoclimate zoning	72
V.I. Demin	Air temperature dynamics in the Kola Peninsula and determination of optimal time period for calculation of climatic parameters	73
V.I. Demin, M.I. Beloglazov	Surface ozone variations during snowstorm and drifting snow	73
V.I. Demin, M.I. Beloglazov	Mountain and valley circulation in the Khibiny mountains	73

N.M. Gavrilov, S. Fukao, M. Fujiwara, H. Hashiguchi, T. Koide, Mamoru Yamamoto and Masayuki Yamamoto	Ozone and turbulence in the tropo-stratosphere from simultaneous radar and ozonesonde measurements in Japan and Indonesia	73
V. Guineva, R. Werner, I. Vince	High resolution spectroscopic measurements and theoretical absorption spectra of the O <sub>2</sub> atmospheric system	74
A.A. Krasilnikov, L.M. Kukin, Y.Y. Kulikov, V.G. Ryskin	Millimeter-wave measurements of the variability of the mesospheric ozone in polar latitudes	74
Y.Y. Kulikov, M.B. Emelyanov, A.A. Krasilnikov, L.M. Kukin, L.V. Lubyako, A.V. Poberovskiy	The response of the ozone and dioxide of nitrogen of the middle atmosphere to the solar irradiance variability during total eclipse August 1, 2008 in Siberia (mountain Altai)	75
A.A. Lubchich	Peculiarity of behavior of temperature in St.-Petersburg during last 25 years	75
E.A. Mareev	Recent progress in the global electric circuit research	75
I.V. Mingalev, K.G. Orlov, V.S. Mingalev	A simulation study of the transformation of circumpolar vortex flows of the lower and middle atmosphere during the period from January to June	76
I.N. Myagkova, A.V. Kukoleva, A.A. Krivolutsky, T.Yu. Vyushkova, A.A. Kuminov	The ionization of the Earth's atmosphere and ozone layer's variations after solar proton events during January 2005	77
V.V. Pchelkin, M.I. Beloglazov, A.N. Vasiljev, A.I. Voronin	Study of Q-type ELF bursts in the Shuman resonance frequency range	77
A.B. Ponomarev, L.I. Miroshnichenko, A.S. Kirillov	Vertical profiles of NO <sub>x</sub> in the middle atmosphere at high latitudes during quiet period and solar proton events	77
O.M. Raspovov, V.A. Dergachev	Response of the atmosphere-ocean system to solar activity variations of different time scales	78
O.M. Raspovov, S.V. Veretenenko	Effects of solar activity and cosmic rays on the lower atmosphere (on memory and the 75th anniversary of PGI seminar founder prof. M.I. Pudovkin)	78
O.A. Rubtsova, V.A. Kovalenko, S.I. Molodykh	Peculiarities of connection between space-time variations of precipitation and geomagnetic activity	78
O. Troshichev, L.V. Egorova, A.S. Janzhura and V.Ya. Vovk	Solar wind influence on atmosphere processes in winter Antarctica	79
O.S. Ugolnikov, I.A. Maslov	Polarization detection of dust and aerosol in the middle and upper atmosphere	79
O.S. Ugolnikov, I.A. Maslov	Lunar eclipses optical profiles: Aerosol, water vapor and ozone relations	79
R. Werner, K. Stebel, H.G. Hansen, U.-P. Hoppe, M. Gausa, R. Kivi, P. von der Gathen, Y. Orsolini, N. Kilifarska	Near tropopause inter-annual ozone variation at European high latitudes	80

A.M. Zvyagintsev, L.B. Ananiev, and A.A. Artamonova	Total ozone variability over the Russian territory during the period 1973- 2008	81
A.M. Zvyagintsev, I.N. Kuznetsova, E.A. Lezina, Ya.O. Romaniuk, M.G. Sosonkin	Surface ozone variations in Moscow and Kyiv	81
B.Г. Вяткин, B.В. Клименко, Ю.В. Шлюгаев	Детектирование планетарного числа молний на основе статистического анализа характеристик электромагнитного шума в диапазоне шумановских резонансов	81

## SESSION 7. HELIOBIOSPHERE

N. K. Belisheva	Functional state of human organism depends on intensity of cosmic rays modulated by solar cyclic activity	85
N.K. Belisheva, N.A. Melnik, S.A. Chernouss, O.V. Antonenko, E.V. Perminova, A.L. Kosova, A.N. Vinogradov, T.B. Novikova	Comparison studies exposure of human organism to cosmic rays in control group and under chronic irradiation by natural radio nuclides	85
A.А. Алхимчиков, Н.К. Белишева, И.В. Калашникова	Зависимость состояния лесов Мурманского региона от вариаций гелиофеофизических агентов	86
В.М. Воробейчиков, О.А. Троицhev, Э.С. Горшков, В. В. Степанов	Влияние гравитационных возмущений на аномальное поведение человека и высших животных	87
В.В. Иванов, Э.С. Горшков, Н.К. Белишева, В.В. Мещеряков	О восприятии времени в экстремальных условиях Арктики и Антарктики	88
Т.Г. Кузнецова, В.В. Иванов, Э.С. Горшков	К вопросу о сравнительной адаптации сердечно-сосудистой системы и дыхания при смене климатографического района и остром инфекционном заболевании	88
С.А. Черноус, В.А. Шишаев, О.В. Антоненко, М.И. Белоглазов	Экспериментальные исследования ослабления биологически активного солнечного излучения по измерениям в Апатитах	89
Author index		91



*Geomagnetic Storms and Substorms*



Narrow field of view auroral TV camera in Apatity



## Features of high latitude magnetospheric topology, magnetospheric substorms and storms

E.E. Antonova<sup>1,2</sup>, I.P. Kirpichev<sup>2,1</sup>, K.G. Orlova<sup>1</sup>, I.L. Ovchinnikov<sup>2</sup>, S.S. Pulinets<sup>1</sup>,  
S.S. Rossolenco<sup>1,2</sup>, M.V. Stepanova<sup>3</sup>, V.V. Vovchenko<sup>2</sup>

<sup>1</sup>*Skobeltsyn Institute of Nuclear Physics Moscow State University, Moscow*

<sup>2</sup>*Space Research Institute RAS, Moscow, Russia*

<sup>3</sup>*Physics Department, Universidad de Santiago de Chile, Chile.*

Structure of high latitude magnetospheric plasma domains is analyzed taking into account the latest results of THEMIS project observations. Averaged radial distribution of plasma pressure near noon is obtained. Daytime compression of magnetic field lines and the existence of magnetic field minima far from the equatorial plane are taken into account. Dayside integral transverse currents at the geocentric distances 7-10  $R_E$  are calculated in the suggestion of the validity of the condition of magnetostatic equilibrium and compared with nighttime transverse currents. Arguments supporting the hypothesis on the existence of high latitude continuation of the ordinary ring current (the existence of cut-ring current - CRC) till geocentric distances  $\sim 10$   $R_E$  are summarized. The role of CRC, partial ring current and tail current in geomagnetic substorms and storms is discussed.

## Relationship between space-time variations of the ground geomagnetic field and plasmasphere at the recovery phase of geomagnetic storm

O.M. Barkhatova<sup>1,2</sup>, P.A. Bespalov<sup>3</sup>, A.E. Levitin<sup>4</sup>

<sup>1</sup>*Radiophysical Research Institute (NIRFI), 603950 Nizhny Novgorod, Russia*

<sup>2</sup>*Nizhniy Novgorod State Pedagogical University, 603950 Nizhny Novgorod, Russia*

<sup>3</sup>*Institute of Applied Physics, Russian Academy of Sciences, 603950 Nizhny Novgorod, Russia*

<sup>4</sup>*Pushkov Institute of Terrestrial Magnetism, Ionosphere and Propagation of Radio Waves (IZMIRAN), Russian Academy of Sciences, 142190, Troitsk, Russia*

Spectra of variations of geomagnetic field observed at network of ground stations at latitudes (37°-74°) during weak geomagnetic activity after magnetospheric storms are compared at different locations relatively to projection of plasmapause. At locations mapped onto the dayside plasmaspheric bulge (50-60°) an enhancement of the high-frequency part of spectra was noticed. At higher latitudes the general falling spectra was observed. Also, it was shown that horizontal components of geomagnetic field vary synchronously at stations mapped onto the dayside bulge. Correlation coefficients of variations at different stations were not less than 0.9. For stations mapped outside the dayside plasmaspheric bulge the variations of the geomagnetic field were different, and correlation coefficients did not exceed 0.3.

Thus, it was shown that existence of the dayside and evening plasmaspheric bulges influences on the magnetic disturbances on the ground. Difference in the latitudinal ranges, where this influence was noticed, can be explained by more significant localization of the dayside plasmaspheric bulge in comparison with that in the evening. The considered magnetic disturbances correspond to geomagnetic pulsations Pc-4. According to the up-to-day view these pulsations represent resonance oscillations of magnetic field lines. As the main source of these pulsations, some processes on the periphery of magnetosphere are often discussed. However, in paper [1] some arguments in favor of generation of such kind of pulsations in the region of field aligned currents at relatively low altitudes are presented.

In our opinion, at the recovery phase of the magnetic storms it is naturally to expect the development of the field-aligned currents in the vicinity of the plasmaspheric bulges. The currents should occur due to interaction of the ring current ions with electromagnetic waves in the region of enhanced plasma density [2].

This work is supported by RFBR grants 08-05-12051.

## References

1. Olson J. V. ULF signatures of the polar cusp. *J. Geophys. Res.*, 1986, V.A9, p.10055-10062
2. Gafe A., Bespalov P.A., Trakhtengerts V.Y., Demekhov A.G. Afternoon mid-latitude current system and low-latitude geomagnetic field asymmetry during geomagnetic storms. *Ann. Geophysicae*, 1997, V.15, p.1537-1547

## **Geomagnetic storms and substorms**

### **Some temporal characteristics of the auroral proton precipitations from groundbase spectroscopic measurements**

L.P. Borovkov (*Polar Geophysical Institute, Apatity, Russia*)

During last 5 years more then 20 auroral proton precipitation events were registered by spectrograph at Apatity in different geomagnetic conditions. Some parameters of the temporal/spatial variations of the H $\alpha$  intensity, which reflects the proton fluxes variations, are presented.

### **Development of substorm bulges during storms of different interplanetary origins**

I.V. Despirak<sup>1</sup>, A.A. Lubchich<sup>1</sup>, V. Guineva<sup>2</sup>

<sup>1</sup>*Polar Geophysical Institute, Apatity, Russia*

<sup>2</sup>*Solar-Terrestrial Influences Laboratory, Stara Zagora, Bulgaria*

Different structures in solar wind are observed depending on the type of solar activity: magnetic clouds (MC), recurrent streams (RS), and regions of their interaction with undisturbed solar wind (Sheath and CIR). Three of these structures, namely, Sheath, CIR, and MC, are the sources of geomagnetic storms. Furthermore, the storms originating from these three sources differ in intensity, recovery phase duration, etc. We will search for distinctions in the development of substorm bulges occurring during geomagnetic storms connected with the MC, Sheath and CIR. Solar wind parameters were taken from the Wind spacecraft observations and the auroral bulge parameters were obtained by data from the Ultra Violet Imager onboard Polar. We determined the longitudinal and latitudinal dimensions of the auroral bulges, the poleward aurora propagation and the onset latitude of auroral bulge. It is shown that auroral bulges development is different for these types of storms. The strongest auroral bulge expansions are found for CIR- and Sheath-storms situations. In contrast to substorms during CIR-storms, during MC-storms the latitudinal expansion of the auroral bulge is less pronounced, but longitudinal expansion is stronger. We suggest the latter feature is explained by different configuration of the near-Earth magnetotail during CIR- and MC-storms.

### **Comparison of different methods of tail magnetic flux calculation**

E. Gordeev<sup>1</sup>, M. Shukhtina<sup>1</sup>, V. Sergeev<sup>1</sup>, A. DeJong<sup>2</sup>

<sup>1</sup>*Institute of Physics, SPbU, St.Petersburg, Russia*

<sup>2</sup>*Department Atmospheric Oceanic and Space Sciences, University of Michigan, Ann Arbor, MI, USA*

One of the basic parameters, characterizing the state and dynamics of the Earth magnetosphere, is the magnetotail magnetic flux  $F$ . However, until recently only rare estimates of the  $F$  value were available. Petrinec and Russell (1996) proposed a method of magnetic flux calculation, based on measured tail lobe magnetic field and the magnetotail radius  $R$  value as well as solar wind dynamic pressure and IMF  $B_z$ . However, the same solar wind conditions may result in different magnetospheric states and, so, in different  $R$  values. We propose an alternative method of  $R$  calculation based on instantaneous pressure balance at the magnetopause.

Recently global MHD modeling of magnetosphere became possible. It gives the opportunity to determine the magnetopause position (i.e. the  $R$  value), the tail magnetic field and, finally, the magnetotail magnetic flux. In the present study we compute magnetic flux for several simulated events. To determine the magnetopause, we compare three different methods, based on: 1) density gradient, 2) current density peak, and 3) fluopause, which is the surface of the boundary solar wind streamlines. All three methods demonstrate a good mutual agreement. Several simulated events (including substorms) are compared using MHD modeling and our empirical method. The results of two methods reasonably agree.

Polar cap images from Polar and IMAGE spacecraft allow determine the polar cap area, i.e. the polar cap magnetic flux. The  $F$  value, obtained from polar cap images in several events (including steady magnetospheric convection, substorms and sawtooth events), are compared with our prediction and show similar behavior, though the values may differ. In conclusion, all three methods demonstrate comparable results. It opens the opportunity of using these methods to monitor the tail magnetic flux on the regular basis, which is important for monitoring of the magnetosphere.

## Data mining in for geophysical tasks

Yu. Katkalov, Ya. Sakharov (*Polar Geophysical Institute, Apatity*)

Some tasks in geophysics are required to obtain data from various storages such as files, databases, remote web sites. It requires the ability to process of various types of data by using different tools and applications. We developed approach which allows to obtain geophysical data from local or remote storages by using specified search criteria. We used this approach to develop the tools for search events with certain level of magnetic activity. We intend to develop a package of tools to automate the data search process in PGI Magnetic Database.

## Magnetic superstorm “Bastille Day Event” (July 15-17, 2000): ULF-pulsations and substorms

N.G. Kleimenova, O.V. Kozyreva (*Institute of the Earth Physics RAS, B. Gruzinskaya 10, Moscow 123995, Russia*)

The superstrong magnetic storm of July 15-17, 2000 with  $Dst \sim -300$  nT was caused by the coronal mass ejection (CME), occurred on 14 July and so it was called “Bastille Day Event”. The front edge of a magnetic cloud formed by this CME was characterised by the large and variable values of IMF (up to 70 nT) and the high solar wind speed (up to 1000 km/s). The aim of our study was the analysis of the peculiarities of the ULF range (1-6 mHz) magnetic pulsations, observed both on the ground and in the space, as well as substorms, exited mostly in the recovery phase of this superstorm. The global maps of the  $Pc5$  amplitude distribution were computed by using the multipoint ground-based observations. It was found that in the storm initial phase the strongest ULF waves were observed at the day-side polar cap. The storm recovery phase was characterized by the bursts of beautiful morning-daytime  $Pc5$  pulsations demonstrating some unusual properties. There were two maxima in the wave spectra. The first spectral maximum at 1-2 mHz was observed at geomagnetic latitudes  $> 62^\circ$  and the second one at 3-4 mHz was observed at the latitudes  $< 62^\circ$ . The 3-4 mHz activity demonstrated the space asymmetry around the noon: the morning-side pulsations were observed at much higher latitudes than the afternoon ones. The ULF waves were extended to the equator, however, only in the 1-2 mHz range.

The strong morning-side polar cap substorm was developed in the early stage of the storm recovery phase under large positive values of  $Bz$  and  $By$  IMF (up to +35 nT) and high solar wind speed (~850-900 km/s). This morning polar substorm led to an unexpected occurrence of the evening ULF activity at the auroral latitudes. Moreover, two hours later the global burst of monochromatic 1-2 mHz waves was exited with the strongest amplitude at the night sector. These ULF waves were propagated from the night-side to the day-side, i.e. opposite direction to the “classical” resonant  $Pc5$  pulsations.

This study was partly supported by the RAS Program № 16.

## Simulation of main ionospheric trough, light ion trough and polar cap patches during substorms

M.V. Klimenko, V.V. Klimenko (*West Department of N.V. Pushkov IZMIRAN, Kaliningrad, Russia, e-mail: maksim.klimenko@mail.ru*)

In this study the numerical calculation results of ionospheric effects of four modeling substorms which have begun in different UT moments are presented. Calculations are executed on the basis of Global Self-consistent Model of the Thermosphere, Ionosphere and Protonosphere (GSM TIP), developed in WD IZMIRAN for vernal equinox conditions in the minimum of solar activity. In calculations we considered the magnetosphere convection electric field with the set of potential differences through polar caps and field aligned currents of the second region with taking into account particle precipitation and dynamo field generated by thermospheric winds. It is shown, that the substorms cause strong positive disturbances in F-region of ionosphere in the night time sector. Negative disturbances are much less and arise, mainly, at night in the middle and low latitudes. During substorms the longitudinal extent of the main ionospheric trough is increased. The substorm with onset at 18:00 UT causes the negative disturbances in high latitudes except for a southern polar cap. Besides, there is the “stratification” of the main ionospheric trough. As a result in southern hemisphere the additional high-latitude trough which is absent in quiet conditions is formed. “Stratification” of the main ionospheric trough occurs in northern hemisphere in 6 hours after the beginning of the substorm. These “stratification” are the consequence of non-stationary magnetosphere convection. The distinction between these events consists that the “stratification” in a southern hemisphere occurs in active phase of substorm, and in northern hemisphere in recovery phase of substorm. During a substorm beginning at 00:00 UT,  $foF2$  increases in the whole of northern polar cap. Calculation results also have shown that the maximal concentration of thermal protons at height of 1500 km during substorms is always higher, than at the same UT moments in quiet conditions. For all substorms calculations show the displacement of the light ion trough to the

## **Geomagnetic storms and substorms**

equator that is in agreement with observations. The formation of polar cap patches during substorm in foF2 and in concentration of hydrogen ions at height of 1500 km is shown.

The present work was done under support of the Russian Foundation of Basic Research (Grant No. 08-05-00274).

## **Study of magnetospheric substorm by auroral TV and THEMIS spacecraft data**

I.A. Kornilov, T.A. Kornilova (*Polar Geophysical Institute, Apatity, Russia. kornilov@pgi.kolasc.net.ru*)

For the season 2007-2008, TV data from Loparskaya and Lovozero observatories were selected and processed combined with THEMIS data for time intervals when two or more spacecraft were located inside the plasma sheet at different distance from the Earth. About 20 days were chosen with 1-4 auroral activations for each day, so in total about 50 events were studied with using all available THEMIS information about the fields, energetic particles and plasma flows. It was found that every detected magnetospheric activity event has many individual features both in TV and THEMIS data, and depends on previous auroral activity, activity in other regions of magnetosphere, longitudinal drift of energetic particles, and so on. Case studies of one or two separate events are not enough for revealing real time delays between different spacecraft measurements and TV data and understanding the sequence of events during magnetospheric substorm. Multi-events and multi-detectors study we have conducted allows making some very preliminary and initial conclusions:

1. Three primary elements of magnetospheric substorm (magnetic field dipolization, auroral breakup and high energy particles injection, probably caused by magnetic reconnection) are not three manifestations of the same process. Those are three different quasi-independent events separated in time and space.
2. Full scale substorm goes through all three stages, and starts from dipolization, then auroral breakup occurs, and the last one is magnetic reconnection. Auroral breakup is definitely a result of dipolization, but not of reconnection; on the contrary, reconnection is a consequence of breakup.

This study is supported by the RFBR grants 09-05-00818 and Program 16 of the RAS Presidium, Program VI.15 of Division of Physical Sciences RAS.

## **Weak auroral activations and THEMIS measurements of electric and magnetic fields, energetic particles and plasma flows**

I.A. Kornilov, T.A. Kornilova (*Polar Geophysical Institute, Apatity, Russia. kornilov@pgia.ru*)

Five identical THEMIS satellites provide excellent information about waves, fields (B and E, three components), energetic particles (electrons and ions) with energies from 30 keV to 6 MeV detected by SST – Solid State Telescope, and from 3 eV to 30 keV detected by ESA – Electrostatic Analyser, plasma concentration, temperature, and velocity. From TV observations for 2007-2008, weak auroral activations (of pseudobreakup type and weaker) were selected that were conjugate with THEMIS observations (about 10 events in total). It was shown that all auroral activations correlate with some perturbations in E and B fields detected by THEMIS satellites (though not always looking like a real dipolarizations), and correlate with an increase in low energy electron and ion fluxes (energy ranging from 5 to 10 keV). But the fluxes of high-energy particles (energies > 30 keV) were much smaller, if occurred at all, than for full-scale breakup. Thus it can be concluded that the weak activations are not accompanied by magnetic field reconnection.

This study is supported by the RFBR grants 09-05-00818 and Program 16 of the RAS Presidium, Program VI.15 of Division of Physical Sciences RAS.

## **Auroral dynamics at different stages of storm recovery phase versus the strength of the main phase**

T.A. Kornilova, I.A. Kornilov (*Polar Geophysical Institute, Apatity, Russia*)

Storm recovery phase is traditionally considered to be connected with the ring current decay, which, in turn, is induced by the charge exchange process. As protons and oxygen ions have different characteristic times of charge exchange, two stages of storm recovery phase exist: the early recovery phase and the late one. Here we present a comparative analysis of spatio-temporal auroral dynamics in the dusk-midnight MLT sector during the early and late recovery phases of 10 magnetic storms, considering Dst minimum value to be the energy characteristics of the storm main phase. TV data of high-latitude observatory Barentsburg and of auroral zone observatories Loparskaya and Lovozero, geomagnetic data, IMF and solar wind data are employed in this study.

It is found that:

- 1) At the early storm recovery phase auroras occupy large latitudinal range (sometimes  $\Phi' \sim 56-78^\circ$ ). During the late storm recovery phase, auroras shift to higher latitudes.
- 2) An anti-correlation between the intensity of storm-time substorms and the intensity of the storm proper is observed when SC event occurs in the course of storm recovery phase.
- 3) Substorms at the early recovery phase display specific features of substorms occurred during the main phase (e.g., long-living stable rays and bright auroral pulsations embedded in diffuse luminosity).
- 4) Peculiarities of auroral dynamics depend on combination of different factors: solar cycle phase, type of the solar source driving the storm, IMF and solar wind parameters, previous magnetic activity, etc.

Difference in auroral dynamics is discussed.

This study is supported by the RFBR grants 09-05-00818 and Program 16 of the RAS Presidium, Program VI.15 of Division of Physical Sciences RAS.

### **ULF-index variations during strong magnetic storms**

O.V. Kozyreva<sup>1</sup> and N.G. Kleimenova<sup>1,2</sup>

<sup>1</sup>*Institute of the Earth Physics RAS, B. Gruzinskaya 10, Moscow 123995, Russia*

<sup>2</sup>*Space Research Institute RAS, Profsoznaya 84/32, Moscow, 117997, Russia*

Using new wave ULF- index we have carried out the statistic study of the wave geomagnetic activity level in the morning, afternoon and night sectors during the strong magnetic storms ( $Dst_{min}$  from -100 to -150 nT). It was found, that during the initial phase of the magnetic storm the greatest intensity of the geomagnetic pulsations in the frequency range 2-7 mHz was observed in the polar latitudes in the morning sector and in the auroral latitudes in the night. During the main phase of the magnetic storm the greatest wave activity was unexpectedly observed in the morning sector of auroral zone, not in the night: the intensity of pulsations in the night sector was two times lower than in the morning. The basic contribution to the morning wave activity gave the geomagnetic pulsations of the recovery phase of magnetospheric substorms associated with the storm main phase. During the recovery phase of the magnetic storm the ULF wave activity in the auroral zone decreased and the level of the morning and night pulsations became compared. The night ULF activity could be noted also in the subauroral latitudes.

### **Model of magnetic disturbances during the historic extreme magnetic storm of 1-2 September 1859**

A.E. Levitin<sup>1</sup>, L.A. Dremukhina<sup>1</sup>, L.I. Gromova<sup>1</sup>, N.G. Ptitsyna<sup>2</sup>

<sup>1</sup>*Pushkov Institute of Terrestrial Magnetism, Ionosphere, and Radiowave Propagation, Troitsk, Moscow region, Russia*

<sup>2</sup>*St. Petersburg Branch of Pushkov Institute of Terrestrial Magnetism, Ionosphere and Radio Wave Propagation, St. Petersburg, Russia*

The 1-2 September 1859 magnetic storm was the most intensive magnetic storm in recorded history. Very large negative values of the H-component of the geomagnetic field (up to -1600 nT) in observatory Colaba (India) were noted. The magnetic disturbance in Colaba were estimated using the model of magnetospheric current systems. It is shown that the very rapid decreasing of H-components during the main phase of the magnetic storm and its rapid recovery are caused by the temporal variation of intensity of the magnetospheric tail current system. During the main phase of the magnetic storm the inner edge of plasma sheet rapidly shifts close to the Earth and then rapidly returns to the magnetospheric tail.

This work is supported by RFFI grants 08-05-00896, 07-05-13524

### **Simultaneous analysis of daily variations in the overshoots of the magnetic field background in the SHR frequency range and in the atmospheric electric field**

V.V. Pchelkin, O.I. Akhmetov (*Polar Geophysical Institute RAS, Apatity, Murmansk region, Russia*)

Daily variations in the overshoots of the magnetic field background in the SHR (Shuman resonance) frequency range are constructed by ELF (extremely low frequencies) magnetometer data in Lovozero observatory. These variations are compared with those in the vertical component of the atmospheric electric field. The correspondence

## **Geomagnetic storms and substorms**

in the main maximum location is found for both types of variations. The correlation between main maximum amplitudes is investigated.

This work was supported by the Fundamental Research Program of RAS Physical Science Department (Project 4.5).

## **Geomagnetic disturbances and railway automatic failures at Oktybrskaya railway**

Y.A. Sakharov<sup>1</sup>, N.V. Kudryashova<sup>1</sup>, A.N. Danilin<sup>2</sup>, S.N. Saranskiy<sup>3</sup>

<sup>1</sup>*Polar Geophysical Institute RAS, Apatity*

<sup>2</sup>*Kola Science Center RAS, Apatity*

<sup>3</sup>*Oktybrskaya railway, Murmansk*

*e-mail: sakharov@pgia.ru*

Geomagnetic disturbances at polar region are related with solar activity and leads to generation of geomagnetically induced currents (GIC) in any long conducting systems as power lines, pipe lines or telemetry systems. We analyzed the list of failure reports of signaling system from Oktybrskaya railway in comparison with magnetic recordings from ground based stations. At least 11 events of false operation during magnetic disturbances were found in 2003 that support the idea of space weather impact to railway automatic systems.

## **Geomagnetically induced currents in power systems of the Kola peninsula**

Ya.A. Sakharov<sup>1</sup>, A.N. Danilin<sup>2</sup>, V.N. Selivanov<sup>2</sup>, R.M. Ostafiychuk<sup>3</sup>, Yu.V. Katkalov<sup>1</sup>, N.V. Kudryashova<sup>1</sup>

<sup>1</sup>*Polar Geophysical Institute RAS, Apatity*

<sup>2</sup>*Kola Science Center RAS, Apatity*

<sup>3</sup>*Military Technical University, St-Petersburg*

*e-mail: sakharov@pgia.ru*

The results of permanent registration of GIC in the power systems of the Kola Peninsula are presented. We have registered DC in dead-grounded neutral of the power autotransformer at the power system substations of 110-330 kV class. GIC response in power lines is estimated for different level of magnetic activity in auroral zone.

## **Evolution of geomagnetic perturbations and aurora dynamics during the strong magnetic storms events**

S.I. Solovyev, R.N. Boroyev, A.V. Moiseyev (*Yu.G. Shafer Institute of cosmophysical research and aeronomy SB RAS, Yakutsk, Russia*)

The results of a study of high-, low-latitude geomagnetic disturbances and aurora reaction to variations of solar wind parameters and Dst according to the satellite and ground observations during periods of strong magnetic storms with  $Dst \leq 400$  nT of October-November, 2003, 2004 are presented.

The following results are obtained:

1. It is shown that : a) impulsive (substorm) electrojet component leads to positive disturbances  $dH$  at low latitudes with magnitude of  $\sim 30-100$  nT in premidnight-morning sector; b) regular (convection) electrojets component is one of the possible reason of negative  $dH$  values at low latitudes and Dst growth.

2. It is shown that the growth of solar wind dynamic pressure ( $P_d$ ) leads to positive variations of geomagnetic field  $dH$ -component of low-latitude geomagnetic disturbances but only during IMF  $B_z$  positive. During the periods of the negative IMF  $B_z$  with the same  $P_d$  magnitude at  $B_z > 0$  the negative  $dH$  disturbances at low latitudes are registered. One of the reason of negative  $dH$  is the increase of Region 1 FACs at  $B_z < 0$ .

3. It is established, that maximal negative values of  $dH$ -component of geomagnetic field at low latitudes in 18-24 MLT observed during most southern position of equatorward boundary of auroral luminosity during the growth of negative IMF  $B_z$ .

It is supposed, that in the magnetic storm the enhancement of partial-ring current which closed to the ionosphere by the region 2 FACs at equatorward boundary of aurora oval is the main reason of geomagnetic field depression at low latitudes.

The work was supported by RFBR grant № 09-05-98546 and partially by the SB RAS project № 69.

## Bay-like magnetic disturbances occurring in the auroral zone during periods of intense and long-duration magnetic activity: Inconsistency with behavior of aurora

O. Troshichev and A. Janzhura (*Arctic and Antarctic Research Institute, St.Petersburg, Russia*)

Relationships between the magnetic disturbances in the auroral zone, aurora dynamics and particles injections at the geostationary orbit have been analyzed for 62 of the bay-like magnetic disturbances repetitively occurring in the auroral zone during intense long-duration activity. It is shown, that lack of the auroral breakup is typical of the powerful disturbances and, therefore, these disturbances can not be assigned as the classical magnetospheric substorms. In these cases aurora in the oval keep the marginal luminosity or, on the contrary, demonstrate the high activity well before (up to few hours) the magnetic disturbance sudden onsets. The distinguishing feature of the aurora activity is the double oval structure, which is the most noticeable near the dusk meridian. It is suggested that the electric field variations, not auroral particle precipitation, is the dominating factor in generation of the westward electrojet, which can extend from dawn to dusk in course of these bay-like disturbances. The close relation of the aurora behavior to the substorm signatures at geostationary orbit breaks down as well. The conclusion is made, that the powerful repetitive magnetic disturbances present quite another, than classical substorm, kind of the magnetosphere disturbance.

## The effect of electric field increasing on the substorm currents formation

M.A. Volkov (*Murmansk State Technical University, 13 Sportivnaya Str., Murmansk, 183010, e-mail: mavol2006@yahoo.com, volkovma@mstu.edu.ru*)

The stable state of the magnetic flux tube with the current and with the finite magnetosphere conductivity has been studied in this work. The appearance of the finite anisotropic conductivity can be caused by thinning of the near-Earth plasma sheet in the night- side magnetosphere. The finite conductivity leads to the increasing electric field and to the formation of the longitudinal plasma pressure gradients also. The field-aligned currents flowing out of and into the ionosphere ( the currents of the expansive phase of the substorm) appear in this region of the magnetosphere.

## Visual luminosity equatorwards of the auroral oval during magnetic storms

V.L. Zverev<sup>1</sup>, Ya.I. Feldstein<sup>2</sup>, V.G. Vorobjev<sup>1</sup>

<sup>1</sup>*Polar Geophysical Institute, Apatity, Russia*

<sup>2</sup>*Institute of Terrestrial Magnetism and Radiowave Propagation, Troitsk, Russia*

The comparison between equatorial boundaries of auroral discrete forms (auroral oval) and diffuse auroral luminosity was carried out for periods of magnetic storms. Position of equatorial boundary of the night-side auroral oval depending on the value of the Dst index was taken from the paper by Starkov [1993]. The limit of corrected geomagnetic latitude (CGL) of visual auroras which were observed overhead of stations was received on the basis of visioplots for IGY period [Auroral visioplots, 1964]. Twenty six magnetic storm events were used to determine the equatorward boundary of visual auroral luminosity during  $Dst < -100$  nT. When Dst changes from  $-100$  nT to  $-400$  nT the boundary of the visual auroral luminosity moves from about  $51^\circ$  to  $44^\circ$  CGL. According to visioplots the equatorward boundary of the visual auroral luminosity shifts on about  $7^\circ$  to lower latitude from the equatorward boundary of the auroral oval in intervals of magnetic storms. The auroral luminosity was registered at all latitudes between equatorward boundaries of the visual auroral luminosity and the auroral oval. It means that during magnetic storm the equatorward boundary of visual luminosity according visioplots does not reflect the location of discrete auroral forms boundary. It is well known that a diffuse aurora equatorward of discrete auroral forms can intensify considerably in intervals of magnetic storms. This special type of the auroral luminosity at mid-latitudes in the forms of stretched diffuse areas is associated generally with the atomic oxygen 630.0 nm emission. Therefore the lowest latitude of auroral luminosity on visioplots characterizes the equatorial boundary of diffuse auroras. The region of red diffuse luminosity spatially coincides with region of diffuse electron precipitation covering the region equatorward of the auroral oval up to latitudes of the main ionospheric trough. An electron energy flux and their average energy sharp decrease from oval to lower latitudes. It leads to decrease of the diffuse aurora intensity and respectively to the increase in the height the luminosity at lower latitudes. The intensification of the 630.0 nm luminosity at mid-latitudes near of the main ionospheric trough was called stable auroral red arc (SAR-arcs).

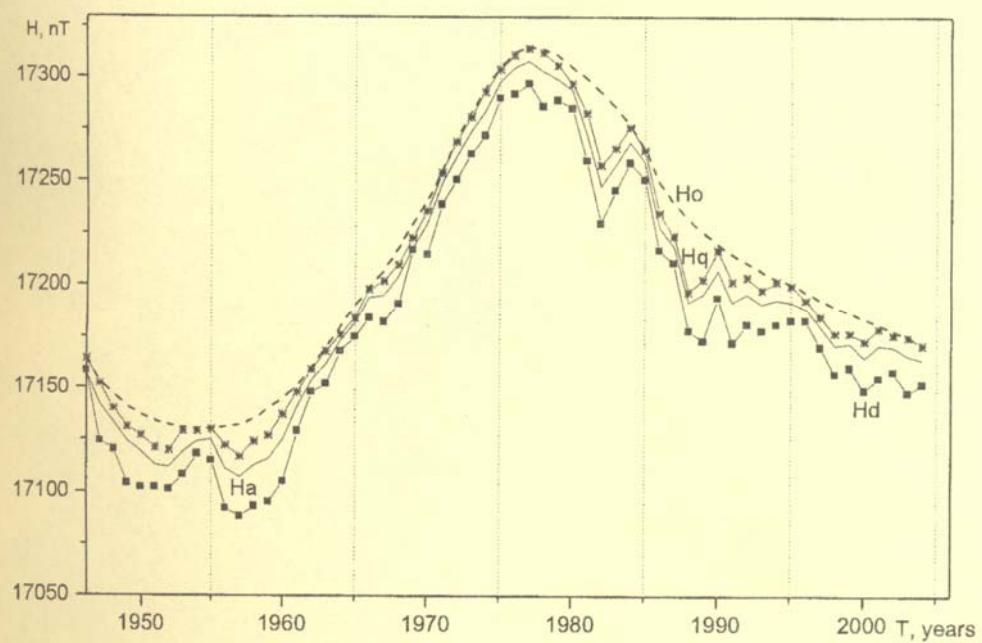
### ***Geomagnetic storms and substorms***

Between usual auroras and SAR-arcs does not exist an auroral gap. The latitudinal interval between the auroral oval and SAR-arcs is filled by auroral particle precipitations and diffuse luminosity. Intensity of a diffuse luminosity decreases to lower latitude becoming very weak or subvisual before SAR-arc.

References:

Starkov G.V. Planetary morphology of auroras // Magnetosphere-Ionosphere Physics: Brief reference book. Ed. Yu.P. Maltsev. St. Petersburg.: The Science. 184 p. 1993.  
Annals of the International Geophysical Year. Vol. XXIX. I.G.Y. Auroral visoplots. Ed. B. McInnes. Pergamon Press Ltd. 507 p. 1964.

*Fields, Currents, Particles in the magnetosphere*





## **Ionospheric convection from Cluster EDI measurements: Comparison with the ground-based IZMEM ionospheric convection model**

M.Foerster<sup>1</sup>, Y.I.Feldstein<sup>2</sup>, S.E. Haaland<sup>3,4</sup>, L.A. Dremukhina<sup>2</sup>, L.I. Gromova<sup>2</sup>, A.E. Levitin<sup>2</sup>

<sup>1</sup>*Helmholtz-Zentrum Potsdam, GeoForschungZentrum (GFC), 14473 Potsdam, Germany*

<sup>2</sup>*Pushkov Institute of Terrestrial Magnetism, Ionosphere and Radiowave Propagation, Troitsk, Moscow region, Russia*

<sup>3</sup>*Max-Planck-Institut für Sonnensystemforschung, Lindau-Katlenburg, Germany*

<sup>4</sup>*Department of Physics and Technology, University of Bergen, Norway*

Cluster/EDI electron drift observations above the Northern and Southern high-latitude areas for more than six and a half years (Feb 2001 till Oct 2007) have been used to derive a statistical model of the electric potential distribution for summer conditions. Based on potential pattern for different orientations of the interplanetary magnetic field (IMF) in the GSM y-z plane, basic convection pattern (BCP) were derived, that represent the main characteristics of the electric potential distribution in dependence on the IMF. The BCPs comprise the IMF-independent potential distribution as well as patterns, which describe the dependence on positive and negative IMF  $B_z$  and IMF  $B_y$  variations. The full set of BCPs allows to describe the spatial and temporal variation of the high-latitude electric potential (ionospheric convection) for any solar wind IMF conditions near the Earth's magnetopause. The comparison of the Cluster/EDI model with the IZMEM ionospheric convection model, which was derived from ground-based magnetometer observations, shows a good agreement of the basic patterns and their variations with the IMF. According to the statistical model, there is a two-cell antisunward convection within the polar cap for northward IMF  $B_z^+ \leq 2nT$ , while for increasing northward IMF  $B_z^+$  there appears a region of sunward convection within the high-latitude daytime sector, which assumes the form of two additional cells with sunward convection between them for IMF  $B_z^+ \sim 4 \div 5nT$ . This results in a four-cell convection pattern of the high-latitude convection. In dependence of the  $\pm$ IMF  $B_y$  contribution during sufficiently strong northward IMF  $B_z$  conditions, a transformation to three-cell convection patterns takes place.

This work is supported by Deutsche Forschungsgemeinschaft (DFG), Norwegian Research Council, RFFI grants 08-05-00896, 07-05-13524

## **Interpretation of wavelet spectra of high-latitude low-frequency electric field fluctuations**

I.V. Golovchanskaya (*Polar Geophysical Institute, Apatity, Russia*)

An attempt to find signatures of MHD turbulence in the spectra of electric field fluctuations measured by the *Dynamics Explorer 2* spacecraft with 16 Hz ( $\sim 500$  m) resolution is performed. The refinements compared to the earlier studies include (1) more indicative frequency range; (2) application of the discrete wavelet transform method developed for estimating scaling data instead of conventional Fourier analysis; (3) discrimination between fluctuations on the open and closed magnetic field lines. Power law spectral index (slope) of  $-1.66 \pm 0.1$  is clearly demonstrated for scale lengths  $> 32$  km. At sizes  $< 32$  km and down to the resolution limit the slope changes for  $\sim -2$  both in the auroral zone and the polar cap. Such spectral behavior can hardly be interpreted as a Kraichnan regime of 2D ionospheric turbulence, a scenario proposed by *Kintner and Seyler* [1985]. Nor can it be explained by scale-dependent mapping of magnetospheric turbulence to ionospheric heights, as suggested by *Weimer* [1985]. It is more likely that in addition to electrostatic turbulent fields originating in the magnetosphere and characterized by the spectral index of  $-5/3$ , an electromagnetic component (incident and reflected Alfvén waves) is present in the signal, which influences the spectral shape in the higher frequency range.

## **Two regimes of ion non-adiabatic acceleration in the Earth magnetotail. Geotail and Cluster observations**

E.E. Grigorenko<sup>1</sup>, L.M. Zelenyi<sup>1</sup>, M. Hoshino<sup>2</sup>, J.-A. Sauvaud<sup>3</sup>

<sup>1</sup>*Space Research Institute of RAS, Moscow, Russia*

<sup>2</sup>*University of Tokyo, Tokyo, Japan*

<sup>3</sup>*CESR, Toulouse, France*

Plasma Sheet Boundary Layer (PSBL) of the Earth magnetotail is an interface region where the manifestations of powerful acceleration processes occurred in the Current Sheet (CS) in the vicinity of magnetic separatrix between

## **Fields, currents, particles in the magnetosphere**

open magnetic field lines and already closed field lines are observed. The phenomenon most frequently observed in PSBL is highly accelerated (up to tens keV) field-aligned plasma beams streaming along the magnetic field lines from the acceleration source. The characteristics of their ion and electron velocity distribution functions reflects spatial and temporal properties of the acceleration sources which, in turn, are defined by the magnetic field topology in vicinity of separatrix. Our observations in the PSBL of the Earth's magnetotail revealed two different types of plasma beams. The first type represents energy collimated ion beams having a rather long duration (up to 20 min) and energies  $\leq 20$  keV observing along with isotropic electron distributions. Multipoint Cluster observations revealed that such beams represent plasma filaments elongated along the lobe magnetic field ( $\sim$ tens  $R_E$ ) and strongly localized ( $< 1 R_E$ ) in the direction transverse to the magnetic field. Moreover, the overlapping of two ion beams having very different field-aligned velocities was often observed in PSBL. These observational features may be reproduced in large scale kinetic model of ion resonant acceleration in the CS with distant X-line. According to this approach the acceleration source can not be considered as "uniform" one but represents wide region of CS with finite  $B_z > 0$  and consisting of several spatially localized sites (resonances) at which ions are accelerated almost without scattering and form localized beams in PSBL. In the other places of this acceleration region ions experience strong scattering and are trapped in CS. Electron observations confirm that the acceleration actually occurs in the region with closed magnetic field geometry. Another type of distributions represents powerful (up to 100 keV) ion beams with large parallel temperatures. They are observed along with the anisotropic electron velocity distributions. This feature is peculiar for the magnetic separatrix and indicates that the spacecraft crossed yet open or recently closed magnetic field lines. Such ion beams may be produced by the spatially extended "merged" acceleration source which is formed due to the overlapping of initially spatially separated resonances near X-line.

## **The contribution of the external geomagnetic field to the average amplitude of the Earth's magnetic field recorded by a magnetic observatory**

A.E. Levitin, L.A. Dremukhina, L.I. Gromova, E.G. Avdeeva (*Pushkov Institute of Terrestrial Magnetism, Ionosphere, and Radiowave Propagation, Troitsk, Moscow region, Russia*)

Annual and secular variations of the geomagnetic field are caused by variation of Main Earth's Magnetic field, generated of internal sources in the Earth's core; variation of the field of magnetic anomalies; variation of the intensity of magnetospheric current systems, generating the external geomagnetic field; variation of the intensity of telluric currents. The contribution of the external geomagnetic field controlled by solar activity to the annual amplitudes of the geomagnetic field is examined. Processing of geomagnetic data of some observatories for long time interval (1950-1985) allows to estimate contribution of each monthly amplitude to the annual amplitude of the geomagnetic field and the temporal changes of this contribution from year to year, and to analyze relation of monthly variations of the geomagnetic field with indices of the solar activity (F10.7), components of Interplanetary Magnetic Field, velocity and density of Solar Wind. It is demonstrated dependence of variation of the geomagnetic field on solar activity cycles, possibility to calculate secular variation of the geomagnetic field based on monthly amplitudes, to estimate contribution of the external geomagnetic field to the secular variation of Main Earth's Magnetic field.

This work is supported by RFFI grants 08-05-00896, 07-05-13524.

## **Ion energy spectra at $L \sim 3.6 - 6.7$ during disturbed geomagnetic conditions**

T.V. Kozelova<sup>1</sup>, L.L. Lazutin<sup>2</sup>, B.V. Kozelov<sup>1</sup>

<sup>1</sup>*Polar Geophysical Institute, Apatity, Russia*

<sup>2</sup>*Space Science Division, Scobeltsyn Institute for Nuclear Physics of Moscow State University, Russia*

Differential energy spectra of ions with the energies 0.1-3200 keV has been considered using the CRRES data at  $L \sim 2.3 - 6.7$  in the nightside magnetosphere. During the events under consideration the CRRES was located near the equatorial plane and crossed the inner part of the plasma sheet and the radiation belts.

It was shown that the ion differential energy spectra at  $L \sim 3.6-4.5$  consists of two different groups of ions, one of them is populated by ions with energy below  $\sim 20$  keV and another one — by ions with energy above  $\sim 70$  keV. Those parts of the spectra may be described by the thermal (Maxwellian) forms. The characteristic energy evens  $\sim 10$  keV for low-energy portion of ion spectra. For high-energy portion the characteristic energy changes with the  $L$  value according to adiabatic law  $\sim L^{-3}$ . The ion flux for intermediate energies 20–70 keV increases with increasing  $L$  and forms the kappa distribution which frequently characterize the energy spectra observed during low AE periods.

Then, this spectral shape at  $L \sim 5.5$  changes from the kappa form to the Maxwellian one with the energy peak on 25 keV.

At  $L \sim 5.9 - 6.6$  the ion spectra in two energy ranges,  $E < 7$  keV and  $E > 70$  keV, may be approximated by the same kappa form, which remains nearly unchanged during the substorm growth phase and the small activations. The spectral shape in the energy range 7-70 keV may be fitted by the Maxwellian form.

During the substorm expansion phase, the spectral shape was significantly variable above the knee of the ion spectra ( $\sim 35$  keV). The energy spectrum clearly manifestates the drop in the flux at lower energies and the enhancement at the higher energies. As a result, a new knee forms with the extreme energy  $\sim 250$  keV. As a whole, as a result of the substorm particle injection the characteristic energy of the Maxwellian shape changes from 10 keV to 22 keV.

We discuss the spectrum-preserving and spectrum-altering magnetospheric processes and compare our results with other observations and model predictions.

### **Energetic electron precipitation measured by CORONAS-F satellite and polar magnetic disturbances**

O. Kozyreva<sup>1</sup>, I. Myagkova<sup>2</sup>, N. Kleimenova<sup>1,3</sup>

<sup>1</sup>*Institute of the Earth Physics RAS, B. Gruzinskaya 10, Moscow 123995, Russia*

<sup>2</sup>*Skobeltsyn Institute of Nuclear Physics, Moscow State University, 119191, Moscow, Russia,*

<sup>3</sup>*Space Research Institute RAS, Profsoyuznaya 84/32, Moscow, 117997, Russia*

The energetic (300-600 keV) electron precipitation at polar latitudes has been investigated on the base of CORONAS-F satellite measurements. Low altitude (500-350 km) CORONAS-F satellite has a circular orbit with an inclination of  $\sim 82.5^\circ$  and orbital period ( $\sim 1.5$  hours), it corresponds to about 15 circuits per day. The data of the polar cap passes on December 13, 2003 has been analyzed and compared with ground geomagnetic observation from the stations located near footprint of the satellite pass in each given moment. We found that some polar cap substorm activations were accompanied by the strong electron precipitation which observed during the substorm growth as well as the recovery phase. The satellite data we compared with ground high latitude riometer measurements at Hornsund station and ASC keogram.

### **Energetic electron flux precipitations near the outer ERB's boundary and auroral oval position**

I.N. Myagkova, E.E. Antonova, M.O. Riazantseva, B. V. Marjin (*Skobeltsyn Institute of Nuclear Physics, Moscow State University, 119191, Moscow, Russia*)

The peculiarities of electron precipitation (with the energies more than 300 keV) to the pole of outer Earth's radiation belt observed during August-September 2003 are studied. Observations of CORONAS-F and Meteor-3M satellites were used. Low altitude polar orbit (about 430-460 km, an inclination of  $\sim 82.5^\circ$ ) of CORONAS-F satellite permits to observed electron precipitations in North and South polar regions every 1.5 hours. Energetic electrons in different energy ranges (0.3-12 MeV) were measured by semiconductor and plastic scintillator telescopes. Localized electron precipitations were observed to the pole from the external boundary of the outer radiation belt. It is shown, that such kind of precipitations can be observed for more than a half of polar crossings and part of them are observed for more than 2 consequent satellite orbits. Results of observations are compared with data of auroral satellite Meteor-3M. The detailed investigation of observed such as their asymmetry, frequencies, MLT-distribution. The nature of observed phenomena is discussed.

This work was partly supported by RFBR foundation grants 07-02-92004-HHC\_a.

### **Comparison between substorm current wedges and dipolarizations during 2008 THEMIS tail season**

A. Nikolaev, V. Sergeev, N. Tsyganenko (*St. Petersburg State University, St.-Petersburg, Russia*)  
V. Angelopoulos (*UCLA, Los Angeles, USA*),  
H. Singer (*NOAA, Boulder, USA*)

The substorm-related magnetic field dipolarizations are contributed by different processes, including the global reconfigurations, the effects of the substorm current wedge (SCW) and meso/small scale features associated with inward-propagated sharp fronts and structures. We compare the observations of dipolarizations made by four GOES

## **Fields, currents, particles in the magnetosphere**

spacecraft and five Themis spacecraft with SCW boundary locations and intensity. These parameters were estimated based on interpretation of midlatitude ground magnetic measurements using the inversion algorithm. Preliminary results from statistical comparison of the SCW and dipolarizations during THEMIS tail season in January-March 2008 are shown and comparisons with a new SCW magnetospheric model are presented.

## **Small-base gradient analysis of high-latitude magnetic pulsations field by usage virtual stations of BEAR network**

A.V. Petlenko, Yu.A. Kopytenko (*St-Petersburg Filial of Institute of Terrestrial Magnetism Ionosphere and Radio Wave Propagation RAS (SPbF IZMIRAN), St-Petersburg, Russia*)

Virtual stations of BEAR magnetometers network were used for small-base gradient analysis of high-latitude ionosphere magnetic pulsations field emulating. This allowed to determine parameters of movement of geomagnetic pulsations sources even in the case when their size was too small in comparison with a distance between real magnetic stations.

## **Origins of plasma sheet By magnetic field**

A.A. Petrukovich (*Space Research Institute, Moscow, Russia*)

With 11 years of Geotail measurements we construct a model of plasma sheet  $B_y$ , depending on IMF  $B_y$ , coordinates  $X$ ,  $Y$ , and geodipole tilt angle. At midnight and pre-midnight local times  $B_y$  is positively correlated with tilt (positive in summer). Thus in summer  $B_y$  is shifted towards positive values and in winter towards negative values, so that up to several nT could be added to the IMF influence. The dawn side plasma sheet  $B_y$  generally does not exhibit any tilt dependence, but within 15 Re the weaker negative correlation with tilt was revealed. The tilt can control plasma sheet  $B_y$  via distribution of the region 1 FAC. Similar coupling between tilt and IMF  $B_y$  was earlier found in the ionospheric convection patterns. Besides this average response, extreme  $B_y$  ( $|B_y| > 5$  nT,  $B_y > \text{IMF } B_y$ ) were often observed (up to 20-25% of cases during solar maximum and in the pre-midnight sector within 20 Re). They can not be explained by our statistical model and are preliminary interpreted as an "over-reaction" of the magnetosphere in some individual events. Large  $B_y$  field radically changes dynamics of the current sheet and has to be taken into account during substorm-related studies.

## **Comparison of saw-teeth oscillations at GOES and GEOTAIL satellites**

V.C. Roldugin (*Polar Geophysical Institute, KSC RAS, Apatity*)

The oscillations of magnetic field in the magnetosphere with period about 2-4 hours (saw-teeth event) at GOES-8 and GOES-10 have been examined jointly with GEOTAIL data for several cases. During GEOTAIL being in the geomagnetic tail, the oscillation periods are the same. There are phase shifts between the satellites from several minutes to half an hour, the propagation direction occurs both earthward and anti-earthward, and there are changes of character of disturbance in the tail depending on GEOTAIL position in the tail. The explanation of these specific features of saw-teeth event is given on the base of the theory of tail oscillation made by Ershkovich with colleagues.

## **Propagation of oblique interplanetary shocks through the magnetosheath**

A.A. Samsonov (*Institute of Physics, St. Petersburg State University, St. Petersburg, Russia*)

We use a three-dimensional MHD model of the Earth's magnetosheath to simulate the interaction of interplanetary shocks (IS) with the bow shock and following variations in the magnetosheath for two cases. In first case, an IS has the normal along the Sun-Earth line, in second case, another IS with the same density jump has the angle between the shock normal and the Sun-Earth line equal to 41 degrees (we would call them the direct and oblique shocks respectively). We find that a forward fast shock and a following train of discontinuities propagate through the magnetosheath in both cases. The oblique fast shock crosses the flank magnetosheath in about 1 minute, and the direct fast shock needs nearly the same time to cross the subsolar magnetosheath. We make simple estimations of the shock propagation time in the magnetosphere to determine the time when the sudden impulse will be registered by ground magnetometers. The theoretical predictions agree with observational facts.

## Generation of the field-aligned currents associated with the geomagnetic sudden impulse

A.A. Samsonov<sup>1</sup>, D.G. Sibeck<sup>2</sup>

<sup>1</sup>*Institute of Physics, St. Petersburg State University, St. Petersburg, Russia*

<sup>2</sup>*Goddard Space Flight Center, Greenbelt, Maryland, USA*

We present results of the global MHD modeling of interaction between an interplanetary shock (IS) and the Earth's magnetosphere for the northward IMF orientation. It is known that the solar wind dynamic pressure is larger downstream of the IS what results in magnetospheric compression. The geomagnetic sudden impulse or sudden commencement is a global increase of the H-component observed by all ground stations. In addition to the global variation, there is a double-pulse structure observed at high latitude stations and connected with variations of the field-aligned currents (FAC). The numerical MHD modeling predicts the evolution of the FACs caused by the IS passage. In the case of northward IMF, the model describes two current systems which correspond to the NBZ and Region 1 currents. In the course of the shock's propagation, these currents intensify successively. The NBZ current peaks as the shock front reaches the terminator plane, while the Region 1 current peaks about 2-3 minutes later. These currents are generated by dynamo regions in the magnetosphere. Using (E-J) contours, we observe intensifications of the magnetospheric dynamo which we relate to intensifications of the FACs. The purpose of our work is to describe the geometry of the magnetospheric-ionospheric currents which can be also applied to stationary magnetospheric conditions.

## Themis observations of dipolarizations and plasma injections associated with substorm current wedge

V. Sergeev<sup>1</sup>, V. Angelopoulos<sup>2</sup>, T. Sugak<sup>1</sup>, S. Apatenkov<sup>1</sup>, I. Kornilov<sup>3</sup>, T. Kornilova<sup>3</sup>, J. McFadden<sup>4</sup>, D. Larson<sup>4</sup>, J. Bonnell<sup>4</sup>, M. Fillingim<sup>4</sup>

<sup>1</sup>*St. Petersburg State University, St. Petersburg, Russia*

<sup>2</sup>*University of California, Los Angeles, USA*

<sup>3</sup>*Polar Geophysical Institute, Apatity, Russia*

<sup>4</sup>*University of California, Berkeley, USA*

We briefly present a summary of recent results concerning the dipolarizations and plasma injections during the 2008 tail season of Themis. We found that the major plasma response to dipolarizations in this entry region consists of the increase of plasma pressure, decrease of plasma tube entropy and (usually) density, combined with an increase of plasma temperature and high energy particle flux. Dipolarisation-related response displays two distinct phases. Prior ( $\sim 1$ min) to the arrival of sharp dipolarization front (SDF), the large scale increase of plasma flow (up to km/s) and pressure (up to 20-30%) is observed withing 1min from the ground Pi2 onset, this perturbation seems to be the interaction region (sheath) of plasma structure intruding Earthward from the tail. The dipolarization front propagates radially at slower speed ( $< 100-200$ km/s). Following its arrival the plasma entropy decreases and flow intensifies but loses a coherence at closely-spaced spacecraft. We interpret this stage as an encounter with the compact plasma structure (bubble?), which is distinct by its sharp boundary as well as by its highly structured/granulated proper. We were also able to identify the auroral signatures of the dipolarization region, whose observation indicate a dynamical grainy structure of the injection proper and which may be a unique tool for further studies of plasma injections.

## Seasonal effect in the latitudinal position of night - and dayside precipitation boundaries

V.G. Vorobjev, O.I. Yagodkina (*Polar Geophysical Institute, Apatity, Murmansk region, 124200, Russia*)

Auroral particle precipitation observed from DMSP F7 spacecraft for 1986 were used to examine seasonal variations in the position of auroral precipitation boundaries. Average corrected geomagnetic latitudes (CGL) of different auroral boundaries were calculated in the dependence on the geomagnetic activity level (AL index) for winter, summer, spring and autumn seasons separately. In the northern hemisphere the most poleward boundary of the nightside auroral precipitation ( $SDP_{pol}$ ) and the poleward boundary of the structured precipitation ( $AOP_{pol}$ ) were found to be about  $2^\circ$  CGL in higher latitude during local winter than during local summer for all geomagnetic activity levels. While the latitudinal location of the equatorward boundary of both the structured ( $AOP_{eq}$ ) and diffuse

## **Fields, currents, particles in the magnetosphere**

(DAZ<sub>eq</sub>) precipitation did not show a significant dependence on seasons. This result testifies that the winter AOP region is wider than the summer AOP. Spacecraft observations in the southern hemisphere revealed the same results: the nightside poleward boundaries of the SDP and AOP were situated in the highest latitude during local winter. Return results have been received for the position of dayside precipitation boundaries. All poleward and equatorward precipitation boundaries in the northern hemisphere were found in higher latitudes during local summer than winter. According to this result it is possible to assume that the polar cap area does not depend on the season but the polar cap simply moves sunward along the X<sub>GSM</sub> axis during the northern winter and antisunward during the northern summer. However big problems arise there with the magnetic conjugacy because the polar cap movement is opposite in both hemispheres.

This study is supported by the RFBR grants 09-05-00818 and Program 16 of the RAS Presidium.

## **The response of midday aurorae to sharp changes of solar wind dynamic pressure under southward and northward Bz IMF conditions**

V.G. Vorobjev, V.L. Zverev, O.I. Yagodkina (*Polar Geophysical Institute, Apatity, Murmansk region, 124200, Russia*)

Behaviors of midday aurorae associated with sharp increases of solar wind dynamic pressure (SC) occurred during intervals of southward and northward interplanetary Bz were examined by using optical observations at Heiss Island (HIS,  $\Phi \approx 75.0^\circ$  N; MLT  $\approx$  UT + 4.6) and Barentsburg (BAB,  $\Phi \approx 75.1^\circ$  N; MLT  $\approx$  UT + 2.5) stations. Observations by the meridian-scanning photometer (MSP), spectrophotometer and all-sky camera were analyzed in this study. Two SC events registered on December 18, 1985 (at 0647 UT) and on November 28, 1989 (at 0743 UT) were examined in detail. Each event has its own peculiarities. The SC on Dec. 18, 1985 appeared under negative Bz IMF condition. Just after SC the considerable intensification of (OI) 557.7 nm emission relative to (OI) 630.0 nm emission was observed by the HIS's MSP not only equatorward but at latitudes of the dayside red auroral bend. The sharp decrease in the ration of  $I_{6300}/I_{5577}$  testified for precipitation of a few keV magnetospheric electrons on closed magnetic field lines. The SC on Nov. 28, 1989 appeared under positive Bz IMF orientation. The considerable increase of the dayside red auroral bend intensity was observed in a few minutes after SC. The large value of the  $I_{6300}/I_{5577}$  points to the sharp increase of the low energy (a few hundred eV) electron precipitation. The sources of such type precipitation may be the solar wind plasma and/or low latitude boundary layer.

This study is supported by the RFBR grants 09-05-00818 and Program 16 of the RAS Presidium.

## **Magnetic field distortion in the process of plasma convection in the magnetosphere of the Earth: Preliminary results of modeling**

V.V. Vovchenko<sup>1</sup>, E.E. Antonova<sup>2,1</sup>

<sup>1</sup>*Space Research Institute RAS, Moscow, Russia*

<sup>2</sup>*Skobeltsyn Institute of Nuclear Physics Moscow State University, Moscow*

The increase of plasma convection in the magnetosphere of the Earth leads to the increase of plasma pressure in the inner magnetospheric regions. The effect is especially pronounced during magnetic storms when ion distribution functions become nearly isotropic and plasma transport can have near adiabatic character. The distortion of the magnetic field by the increase of plasma pressure is modeled using self-consistent modified Wolf-like model. Model description is presented. Model describes the formation of asymmetric ring current, systems of transverse and field-aligned currents and electric fields of large-scale magnetospheric convection. It includes the effect of local magnetic field distortion due to the increase of plasma pressure in every point calculated in the suggestion of the validity of the condition of magnetostatic equilibrium. It is shown, that due to magnetic field distortion closed inside the magnetosphere isolines B=const at the equatorial plane which does not surround the Earth can appear.

## Spatial distribution of the auroral precipitations zones depending on different solar wind streams

O.I. Yagodkina<sup>1</sup>, I.V. Despirak<sup>1</sup>, V. Guineva<sup>2</sup>

<sup>1</sup>*Polar Geophysical Institute, Apatity, Russia*

<sup>2</sup>*Solar-Terrestrial Influences Laboratory, Stara Zagora, Bulgaria*

The dynamics of the spatial distribution of the different auroral precipitations zones during different solar wind streams was studied by DMSP satellites data. The examination was implemented depending on the geomagnetic disturbance level, expressed by the AL- and Dst indices. Three precipitation zones were determined: 1) DAZ zone, coinciding with the diffuse auroral glow zone; 2) AOP zone, coinciding with the statical discrete auroral forms oval; 3) the band of soft diffuse precipitations SDP, enveloping the poleward boundary of the AOP zone.

The solar wind streams (recurrent streams from coronal holes and magnetic clouds) were defined by Wind satellite data. The spatial localization of auroral precipitation zones was obtained during two recurrent streams, observed in January and February 1997, and during two magnetic clouds, observed 10 January 1997 and 15 July 2000. The last case was connected to the development of a strong geomagnetic storm excited by the magnetic cloud with extremely high values of the solar wind parameters ( $V_x \sim 1200$  km/s,  $B_z \sim 60$  nT). The different precipitation structure during the specified events was discussed. The obtained dynamics of the precipitation zones during recurrent streams and magnetic clouds is in good agreement with the DMSP observations.

## Dayside aurorae and geomagnetic variations associated with negative and positive solar wind dynamic pressure impulses: case study

O.I. Yagodkina, V.G. Vorobjev, V.B. Belakhovsky (*Polar Geophysical Institute, RAS, Apatity, Murmansk region, 184200, Russia*)

Optical observations in Barentsburg ( $\Phi \approx 75.1^\circ$  CGL,  $MLT \approx UT + 2.4$ ) and geomagnetic variations from IMAGE magnetometer network were used to examine auroral phenomena on November 28, 2000. This day the sharp decrease (SI) and in about two hours sharp increase (SC) in the solar wind dynamic pressure were registered with ACE and Wind spacecraft. The solar wind dynamic pressure drop from about 5 to 2 nPa in two minutes caused about 20 nT decrease in the SYM-H from 0316 UT to 0330 UT. During this time the diffuse auroral luminosity at latitudes below than  $73^\circ$  CGL were observed by all-sky TV camera and meridian scanning photometer in Barentsburg. Fast equatorward movement and auroral luminosity decrease were observed after SI from 0325 to 0330 UT. Simultaneously, the sharp short-time increase in the westward electrojet intensity at the poleward edge of aurorae ( $70^\circ$ - $72^\circ$  CGL) as well as Pc5 geomagnetic pulsation activity at latitudes between  $64.5^\circ$ - $66.5^\circ$  CGL was registered. The SC at 0531 UT was caused by the sharp dynamic pressure increase from about 2 to 7 nPa. About 1 minute increase in diffuse aurora intensity occurred just after SC near the southern horizon of Barentsburg and about 5 min later a new intensification accompanied with the discrete aurorae appearance poleward of the diffuse aurora was observed. Sharp increase in Pc5 geomagnetic pulsation activity arisen from SC occurred from  $66.5^\circ$  to  $71.5^\circ$  CGL (max at  $\sim 70.5^\circ$ ) in the diffuse aurora region observed by IMAGE spacecraft.

This study is supported by the RFBR grant 09-05-00818 and Program 16 of the RAS Presidium.

## Internet as the media for coordinated polar geophysical research

A.N. Zaitsev, V.A. Shilimov (*N.V.Pushkov Institute of Terrestrial Magnetism, Ionosphere and Radiowaves Propagation, RAS, Troitsk, Moscow region, Russia*)

Future development of coordinated polar geophysical research is oriented on the achievements in the Internet network which based on the rapid innovation in information technologies such as personal computers and high speed links. Such new technologies drastically change the style and ways of research as well as access and processing of the data. One of the first sample of the usage such new technologies at 1975-1985 we can refer CDAW - Coordinated Data Analysis Workshops, when a few data intervals (substorms) were analyzed from different points of view. As a result we get an initial unified knowledge about substorms which since that has massive developments, see the reference as NASA source: <http://spdf.gsfc.nasa.gov/spdf.html>. Due to many common interests, common techniques and overlapped activities it was proposed to produce the real-time Internet services as AE-index project, AMIE (Assimilative Mapping of Ionospheric Electrodynamics), <http://amie.engin.umich.edu/~amie/>, and SuperDARN ionospheric radars network, <http://superdarn.jhuapl.edu/>.

## **Fields, currents, particles in the magnetosphere**

Next leap become the space multi-satellite experiments as Interball and Cluster which data base become first sample as the “open source”. At nowadays we enter in the new stage of coordinated projects such as International Polar Year (IPY), electronic Geophysical Year (eGY) and International Heliophysical Year (IHY). The eGY lead to the new understanding what we might expect from coming changes on the “digital road in science”, <http://egy.org/index.php>. Also real breakthrough happened in space experiments due to THEMIS projects, see <http://ds9.ssl.berkeley.edu/themis/news.html>. 5 satellites operate in distant magnetosphere and the data available in real time. In addition to such service the most of scientists are use the same software (IDL) to process the data. Another point of coordinated programs – the virtual observatories with “open source” data bases as well as computer programs. Now we have many data bases which united in one scheme with the same information and communication technologies. As the new results we have a new real-time services in favor of coordinated polar geophysical research programs. The samples already well-known as the real-time magnetometer network in Barents Sea area, <http://geo.phys.uit.no/eljet/>, all-sky camera on South Pole station in Antarctica, [http://aurora.iar.nagoya-u.ac.jp/southpole/2008\\_NRT/](http://aurora.iar.nagoya-u.ac.jp/southpole/2008_NRT/), the web-server of cosmic ray stations in IZMIRAN, <http://helios.izmiran.rssi.ru/cosray>. Almost 20 years we use the Intermagnet system ([www.intermagnet.org](http://www.intermagnet.org)) and now they are make the next step – SuperMAG project (<http://supermag.jhuapl.edu/>), which based on worldwide collaboration of ground based magnetometers generously supported by the National Science Foundation and NASA. The aim of such project is to collect the data from polar magnetometers (variometers) and accept the software to process and to distribute the data. Now SuperMAG include more than 200 stations. It is obvious that our work in future must based on the recent results and methods of informatics (including data integration, data mining, and knowledge extraction), networks, communication engineering, and computer science in space science research. Modern Information Age will open the new possibilities to conduct the polar geophysical research first of all through Internet. The success will be achieved by scientists who will gain enough skill on usage of Internet and new computing technologies. The scientific tasks will exploded as we can approach to detailed description of physical process in the magnetosphere in the format of “space weather”.

## **Мультифрактальные характеристики магнитосферной активности как отклик на стохастическое воздействие солнечного ветра**

Б.В. Козелов (*Полярный геофизический институт КНЦ РАН*)

Одной из до сих пор актуальных задач является поиск связи между характеристиками солнечного ветра и откликом магнитосферно-ионосферной системы. Известно, что эта связь нелинейная, кроме того, структура солнечного ветра также весьма сложна, что ограничивает возможности построения прогнозистических моделей. Развитие численных методов анализа временных рядов даёт новые подходы к решению этой задачи. Недавно было показано, что флюктуации глобальных характеристик в ряде лавинных (модели Bak-Tang-Wiesenfeld и Zhang) и турбулентных (2D Navier-Stokes) систем могут быть описаны стохастическими дифференциальными уравнениями с окрашенным шумом в правой части и диффузионным коэффициентом, зависящим от амплитуды флюктуаций. Для приложения к магнитосферной активности необходимо обобщение данного подхода на случай мультифрактального шума. В докладе обсуждаются результаты анализа мультифрактальных характеристик стохастической компоненты временных рядов индексов геомагнитной активности с разрешением 1 мин. (AE) и 1 час. (Dst) и соответствующих параметров солнечного ветра ( $B_z$ ,  $vB_z$ ,  $|\mathbf{B}|$ ).

## **Влияние анизотропии источников плазмы на структуру тонкого токового слоя в хвосте магнитосферы**

О.В. Мингалев<sup>1</sup>, И.В. Мингалев<sup>1</sup>, Х.В. Малова<sup>2,3</sup>, Л.М. Зеленый<sup>2</sup>

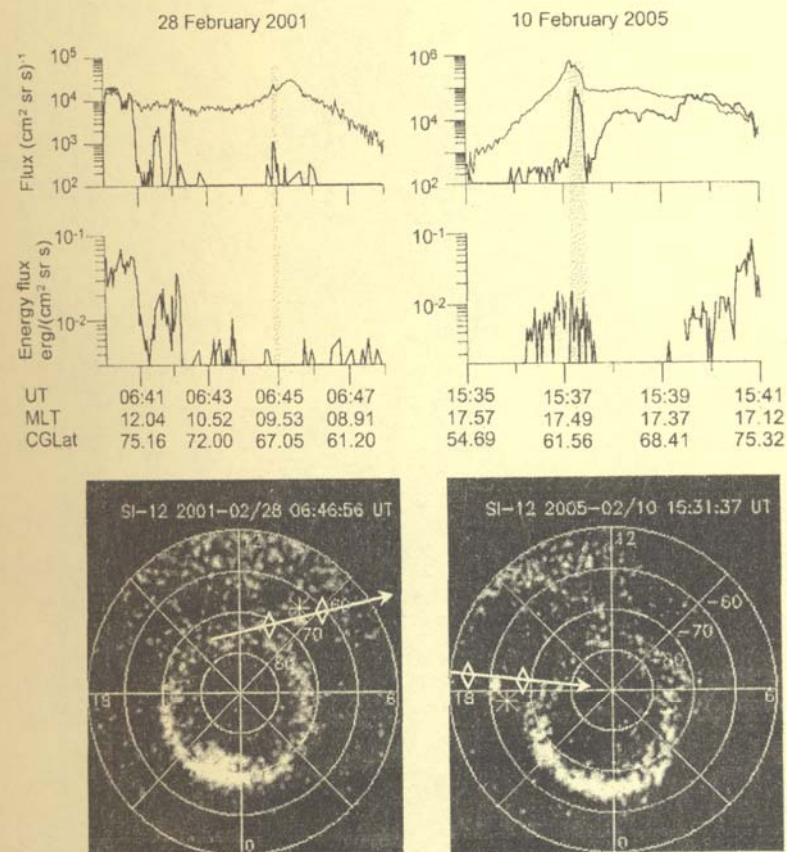
<sup>1</sup>*Полярный геофизический институт КНЦ РАН, Апатиты*

<sup>2</sup>*Институт космических исследований РАН, Москва*

<sup>3</sup>*Научно-исследовательский институт ядерной физики им. Д.В. Скobelьцына МГУ, Москва*

При помощи основанной на методе макро-частиц численной модели тонкого токового слоя (ТТС) исследован вопрос о влиянии на структуру ТТС анизотропии образующих слой источников плазмы в долях хвоста. Показано, что равновесные симметричные конфигурации ТТС существуют для достаточно большого диапазона значений параметра анизотропии источников, равного отношению тепловой скорости к величине гидродинамической скорости, в частности, при очень слабо анизотропных источниках (с большим значением параметра анизотропии).

## Waves, Wave-Particle Interaction





## On existence of the shock wave inside the magnetosphere

V.B. Belakhovsky (*Polar Geophysical Institute of Kola Scientific Center, Apatity, Russia*)

Some shock waves with high magnetosonic Mach number in the solar wind using *ACE* and *WIND* spacecraft were detected. For these shock waves the corresponding disturbances of the plasma parameters inside the magnetosphere using geosynchronous *LANL* and *GOES* spacecrafsts were found. It was selected only those *SSC* events when *LANL* and *GOES* located on the dayside magnetosphere. Alfvénic Mach number for the disturbances inside the magnetosphere was visibly less than unit. Therefore the magnetosonic Mach number was also visibly less than unit. So it was considered that the shock wave does not remain shock inside the magnetosphere at geosynchronous orbit.

## Generation of *Pc5* pulsations under fluctuations of the solar wind dynamic pressure

V.B. Belakhovsky<sup>1</sup>, V.A. Pilipenko<sup>2</sup>

<sup>1</sup>*Polar Geophysical Institute, Apatity*

<sup>2</sup>*Space Research Institute, Moscow*

The intense *Pc5* pulsations at the recovery phase of strong magnetic storm 31 October 2003 are considered. The magnetospheric MHD waveguide turns out to be in a meta-stable state under high solar wind velocities, and quasi-periodic fluctuations of the solar wind plasma density on October 31, 2003 stimulate the waveguide excitation. The peaks in the spectra of magnetic field oscillations in the *Pc5* band at ground-based stations are shifted to higher frequency part in comparison with the peaks in the spectra of the solar wind dynamic pressure fluctuations. We suppose that this effect associated with accelerated motion of the magnetopause. The addition of the inertia force to the force balance at the boundary results in an increase of the Kelvin-Helmholtz instability (KHI) growth rate [Mishin, 1993]. This increase may be visualized as “plug-in” of a Rayleigh-Taylor instability into the KHI. According to this mechanism, the evolution of ULF waves should correspond better to the derivative of pressure than to pressure itself.

The comparison of the simultaneous *Pc5* pulsations on morning and evening side of the magnetosphere show that cross-spectra, azimuthal wave numbers, phase velocities was quite different on both sides. So we consider that the direct driver of the *Pc5* pulsations is disturbances inside the MHD-waveguide, but not disturbances on the magnetopause, excited by the solar wind.

## Generation of magnetic and particle *Pc5* pulsations at the recovery phase of strong magnetic storm

V.B. Belakhovsky<sup>1</sup>, V.A. Pilipenko<sup>2</sup>

<sup>1</sup>*Polar Geophysical Institute, Apatity*

<sup>2</sup>*Space Research Institute, Moscow*

The intense *Pc5* pulsations at the recovery phase of strong magnetic storm 21 November 2003 are considered in detail. A global structure of disturbance is studied using data from a world-wide array of magnetometers and riometers augmented with data from particle detectors and magnetometers on board the geosynchronous *GOES* and *LANL* satellites. The local spatial structure is examined using the Finnish riometer array and *IMAGE* magnetometers. Though a general similarity between the quasi-periodic magnetic and riometer variations is observed, their local propagation patterns turn out to be different. To interpret the observations, we suggest a hypothesis of coupling between two oscillatory systems – magnetospheric Alfvén resonator and the system turbulence + electrons. The observed *Pc5* oscillations are supposed to be a result of the MHD waveguide excitation at the dawn and dusk flanks of the magnetosphere. The magnetospheric MHD waveguide turns out to be in a meta-stable state under high solar wind velocities. On November 21, 2003 a comparison of electron fluxes at *LANL* and ground ULF observations shows that the magnetospheric waveguide is excited by particle injection into the morning side of the magnetosphere.

## Generalization of the linear theory of absolute instability of whistler-mode waves in the Earth's magnetosphere

A. A. Bespalov,<sup>1</sup> A. G. Demekhov<sup>2</sup>

<sup>1</sup>*N. I. Lobachevsky State University of Nizhny Novgorod, Nizhny Novgorod, Russia*

<sup>2</sup>*Institute of Applied Physics, Nizhny Novgorod, Russia*

We perform a detailed analytical study of the linear stage of the backward-wave oscillator (BWO) regime in a whistler-mode cyclotron maser in both homogeneous and inhomogeneous magnetic field. We obtain analytical expressions for the growth rate of absolute instability of whistler-mode waves in the case where the unperturbed distribution function has a step-like deformation in parallel velocities. This case corresponds to the favorable conditions for the generation of VLF chorus emissions in the Earth's magnetosphere. The obtained expressions cover the ranges of both small and large excess over the instability threshold, and they agree with numerical results. Along with pure theoretical value, this result is important due to the fact that, according to the BWO model for VLF chorus emissions, it is the linear growth rate which determines characteristic wave amplitude at saturation and the frequency drift rate in individual chorus elements.

## Nonlinear dynamics of a magnetospheric VLF backward-wave oscillator: Possible influence of bounce oscillations of energetic electrons

A.G. Demekhov (*Institute of Applied Physics, Nizhny Novgorod, Russia*)

We present some results of numerical simulations within the framework of a simplified nonlinear model of the backward-wave oscillator (BWO) regime in a whistler-mode magnetospheric cyclotron maser. In particular, we study the possible influence of bounce motion of energetic electrons in a geomagnetic trap on the nonlinear stage of generation of VLF chorus emissions in the Earth's magnetosphere. If the particles coming back to the generation region due to their bounce motion preserve the phase bunching they acquired during the previous pass through this region, then falling tones can be generated in the system. The obtained result can be explained by the fact that in the presence of an initial phase bunching, the interaction is more intense in the region where the particles move towards the decreasing geomagnetic field and, hence, are adiabatically accelerated along their motion. This increase in the parallel velocity corresponds to a decrease in the cyclotron-resonance frequency and thus a lower frequency is generated at a later stage of interaction. These results allow us to assume that the generation of chorus elements with falling frequency can take place if the the amplitude of bounce oscillations of the electrons generating chorus is close to the characteristic length of the generation region.

## Self-consistent model for cyclotron acceleration of radiation belt electrons by noise-like whistler-mode wave emissions

A.G. Demekhov<sup>1</sup>, A.V. Bashinov<sup>2</sup>, and V.Yu. Trakhtengerts<sup>1†</sup>

<sup>1</sup>*Institute of Applied Physics, Nizhny Novgorod, Russia*

<sup>2</sup>*N. I. Lobachevsky State University of Nizhny Novgorod, Nizhny Novgorod, Russia*

<sup>†</sup>*deceased*

We develop a self-consistent analytical model for the acceleration of relativistic electrons in the Earth's magnetosphere by noise-like VLF emissions generated due to the cyclotron instability of whistler-mode waves. Within the framework of this approach, both the intensity of generated waves and the accelerated-electron flux are determined by the power of particle source (injection) in the weakly-relativistic range of energies (10-100 keV). The wave generation is described in the low-frequency approximation which allows one to neglect the energy diffusion. We obtain an analytical solution for the stationary spectrum of accelerated electrons in the case of their almost isotropic velocity distribution. This solution yields the relationship between the rate of injection of weakly relativistic electrons, generating the waves, into the geomagnetic trap and the accelerated-electron flux. We demonstrate that such an acceleration regime is most efficient at sufficiently large L shells.

## Peculiarities of sudden commencement manifestation in geophysical phenomena on subauroral and auroral latitudes

A.V. Moiseyev, V.A. Mullayarov, S.N. Samsonov, S.I. Solov'yev (*Yu.G. Shafer Institute of cosmophysical research and aeronomy SB RAS, Yakutsk, Russia*)

Features of the connection of parameters variations of geomagnetic field, of VLF emission, and precipitation of energetic particles (absorption of space radionoise) during periods of magnetic storm sudden commencements (SC) for 2001-2002 are considered.

VLF emission on the st. Yakutsk  $L \sim 3$ , geomagnetic field and riometric absorption measurements in Yakut meridional chain of stations ( $\sim 190$  magnetic meridian) were conducted, but most of riometric observations made at the Tiksi station  $L \sim 6$ . It was found that at the subauroral latitudes the SC events were accompanied by variations in the VLF emission (SCvlf) in 38% of events, and riometric absorption (SCrp) - in 22% of events. Simultaneous events SCvlf and SCrp in 40% of all the SCs were registered.

An analysis of the solar wind and the IMF parameters variations during the time the relevant points before SC, showed that when the events appeared only in SCvlf, they occur at higher initial density and velocity of solar wind particles.

The study of MLT SCvlf and SCrp events occurrence showed that the majority of the events recorded in the evening-night sector. However, some of the events, occurring only in the VLF emission recorded in the 6-13 MLT sector, in which the simultaneous events and events manifested only in riometric absorption are not available.

Considered peculiarities of the effects of SC in the VLF emission and riometric absorption, showed some differences between the characteristics of energy spectra of particles responsible for these phenomena at subauroral latitudes.

The work was supported by RFBR grant № 09-05-98546 and partially by the SB RAS project № 69.

## Spectrum of VLF signals from lightning in far-field region

A.A. Ostapenko<sup>1</sup>, E.E. Titova<sup>1</sup>, T. Turunen<sup>2</sup>, J. Manninen<sup>2</sup>, T. Rajta<sup>2</sup>

<sup>1</sup>*Polar Geophysical Institute, Apatity, Russia*

<sup>2</sup>*Sodankyla Geophysical Observatory, Sodankyla, Finland*

Analysis of VLF signals from lightnings (atmospherics) in far-field region was performed using ground-based observations in Northern Finland at the frequency range of 0-10 kHz. Using a wave equation the characteristics of resonance waves of the Earth – ionosphere waveguide were computed to interpret an observed narrow-band maximum of the amplitude in the vicinity of the first critical frequency ( $f \sim 1.6\text{-}2.2$  kHz). The dynamic spectrum and the values of wave fields in far-field zone at different distances from a source were calculated. Interference of wave modes propagating in a waveguide with different phase speeds was computed, and the results correspond with the experimental observations. The interference of modes can be used for estimating the distances to sources of the VLF signals.

## Mechanisms of the cusp-related Pc3-4 waves

V. Pilipenko<sup>1,2</sup>, O. Chugunova<sup>1,2</sup>, M. Engebretson<sup>3</sup>, T. Yeoman<sup>4</sup>, and M. Vellante<sup>5</sup>

<sup>1</sup>*Institute of the Physics of the Earth, Moscow*

<sup>2</sup>*Space Research Institute, Moscow*

<sup>3</sup>*Augsburg College, Minneapolis, MN*

<sup>4</sup>*University of Leicester, Leicester, UK*

<sup>5</sup>*l'Aquila University, Italy*

Pc3-4 pulsations were found to be an ubiquitous element of dayside ULF wave activity both at low-latitude and in the cusp region. We compare simultaneous observations of Pc3-4 wave activity by search coil magnetometers at three locations on Svalbard, covering geomagnetic latitudes  $74^\circ\text{-}76^\circ$ , and by the low-latitude SEGMA magnetometer array ( $36^\circ\text{-}43^\circ$ ). The ULF meridional spatial structure is examined using the amplitude-phase gradient technique. The cross-spectrum between low-latitude stations shows a typical pattern – maximal phase delay at specific resonance frequency, which confirms that the ground ULF response at low latitudes is formed due to the conversion

## **Waves, wave-particle interaction**

of external band-limited disturbances into standing field line oscillations. At the same time, the gradient analysis shows no specific mode conversion pattern near the cusp region. The amplitude gradient mainly has the same direction at all frequencies, and only during periods when the cusp is shifted to very high latitudes, the gradient may change sign. The phase delay is chaotic and does not show any consistent pattern. This behavior corresponds to the occurrence of a localized peak in the latitudinal distribution of Pc3-4 power not under the cusp proper as was previously thought, but about several degrees southward from the equatorward cusp boundary. We suggest the occurrence of different simultaneously operating mechanisms of propagation of upstream wave energy to the ground. The estimate show that compressional Pc3 fluctuations leaking from the magnetosheath into the entry layer of the magnetosphere can modulate the precipitating electron fluxes, which produce the ground response. This study is supported by INTAS grant 05-1000008-7978.

## **Solar wind dynamic pressure pulses, subauroral proton flashes, and Pc1 bursts**

T.A. Popova<sup>1</sup>, A.G. Yahnin<sup>1</sup>, and H.U. Frey<sup>2</sup>

<sup>1</sup>*Polar Geophysical Institute, Apatity, Russia*

<sup>2</sup>*Space Sciences Laboratory, University of California, Berkeley, California, USA.*

Among lots of isolated, sharp increases of the solar wind dynamic pressure registered in 2001-2005, those occurring during proton aurora observations from IMAGE spacecraft were selected for this study (61 events). The plasma pressure pulses were divided into two groups: 1 – those correlated with a sharp increase of the interplanetary magnetic field (38 events), and 2 – those accompanied by a sharp decrease of the magnetic field value (23 events). In agreement with some previous observations, many, but not all solar wind pressure increases were associated with subauroral proton aurora flashes on the dayside (42 events). Most proton flashes (34, that is, 81%) were associated with plasma pressure pulses of group 1, and only 8 (that is, 19%) with pressure pulses of group 2. Correspondingly, most events without proton flashes were connected to pressure pulses associated with a magnetic field decrease. In addition, ground observations of geomagnetic pulsations in the Pc1 range in Lovozero (Kola Peninsula) were considered. When the ground station was conjugated with a proton flash (20 events), a specific type of Pc1 pulsations, called hydromagnetic emission bursts or Pc1 bursts, were always observed. During 22 other flashes the ground station was far away (more than 2 hours of MLT) from the subauroral proton aurora region. In such cases the Pc1 bursts were registered only in two events. In 18 of 20 remaining events either irregular (PiB/PiC-like) noise was observed or pulsations were absent. In two cases an intensification of regular Pc1 was noted during the proton flashes. Only one of 19 plasma pressure increases without subauroral proton flashes was associated with Pc1 bursts; others were not.

The good correlation of proton aurora flashes and Pc1 bursts agrees with the suggestion that both phenomena are consequences of the ion-cyclotron instability developing in the near-Earth equatorial dayside magnetosphere during magnetosphere compression. In turn, the compression is more pronounced for those solar wind pressure pulses, which relate to a simultaneous increase of the interplanetary magnetic field.

## **Connection between geomagnetic Pc4 – 5 and auroral pulsations in Barentsburg observatory**

V.C. Roldugin and A.V. Roldugin (*Polar Geophysical Institute, KSC RAS, Apatity*)

Several occurrences of regular geomagnetic pulsations Pc4-5 and about 10 minutes, observed at Spitzbergen and Bjornaja in December 2007 – January 2008, are compared with photometric data in Barentsburg. Auroral pulsations have a place in all cases. The sign of polarization of geomagnetic pulsation components in an auroral peak has been studied subject to aurora location relatively a magnetic observatory.

## Parameters of auroral Pc5/Pi3 pulsations and geostationary electron flux at relativistic and keV energies

N.V. Yagova<sup>1</sup>, V.A. Pilipenko<sup>1,2</sup>

<sup>1</sup>*Institute of the Physics of the Earth, Moscow*

<sup>2</sup>*Space Research Institute, Moscow*

A correlation exists between spectral power  $S$  of long period auroral ULF geomagnetic pulsations (Pc5/Pi3) and electron flux  $J_e$  in the radiation belt. The  $J_e - S$  correlations for short-time irregular variations is positive at zero timeshifts for energies below 300 keV, while for relativistic energies positive correlation exists only at timeshifts more than one day. In the present paper the details of temporal behavior and spatial distribution of  $J_e - S$  correlation are analyzed. It is found that maximal correlation exists not at conjugated position, but for observatories shifted at about  $\pi/2$  from it. The absolute values and timeshifts of maximal correlation depend also on ULF spectral and polarization content and spatial scale.

## Statistical study of properties of Intervals of Pulsations of Diminishing Periods (IPDP) and their relation to subauroral proton arcs

T.A. Yahnina<sup>1</sup>, A.G. Yahnin<sup>1</sup>, H.U. Frey<sup>2</sup>, J. Manninen<sup>3</sup>

<sup>1</sup>*Polar Geophysical Institute, Apatity, Russia*

<sup>2</sup>*Space Sciences Laboratory, University of California, Berkeley, USA*

<sup>3</sup>*Sodankyla Geophysical Laboratory, Sodankyla, Finland*

We performed a statistical analysis of IPDP properties on the basis of data from three stations (IVA, OUL, NUR) of the Finnish meridional chain of induction coil magnetometers for the two-year period 2004-2005. Latitudes of these ground stations are 65.1, 61.7, 56.9 CGLat, respectively. In all, 153 IPDP events were selected that occurred between 12 and 23 MLT. As well known, the end frequency observed in IPDP depends on the latitude of observation: the lower the latitude of a ground station the higher frequency is observed. This agrees with a general view on IPDP as a kind of ion-cyclotron waves generated in the near-Earth equatorial magnetosphere. The end frequency in IPDP tends to increase with MLT at any station. Also, there exists a tendency to observe IPDP at later MLTs at lower latitude stations. This suggests the IPDP source is situated in the day-to-late evening sector of the magnetosphere and elongated from a larger distance from the Earth at its dayside end to a smaller distance in the evening. Comparison with proton aurora observations from the IMAGE spacecraft (35 events) confirms this suggestion. We found that IPDP are associated with the appearance of subauroral proton arc-like structures. These "arcs" are observed in the evening sector equatorward of the proton oval. Typically, the dayside (westward) end of the "arc" collocates with the equatorial edge of the proton auroral oval while the nightside (eastward) end is detached from the oval. It is known that such arcs are mapped onto the equatorial plane to the plasmaspheric plume, which geometry is similar to that of the IPDP source deduced from the above-mentioned morphological properties of IPDP. In addition, we noted a close correlation of IPDP and the appearance of the proton arcs with substorm-like proton injections. We conclude that both IPDP and associated proton arcs are the result of the ion-cyclotron instability developing when the proton cloud injected on the night side contacts the cold plasma of the plasmaspheric plume.

## Распределение по небесной сфере интенсивности синхротронного радиоизлучения релятивистских электронов, захваченных в дипольном магнитном поле Земли

В.В. Клименко (*Институт прикладной физики РАН, г. Нижний Новгород*)

Эта работа дополняет ряд публикаций, содержащих вычисления характеристик синхротронного излучения электронов в дипольных магнитных полях, в частности в радиационных поясах Земли. Здесь выполнены расчеты интенсивности синхротронного радиоизлучения радиационного пояса, сформированного электронами с релятивистской максвелловской функцией распределения по энергиям, питч-угловым распределением  $\sim \sin^n \alpha$  и с гауссовским пространственным распределением в экваториальной плоскости  $N_e \sim \exp[-(L-L_{max})^2/\Delta L^2]$ ,  $L$  – параметр Мак-Илвайна. Получены двумерные распределения радиояркости в координатах азимут-зенитный угол для наблюдателя, расположенного на поверхности Земли. Детектирование синхротронного излучения с помощью наиболее распространенного типа приемников –

риометров 30-40 МГц, практически осуществимо, если потоки релятивистских электронов ( $\sim 1$  МэВ) в вершине силовой трубы превышают  $\sim 10^7$  см $^{-2}$ с $^{-1}$ .

Помимо достоверного случая регистрации синхротронного излучения от искусственного радиационного пояса во время ядерного эксперимента в магнитосфере в 1962 г. [Операция «Морская звезда». Сборник статей. Под ред. И.А. Жулина. М.: Атомиздат, 1964.] известен еще ряд очевидных наблюдений интенсивного радиоизлучения из возмущенной магнитосферы (ионосферы) на частотах от 30 до 225 МГц, которые с большой вероятностью являются результатом синхротронного излучения в моменты усиления потоков релятивистских электронов выше  $\sim 10^7$  см $^{-2}$ с $^{-1}$ .

### **Закономерности магнитосферного отклика на большие и резкие скачки потока солнечного ветра в геомагнитных пульсациях частотного диапазона 0.2 - 5 Гц**

В.А. Пархомов <sup>1</sup>., Г.Н. Застенкер <sup>2</sup>, М.О. Рязанцева <sup>2,4</sup> , Б. Цэгмэд <sup>3,6</sup> , Т.А. Попова<sup>5</sup>

<sup>1</sup>*Байкальский государственный университет, Иркутск*

<sup>2</sup>*Институт космических исследований РАН, Москва.*

<sup>3</sup>*Институт солнечно-земной физики СО РАН, Иркутск*

<sup>4</sup>*НИИЯФ МГУ имени Д.В. Скobel'цина .*

<sup>5</sup>*Полярный геофизический институт КФ РАН.*

<sup>6</sup>*Центр исследований по геофизике и астрономии АН Монголии*

На основе наблюдений вариаций потока солнечного ветра на спутнике Интербол-1 и геомагнитных пульсаций на двух среднеширотных и одной авроральной обсерваториях представлены результаты исследования магнитосферного отклика на большие скачки потока (давления) солнечного ветра ( $\sim 4 \times 10^8$  см $^{-2}$ с $^{-1}$ , при длительности скачка не более 60 секунд).

Показано, что такие возрастания потока ионов солнечного ветра как при неизменной скорости, так и для случаев прихода к Земле межпланетных ударных волн, при различном направлении вертикальной компоненты межпланетного магнитного поля, могут вызвать магнитосферный отклик в виде усиений токовых систем – кольцевого тока (положительное возрастание SYM H), западной и восточной электроструй (возрастание AU и AL), сопровождаемых тремя видами режимов возбуждения геомагнитных пульсаций:

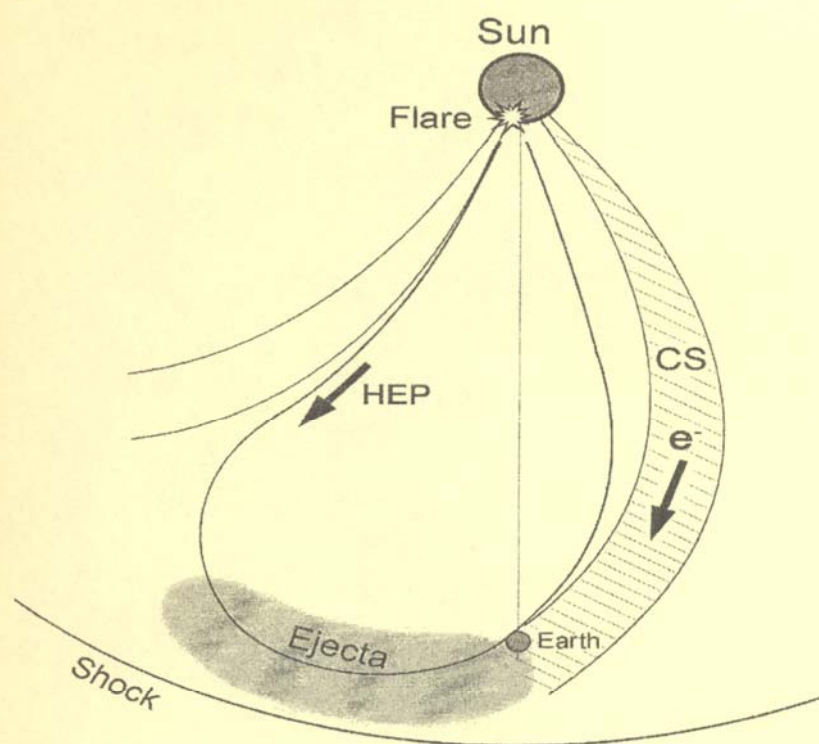
1) генерацией кратковременного всплеска широкополосных пульсаций типа Pi, имеющих шумоподобный спектр;

2) генерацией кратковременных колебаний с изменяющейся частотой PCF в диапазоне 0.2 – 5 Гц с девиацией частоты около 0.4 Гц/мин.;

3) отсутствием пульсаций в частотном диапазоне 0.2 – 5 Гц при наличии низкочастотных пульсаций типа Psc 3 - 5.

Первый и второй виды пульсаций наблюдаются только для 20% событий со скачками потока, а все остальные такие события относятся к третьему типу. Однако почти для всех случаев прихода межпланетных ударных волн наблюдается возбуждение геомагнитных пульсаций первого или второго типа. Отмечено существенное влияние направления межпланетного магнитного поля на возбуждение пульсаций разных типов. Обсуждаются возможные механизмы наблюдаемых закономерностей.

*The Sun, Solar Wind, Cosmic Ray*





## **Real-time forecast of radiation-hazardous fluxes of solar cosmic rays on the data of the neutron monitor network**

Yu.V. Balabin, E.V. Vashenyuk, B.B. Gvozdevsky (*Polar Geophysical Institute, Apatity, Russia*)

The worldwide network of neutron monitors remains till now by a sole reliable data source about relativistic solar protons (RSP), registered during Ground Level Enhancement (GLE) events.

The parameters of RSP are obtained by methods of optimization (least square procedure) from the neutron monitor network data. No less than 25-35 stations are required for such analysis. The detailed computations of asymptotic viewing cones of the neutron monitors in modern models of a geomagnetic field are required also. And a huge bulk of accounts takes the solving of a least square problem of definition of the solar proton parameters from the neutron monitors data. In a task of early operative definition of radiation-hazardous fluxes of solar cosmic rays the basic goal is the estimation and forecast of solar proton spectrum in the energy range of tens and hundreds MeV. This is at the lower edge of a spectrum of solar protons determined on the data of neutron monitors. It is clear that applying of the above mentioned technique for the purposes of the operative forecast of radiation hazard is inexpedient because of required large number of stations, and also large bulk of calculations. We developed the short cut technique of definition of a spectrum of solar protons on the data of the limited number of neutron monitor stations (less than 20) and with the simplified procedure of accounts adapted for the purposes of the operative forecast. The results of computations of spectra of solar protons with the short-cut technique practically do not differ from spectra obtained with a complete technique at energies less than 5 GeV. Thus the good agreement between derived from the neutron monitor data intensities of solar protons in an energy range of hundreds MeV with the data of direct measurements of solar protons at GOES-series spacecarts and balloons is observed. The maximum of increase on neutron monitors outstrips on several hours (5-10) an appropriate maximum of radiation-dangerous fluxes, registered by spacecarts of GOES-series. Thus, the technique of the early forecast of radiation hazardous fluxes of solar cosmic rays in space on the basis of the neutron monitors data obtained in real time by the neutron monitors network is created.

## **Numerical simulation of solar cosmic ray acceleration during a flare**

Yu.V. Balabin<sup>1</sup>, I.M. Podgorny<sup>2</sup>, A.I. Podgorny<sup>3</sup>, and E.V. Vashenyuk<sup>1</sup>

<sup>1</sup>*Polar Geophysical Institute RAS, Apatity, Russia*

<sup>2</sup>*Institute for Astronomy RAS, Moscow, Russia*

<sup>3</sup>*Lebedev Physical Institute RAS, Moscow, Russia*

The set of neutron monitors measurements reveals two components of relativistic protons that accompany a flare. The prompt component of relativistic protons is created simultaneously with flare hard X-ray radiation. It possesses information about the mechanism of particle acceleration in a flare up to  $\sim 10$  GeV. Prompt component shows the exponential spectrum with  $W_0$  order of 0.5 GeV. The possibility of particle acceleration in a current sheet has been considered in the frame of the electrodynamical solar flare model. Particles can get energy during acceleration in the Lorenz electric field along a singular line. The similar mechanism of acceleration has been observed in the powerful pinch discharge. In previous simulation work it has been shown that exponential spectrum appears, if the electric field is applied along a magnetic symmetrical X-type singular line. Such simulation can be considered as a first step for reality, because the real field distribution is more complicated. Now numerical simulations have been carried out for the real magnetic and electric configurations calculated in MHD numerical experiments for the famous Bastille flare. The result of simulation shows that the spectrum of accelerated protons during a flare indeed is the exponential one. The rate of reconnection for  $W_0 \sim 0.5$  GeV is order of  $10^7$  cm/s.

## **Variations of aurora emissions during substorms connected with different solar wind streams**

I.V. Despirak<sup>1</sup>, Zh. V. Dashkevich<sup>1</sup>, V. Guineva<sup>2</sup>

<sup>1</sup>*Polar Geophysical Institute, Apatity, Russia*

<sup>2</sup>*Solar-Terrestrial Influences Laboratory, Stara Zagora, Bulgaria*

Spitsbergen photometer data from the 2005/2008 winter seasons have been used to study the variation of auroral 5577 Å and 6300 Å intensity ratio in different conditions of interplanetary medium and various geomagnetic activity. Solar wind and interplanetary magnetic field parameters were taken from CDAWeb

## **The Sun, solar wind, cosmic rays**

([http://cdaweb.gsfc.nasa.gov/cdaweb/istp\\_public/](http://cdaweb.gsfc.nasa.gov/cdaweb/istp_public/)). Using WIND satellite data for the examined periods, the different solar wind streams were revealed: recurrent streams from coronal magnetic holes and magnetic clouds connected with non-stationary processes at the Sun. Substorm onset time and further development were verified by ground-based data of IMAGE magnetometers network and by data of all-sky camera at Spitsbergen. The auroral 5577 Å and 6300 Å intensity ratio behaviour is shown and discussed. The particularities in behaviours of the emission intensities and the 6300/5577 ratio during substorms observed by solar wind recurrent streams and by magnetic clouds are discussed. These estimations were obtained for storm and nonstorm substorms as well.

## **Monitoring of various kinds of cosmic radiation for environmental studies**

A.V. Germanenko, Yu.V. Balabin, E.V. Vashenyuk, B.B. Gvozdevsky, L.I. Schur (*Polar Geophysical Institute, Apatity, Russia*)

In 2008 the monitoring of a gamma-radiation and low energy neutrons at cosmic ray station in Apatity is begun. These kinds of radiations can have the important value for environmental studies. The registration of gamma-radiation is made with the help of a NaJ crystal: 6.3x2 cm and a photo multiplier with two energy thresholds: > 20 and > 100 KeV. The background of low-energy neutrons is measured by a lead free section of a neutron monitor: 4 neutron sensitive counter tubes SNM-15 filled with  $\text{BF}_3$  gas enriched with  $\text{B}^{10}$  isotope. Tubes are surrounded by cylindrical layer (2.5 cm) of polyethylene moderator and are capable detecting atmospheric neutrons of thermal and quasi thermal energies. The standard neutron monitor with tubes covered with the 5 cm of lead has the lower energy limit > 50 MeV for detecting of neutrons.

At registration of gamma-radiation the sporadic increases of count rates correlating with atmospheric precipitations are found out. As the reason of these increases can be bremsstrahlung from particles accelerated in an electric field between clouds and the ground. The probable connection with atmospheric radio nuclides is considered also. The basic source of neutrons registered by the lead free section are the moderated neutrons of secondary cosmic radiation. It is specified by the high correlation between the data of lead free section and the standard neutron monitor. At the same time, in a count rate of lead free section the appreciable contribution is given by particles of a radioactive background of the terrestrial core. It specifies peak in a frequency spectrum with the period of the Moon. Radioactive emanation of the terrestrial core as is known are related with a tidal wave, caused by the Moon.

## **Solar wind dynamic pressure jumps characteristics and their magnetospheric effects**

N.A. Glotova, M.A. Shukhtina (*St. Petersburg State University, St. Petersburg, Russia*)

To study the solar wind - magnetosphere interaction it is necessary to determine the time, when the structures, registered at a distance of 100-200 Re from Earth, come to the Earth bow shock(BS). Until recently, the solar wind parameters were usually transferred by convection time  $dt = dx / V_{sw}$ , implying the front of the structures moving with the solar wind and perpendicular to the Sun-Earth line. However the discontinuity normals, as well as the normals to the solar wind phase fronts, are often tilted to the Sun-Earth line, which is taken into account in the recently created OMNI data base (<http://omniweb.gsfc.nasa.gov>). This base contains solar wind/IMF parameters, transferred to the Earth bow shock, and is created for smooth variations of solar wind parameters. The purpose of our work is to test the OMNI base for interplanetary discontinuities, using ground observations. We study the response time of the ground SYM-index to solar wind dynamic pressure (Pd) jumps, recorded by remote (100-200Re) spacecraft and transferred to BS according to OMNI and by convection time. We also transferred solar wind structures using methods of normal and velocity calculations for given discontinuities. 2 types of discontinuities corresponding to Pd jumps: tangential (TD), and fast shocks (FS) were considered.

Time delays between Pd jumps at the BS, (1) taken from OMNI and (2) transferred by convection on the one hand, and jumps of ground SYM- index (SIs) on the other hand, were studied separately for TDs and FSs. We also compare normals from OMNI and obtained by methods for concrete discontinuities.

62 SYM jumps, corresponding to 35 TDs and 27 FSs, were analyzed. The results are as follows: According to OMNI, TDs come to the bow shock on average 4 min before SIs on the ground. For convection translation the average delays are also 4 min, but the scatter is larger. Thus the OMNI procedure is better compared to the convection one.

For shocks OMNI gives unrealistic results: on average the Pd jumps come to the bow shock 4 min after the ground SIs. As for normals, the average angle between normals from OMNI and our normals for TDs is 13 degrees and 66 degrees for FSs.

We conclude, that the OMNI data base is good for TDs and can not be used for FSs.

When using normal and velocity calculation methods for the FSs, we obtain that the FS on average comes to the BS 5 min before Si.

Our calculations of TD and FS propagation time from the BS to the ground agree with theoretical and MHD estimates.

### **Participation of the Apatity neutron monitor in the international Neutron Monitor Data Base**

B.B. Gvozdevsky, Yu.V. Katkalov, E.V. Vashenyuk (*Polar Geophysical Institute, Apatity, Russia*)

By the end of 2008 the international Neutron Monitor Data Base (NMDB) was created in a frame of the 7-th European Framework Programme (FP7) Project. At present 20 NM stations, mostly European, submit real-time data with 1-minute resolution to the database. Apatity neutron monitor is one of the stations. We have developed a software automatically delivering our data to the database once per minute via Internet. The NMDB server is located at the Christian-Albrechts University of Kiel, Germany. It is running MySQL Server. Our software employs the Perl and SQL functionality to connect to the server and to upload the data, as well as to collect the data of other stations for using. The data of the networks of neutron monitor stations will be used for diagnostics in real time of a state of near-earth space. In particular they will allow operatively detecting a beginning of the GLEs (Ground Level Enhancements), related to solar cosmic rays and Forbush effects. To reveal these events on the data of only one station often is impossible. We also develop a technique of definition of the characteristics of primary solar cosmic rays on the data of neutron monitors which are included in the NMDB network. On the basis of our technique the operative forecast of radiation hazard in space and on the high latitude airline routes, probable effects of cosmic radiations on humans, technological systems, and the environment is possible also.

### **The magnetosphere time response to the IMF Bz turning**

I.M. Ivanova, N.P. Dmitrieva (*St. Petersburg State University, St. Petersburg 198504, Russia*)

We analyzed the time response of the polar cap electric field to the IMF Bz turning. Using the magnetic and plasma data from Wind, ACE, Geotail, Themis B and Themis C spacecraft 39 solar wind directional discontinuities (DD) were examined. 20 events with N-S Bz turning and 19 events with S-N Bz turning were selected. The multi-spacecraft method was used to estimate the propagation time of the DD fronts. The reference time for the electric field response is the moment of DD arrival to the bow shock nose. The uncertainty of the arrival time estimate does not exceed 2 min. PC-index was used as an instrument to observe the polar cap electric field variations. The average time response value  $13.6 \pm 6.4$  min for all events was obtained, this value being  $15.1 \pm 6.7$  ( $12.2 \pm 5.8$ ) min for the N-S (S-N) turning. This result confirms the conclusion of N.V. Erkaev (Planet. Space Sci., 2003, 745-755) whose analytical computation gives the magnetic barrier formation time of about 10 min. for typical solar wind parameters.

### **The short-term forecast of Solar wind magnetic cloud parameters reaching vicinity of the Earth**

E.A. Kalinina <sup>1</sup>, N.A. Barkhatov <sup>1,2</sup>, A.E. Levitin <sup>3</sup>

<sup>1</sup>*Nizhniy Novgorod State Pedagogical University, 603950 Nizhny Novgorod, Russia*

<sup>2</sup>*Pushkov Institute of Terrestrial Magnetism, Ionosphere and Propagation of Radio Waves (IZMIRAN), Russian Academy of Sciences, 142190, Troitsk, Russia*

Geomagnetic storms frequently occur as result of interaction of the magnetosphere with ejection of the solar plasma in a form of magnetic cloud. If key parameters of the magnetic cloud reaching the Earth are known, they can be used for the forecast of intensity and duration of geomagnetic storm. The method of determination of orientation of such magnetic cloud, its cross size, a magnetic field on its axis and impact parameter is presented. It allows concretization of a passage trajectory of the Earth through the cloud using measurements of the interplanetary medium parameters onboard the patrol spacecraft taking place in a libration point.

The method consists in comparison of measured components of the magnetic field vector in a cloud, with their modelled values. For this purpose the data base of the magnetic clouds parameters is created based on experimental data obtained during the real passage of the magnetosphere through the solar plasma ejections. Number of the used modelling clouds representing different possible variants of the Earth passage trajectories and allowing determination of their parameters is about one million. The developed method is tested on statistics of real events.

## ***The Sun, solar wind, cosmic rays***

On the basis of numerical experiments the estimation of quantity of initial measurements onboard the patrol satellite, needed for determination of the magnetic cloud parameters is carried out.

After determination of these characteristics the forecast of the interplanetary magnetic field Bz component, which magnetosphere should meet in a magnetic cloud, is carried out. This enables the forecast of the Dst-variation expected during interaction of the given cloud with magnetosphere. The number of needed initial measurements of interplanetary medium parameters, that is, forecast time from the moment when the patrol spacecraft enters a cloud, appears less for the magnetic clouds having a smaller inclination to the ecliptic plane.

This work is supported by RFBR grants 08-05-12051.

## **Solar wind parameters and relativistic electron flux variations (2001-2005 years) correlations studies**

I.N. Myagkova, A.V. Bogomolov (*Skobeltsyn Institute of Nuclear Physics, Moscow State University, Moscow*)

Dynamics of the relativistic electron flux in the Earth's outer radiation belt of the Earth (ERB) ( $3 < L < 5$ ) and their acceleration mechanisms have been discussed for a long time. However, there is still no clear theory of the acceleration of electrons to the relativistic energies describing all the principal features of their variations. In this work the correlation between the relativistic electrons flux measured at low orbits on board CORONAS-F satellites and solar wind parameters such as velocity and density have been studied during September 2001 – June 2005 year time period.

We have found, that the significant increasing (more than in order) of electron mean flux in the outer ERB was observed during time period from 2001 to 2003 years. The correlation of mean electron flux variations at low altitudes and at geostationary orbit with the solar wind parameters was carefully investigated.

## **Effect of substorm in the propagation of the galactic cosmic rays**

V.V. Pchelkin (*Polar Geophysical Institute RAS, Apatity, Murmansk region, Russia*)

By the method of trajectory calculations with the use of empirical model of the current wedge the influence of substorms on asymptotic directions and cut-off rigidity of the cosmic rays is investigated. It is shown that, to the first approximation, the influence of substorm in the analysis of galactic cosmic rays propagation in the magnetosphere can be neglected.

## **The method of search for possible solar flare positions in the corona**

A. I. Podgorny (*Lebedev Physical Institute RAS, Moscow, Russia*)

To find solar flare positions in the corona above an active region the search of singular magnetic lines in the potential magnetic field usually employed. It is supposed that such method can be used for solar flare prediction. But such approach does not take into account the magnetic field of several current sheets appeared in the corona before the flare. Often for calculations of the potential magnetic field the rough approximation of the active region magnetic field by magnetic charges is used, and the magnetic field between spots is not taken into account. Such an approach often meets difficulties during analysis of complicated active region configurations. Here we present the method of direct search of current sheets in the magnetic field above the active region in a preflare state. The magnetic field configuration in the corona is calculated by MHD numerical simulation with the initial and boundary conditions obtained from observed magnetic maps on the photosphere. The current density local maximum has been found in 3D space. It must correspond to the current sheet center. The current sheet plane must be perpendicular to the plane which contains the point of the current density maximum, and this plane must be perpendicular to the magnetic line passing through this point. Magnetic field lines in this plane correspond to the magnetic configuration of the current sheet. The numerical code of visualization of the field configuration in an arbitrary plane with simultaneous calculation of the current density maximum in 3D space is developed. This code permits prompt finding current sheet position for the flare prediction. Flare positions and field configurations are demonstrated for the active region AR 0365. The method permits to investigate the behavior of the magnetic field and plasma in the current sheet vicinity.

## **Solar flare model – comparison with complex space crafts observation**

I. M. Podgorny<sup>1</sup>, and A. I. Podgorny<sup>2</sup>

<sup>1</sup>*Institute for Astronomy RAS, Moscow, Russia*

<sup>2</sup>*Lebedev Physical Institute RAS, Moscow, Russia*

The solar flare model obtained from 3D MHD numerical simulation has been discussed in previous Apatity conferences. The main point of the model consists in primary energy release in the corona due to magnetic energy dissipation in a current sheet. Now a possibility appears for detail comparison of this model with simultaneous observations of a flare by several space crafts (RHESSI, Stereo A and B, and GOES). An unusual position of the active region and spacecrafts permits to obtain new information about a flare event. The M2 flare 25.11.2007 has been produced above the active region situated behind the solar limb. This active region was observed by Stereo A and Stereo B. RHESSI can measure thermal X-ray emission from the current sheet and X-ray radiation above the flare current sheet. This space craft has been shielded from powerful X-ray radiation in legs of the flare loop by the Sun body that permits to detect very weak radiation from the corona. The weak flux of hard X-ray from corona (above the thermal source) is revealed together with III-type radio emission. The electrons with energy order of 50 keV responsible for these radiations are moving along magnetic lines. They reach the Earth orbit and are observed by GOES. This hard pulse of X-ray shows a thin target spectrum. Electrons producing these radiations are accelerated in field-aligned currents generated by Alfvén wave which is excited by the Hall electric field in the current sheet. The field aligned currents are connected due to Alfvén conductivity. Another system of field aligned currents is connected in the chromosphere, where accelerated electrons produce the thick target power spectrum. Strong flux of hard X-ray radiation is measured by Stereo spacecrafts. All scenario of solar flare development is in agreement with the electrodynamical solar flare model prediction.

## **The beginning of new 24-th cycle in solar and geomagnetic activity generation**

T.E. Val'chuk (*Pushkov Institute of Terrestrial Magnetism, Ionosphere and Radio Wave Propagation RAS, Moscow reg., Troitsk, e-mail: valchuk@izmiran.ru*)

The general solar magnetic field is presented by quasi dipole structure in solar activity minimum. The heliosphere plasma layer (HPL) divides the giant solar wind flow into two regions of preferred polarity in connection with the solar hemisphere polarity. On the Earth orbit the polarity alternation is the interplanetary magnetic field (IMF) sector structure variations. Heliosphere current layer (HCL) is situated inside the HPL. Current layer is much more thin; the IMF polarity changes into opposite polarity after this layer transition. HPL and HCL are the long lived solar activity phenomena. The changing of sector structure boundaries shows the dynamics of solar activity in the equatorial belt of the Sun.

The plasma and IMF data in 2007-2008 were treated with the aim of detailed examination of HPL character in the initial phase of new solar activity grows. Only in the deep solar spot minimum the HPL has the most flattening configuration in heliosphere and near to ecliptic plane.

Solar wind plasma is the fractal medium, reflecting in fractal dimension (FD) the sector structure transitions. The control of HPL variations from one Carrington rotation (CR) to another CR helps to identify the connection between solar wind parameters and solar activity phenomena. The transition of HPL is revealed as the FD diminution (down to 1.5 in the most cases). The sharp decrease of the FD is the feature of another fractal structure in HPL region.

The geomagnetic disturbance is not valuable in the minimum of solar cycle №23. Corotating interaction regions (CIR) were the general reasons of geomagnetic disturbances in 2007-2008. Extra magnetosphere storm, similar to great geomagnetic storm 13-14.12.2006, is absent in two last years.

The last FD result is connected with the coupling two sector boundaries in the middle of Carrington rotations №2060-2064 in the end of 2007. The possible explanation may be proposed: the Wind trajectory is sink into the thickness of HCL, but the heliosphere current layer is not cut in that case. It is the situation of two-sector structure of IMF, but the typical FD diminution is repeated in these CRs on the old places of the sector boundary coupling. It is the situation of HPL flattening. In 2008 2-th sector structure transforms into 4-th sector structure.

## **Коэффициенты транспортного уравнения для ГКЛ в гелиосфере с токовым слоем конечной толщины**

М.С. Калинин, М.Б. Крайнев (*Физический институт им. П.Н. Лебедева РАН, Москва*)

На основе модели гелиосферы с токовым слоем конечной толщины, включающей все три компоненты -  $B_r, B_\theta, B_\phi$  - магнитного поля, предложенной нами ранее, вычисляются кинетические коэффициенты транспортного уравнения для ГКЛ. Усреднённые по азимутальному углу значения коэффициентов используются при численном решении двумерного по пространственным координатам уравнения модуляции ГКЛ. Анализируются пространственные характеристики интенсивности ГКЛ, чувствительные к структуре гелиосферного токового слоя конечной толщины.

## **Модель гелиосферного токового слоя конечной толщины**

М.С. Калинин, М.Б. Крайнев (*Физический институт им. П.Н. Лебедева РАН, Москва*)

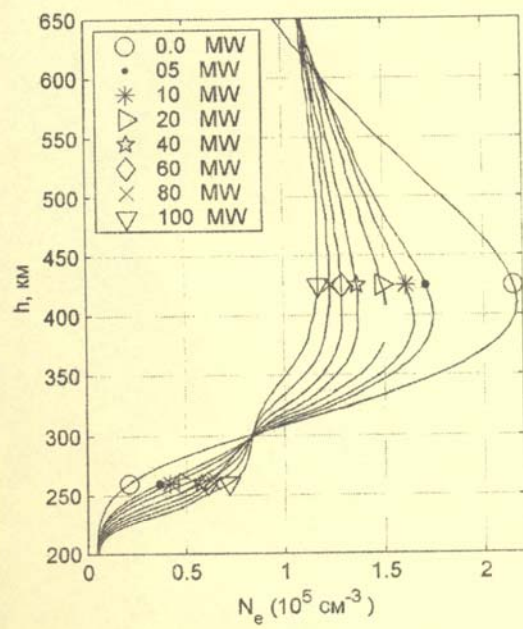
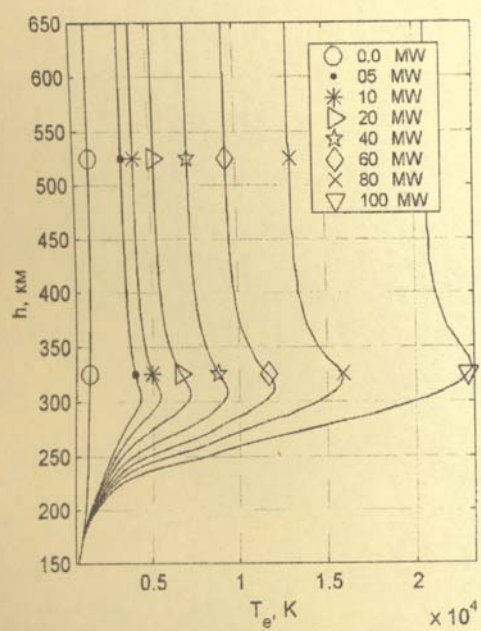
Рассмотрены два механизма образования гелиосферного токового слоя конечной толщины, имеющего все три компоненты -  $B_r, B_\theta, B_\phi$  магнитного поля. Стационарный механизм связан с наличием  $B_\theta$ -компоненты магнитного поля на поверхности источника вблизи токового слоя. Второй механизм связан с нестационарностью самого токового слоя, толщина которого определяется изменением угла его наклона к гелиоэкватору за солнечный оборот. Основные параметры модели оцениваются на основе рассчётов магнитного поля на поверхности источника в рамках потенциального приближения (модель Стенфордского университета, США). Модель может быть применена для теоретических исследований модуляции ГКЛ на основе транспортного уравнения.

## **Взаимодействие падающей гидродинамической волны с ударной волной: сравнение между аналитическим решением для идеальной среды и численными расчетами для вязкой среды**

А.А. Любич, И.В. Дэспирак (*Полярный геофизический институт КНЦ РАН, Анадырь, Россия*)

Проведено численное моделирование взаимодействия падающей гидродинамической волны с ударной волной для вязкой среды с числом Прандтля  $Pr = 3/4$ . Рассматривались случаи падения звуковой волны со стороны сжатой среды, а также прямой и обратной звуковой волны и энтропийной волны со стороны несжатой среды. На границах области моделирования, включающей ударную волну, задавались граничные условия исходя из аналитических решений соответствующей задачи в идеальной среде, описываемой уравнением Эйлера. Для сравнения использовались два типа решений, которые дают разные граничные условия. Одно из них учитывает динамический и кинематический эффекты, связанные с колебаниями поверхности ударной волны, а второе – только кинематический эффект. Эти решения по-разному описывают результат взаимодействия падающих волновых возмущений солнечного ветра с лобовой ударной волной и дают разные условия, при которых возможно спонтанное излучение волн ударной волной. В результате численного моделирования определялась амплитуда колебаний центра ударной волны. Эта величина сравнивалась со значениями, даваемыми аналитическими решениями. Было показано, что результаты численного моделирования в вязкой среде хорошо согласуются с аналитическими решениями в идеальной среде для всех рассматриваемых типов падающих волн. Согласие является одинаково хорошим для аналитических решений, полученных как при учете динамического эффекта, так и без его учета. Сделан вывод о том, что только сравнение полученных решений с экспериментальными результатами позволит определить, какой из двух типов решений является физически корректным.

## *Ionosphere and Upper Atmosphere*





## Appearance and interpretation of a Broadband Spectral Maximum (BSM) in low latitude ULF magnetic noise observations: effect of a MHD cavity in the ionospheric E-F1 valley

T. Bösinger<sup>1</sup>, A. G. Demekhov<sup>2</sup>, and C. Haldoupis<sup>3</sup>

<sup>1</sup>*Department of Physical Sciences, University of Oulu, Finland*

<sup>2</sup>*Institute of Applied Physics, 46 Ulyanov st., 603950 Nizhny Novgorod, Russia*

<sup>3</sup>*Physics Department, University of Crete, Iraklion, Greece*

We demonstrate by frequent observations and modeling that the concept of the so called broad-band spectral maximum (BSM) in the ULF magnetic noise is fully valid and applies excellently to observations made at a low latitude station. This spectral feature was introduced by Belyaev et al. (2002), and its first rigorous model based on the resonant properties of the ionospheric E/F1 region valley was suggested by Ermakova et al. (2007). In contrast to the reported mid and high latitude observations, the BSM phenomenon seems to be a regular feature detected every night on the island of Crete ( $L = 1.4$ ). It shows up in a broad band maximum in the power spectral density below the first Schumann resonance but typically above the frequency range carrying IAR signatures. The phenomenon is, however, best portrayed in the behavior of the ellipticity which reveals another signature of the phenomenon: long (several hours), quasi-periodic pulsations of the ellipticity just in the BSM frequency range indicating ongoing, large scale changes in the ionospheric E/F1 valley.

### References

P. P. Belyaev, S. V. Polyakov, E. N. Ermakova, et al. // *Izv. Vyssh. Ucheb. Zaved., Radiofiz.* 2002. V. 50, No. 2. P. 151–162 (*Radiophys. Quantum Electron.*, **45**, No. 2, 135–146, 2002).  
 E. N. Ermakova, D. S. Kotik, S. V. Polyakov, and A. V. Shchennikov // *Izv. Vyssh. Ucheb. Zaved., Radiofiz.* 2007. V. 50, No. 7. P. 607–623 (*Radiophys. Quantum Electron.*, **50**, No. 7, 555–569, 2007).

## Display of magnetogravitation waves caused by auroral electrojet dynamics in traveling ionospheric disturbances

O.M. Barkhatova<sup>1,2</sup>, N.A. Barkhatov<sup>1,2</sup>, G.I. Grigor'ev<sup>1</sup>

<sup>1</sup>*Research Radiophysical Institutes (NIRFI), 603950 Nizhny Novgorod, Russia*

<sup>2</sup>*Nizhniy Novgorod State Pedagogical University, 603950 Nizhny Novgorod, Russia*

It is known, that due to substorm activity the acoustic-gravitational disturbances of different spatial scales manifested in traveling ionospheric disturbances (TID) appear in high-latitude terrestrial atmosphere. On the other hand slow magnetohydrodynamic (MHD) disturbances can take place in ionosphere. In the density stratified atmosphere these disturbances can involve in the wave movement not only ionized component, but also neutral component. As result, so-called magnetogravitation waves (MGW) are formed which velocity appears above the acoustic-gravitational wave (AGW) velocity, but is lower than MHD wave velocity [1].

Existence of MGW caused by the activity of the eastward and westward auroral electrojets conduces to that substorm activity can be noticed in TID earlier, than one usually suggests. For detection of such MGW feature the experimental data on decametric radiowave propagation on middle-latitude and subauroral traces of inclined ionosphere sounding were used. The traces are Inskip - Rostov -Don, Cyprus - Rostov - Don, Irkutsk - Rostov - Don and Norilsk - Rostov -Don. The data were obtained in December 2006 and March, 2007 in conditions of weak geomagnetic disturbances. Maximum observed frequency (MOF) was considered for local day time intervals. This allows to exclude TID connected to passing the terminator passage and to study the effect of substorm activity.

The analysis of linear correlations of MOF for each of inclined sounding traces with AU, AL index values describing intensity of eastward (AU) and westward (AL) electrojets was performed for different time shifts of MOF relatively to the indices. As result, the time shifts between AU, AL and MOF corresponding to the highest correlation were established. These time shifts should correspond to the time needed for transportation of gravitational indignations from auroral zone to points of radiowave reflection. Among the values of the time shifts the times 5-10 minutes were noted representing increased propagation velocity of disturbances in comparison with typical AGW velocity for considered traces. Such cases can be connected to the MGW propagation.

Spectra of disturbances in AU, AL indices and in MOF for cases of their enhanced correlation show coordination of the spectral features. The analysis of MOF spectra calculated along a line of probable propagation of gravitational waves towards equator suggests a weakening of the high-frequency part of spectra at lower latitudes. This can be a

## ***Ionosphere and upper atmosphere***

consequence of the greater attenuation on long-distant traces of middle-scale gravitational waves in comparison with large-scale waves. Also, this can be a possible consequence of interaction AGW with a geomagnetic field with MGW formation.

The performed numerical modelling of the transportation of MHD disturbances demonstrates an opportunity of their generation by electrojet perturbations and their influence on TID observed on the inclined radiosounding traces.

This work is supported by RFBR grants 08-05-12051.

## **References**

1. Sorokin V.M., Fedorovich G.V. Physics of slow MHD-waves in ionosphere plasma. Energoizdat, M. 1982, p.136 (in Russian)

## **VLF characteristics of magnetic cutoff in the cases of ultra relativistic electron precipitations**

M.I. Beloglazov (*Polar Geophysical Institute, Apatity*),  
G.F. Remenets (*Physics Department of St.-Petersburg State University*)

Continuous, synchronous, many year (1982-1986), on ground registration of VLF signals for short (Aldra-Apatity,  $S_1=885$  km,  $f_i = 10.2; 12.1; 13.6$  kHz,  $i = 2, 2, 3$ ) and long (Ragby-Apatity,  $S_2=2400$  km,  $f_4=16$  kHz) radio traces has revealed new geophysical phenomena. The essence of it in the ultra relativistic ( $E_e \sim 100$  MeV) electron precipitation into middle polar atmosphere with the synchronous generation of X-rays of such intensity that they are capable to produce a sporadic D-region middle atmosphere (10 – 40 km) ionization. The effective altitude of such layer of electric conductivity may achieve a value of 30 km. The time scale of the event is equal to 5 min – several hours, the space scale is equal to one thousand – several thousand km. A crucial item in the proof of electron nature of the events is the existence of the magnetic cutoff in the VLF disturbances. The purpose of the report is to represent the quantity VLF characteristics of all anomalous disturbances, which were registered in Apatity in 1982 – 1986 years.

All the anomalous disturbances were divided at 4 classes according to the intensity (to the depth) of compensation between the ground diffraction wave and the first ionosphere ray. These disturbances were named as powerful (Pw), strong (St), moderate (Md) and weak.

For 5 years there were only 4 daytime Pw disturbances (PwDs), which we represent below, indicating the calendar dates, the UT times of beginning ( $T_b$ ), of the disturbance maximum ( $T_m$ ) and of the disturbance end ( $T_e$ ), the amplitude ratios  $\eta_i = (A_i(T_m) / A_i(T_b))$  and the phase decreasings  $\Delta_i = (\varphi_i(T_b) - \varphi_i(T_m))$  for 4 frequencies in mcs with error  $\delta= \pm 5$  mcs. The data for the forth frequency  $f_4$  and the long radio trace with  $S_2$  are distinguished by solid print. The amplitude data were gotten by the help of apparatus, the effective radio band of which was equal to 20 Hz.

22 April 1984 г. 3.20 4.05 7.00	25 March 1986 г. 9.00-11.10-13.20	27 March 1986 г. 12.35-13.10-19.00	23 April 1986 г. 18.30-19.15- 20.00
$0,10 \pm 0,03$ 13,6 мкс	$0,09 \pm 0,04$ 8,5 мкс	$0,09 \pm 0,04$ 19,0 мкс	$0,08 \pm 0,04$ 15,5 мкс
$0,25 \pm 0,03$ 13 мкс	$0,12 \pm 0,03$ 10,5 мкс	$0,18 \pm 0,05$ 10,5 мкс	$0,10 \pm 0,05$ 13 мкс
$0,27 \pm 0,06$ 11 мкс	$0,06 \pm 0,07$ 10,5 мкс	0,0 9,5 мкс	0,0 15,5 мкс
<b><math>0,12 \pm 0,07</math> 11 мкс</b>	<b><math>0,07 \pm 0,03</math> 18,5 мкс</b>	<b><math>0,36 \pm 0,07</math> 9,0 мкс</b>	<b><math>0,27 \pm 0,05</math> 6 мкс</b>

In these cases, just as in all other cases of PwDs, StDs, MdDs, the anomalous VLF disturbances at short radio trace were accompanied by the signal attenuation and signal phase decreasing for the long radio trace. At the same time the maximum phase decreasing never prevailed upon the maximum phase decreasing for short radio trace. That may mean only one experimental fact. That the long radio trace, which is 3 times longer than the short one, is only **partly** disturbed in all cases and that this disturbed part in its length is comparable with the length of the short radio trace. So we have the effect of the magnetic cutoff relative to the charged particle precipitations.

So the experimental data for 111 events for 5 years represented in this report are a solid proof of magnetic cutoff existence in the cases of abnormal VLF disturbances. This fact we declared earlier [1-3] but publicize the corresponding full volume of experimental data at first. Once more we attract attention of a reader to the fact [1-3] that an amount of the abnormal events per year increased monotonously and significantly from 1982 till 1984 (23, 30, 43 events accordingly) before getting its minimum value in the 1985 y (5 events) of Solar activity minimum and getting value 10 in 1986 y.

1. Remenets G. F., Beloglazov M. Iv. Ground VLF monitoring of the ultra relativistic electron precipitations. In: Problems of Geospace 2. - Austria, Vienna: Austrian Academy of Sci. Press, 1999. P. 275-281.
2. Ременец Г.Ф. Исследование ионизации средней атмосферы высоких широт высокоэнергичными релятивистскими и ультрарелятивистскими электронами по СДВ экспериментальным данным // Вестник СПбГУ. Серия 4. 2001. Вып. 3 (No. 20). С. 23-38.
3. Beloglazov M. I., Remenets G. F. Investigation of powerful VLF disturbances // Intern. J. Geom. Aeronom., 2005. Vol. 5. No. 3. April issue.

### About solving ability of the self-consistent method relative to the VLF inverse problem in nonstationary conditions

M. I. Beloglazov (*Polar Geophysical Institute, Apatity*)

M. V. Kukovyakin, G. F. Remenets (*Physics Department of St.-Petersburg State University*)

The results of numerical analysis of an abnormal electric conductivity disturbance of middle auroral atmosphere caused by ultrarelativistic electron precipitation are introduced. The analysis was fulfilled on the basis of PGI RAS experimental data for radio trace Aldra - Apatity (885 km) on 30 April 1992 (13.00 – 13.30 UT) (Fig. 1). These experimental data are the amplitude and phase changes in time of the radio signals with frequencies  $f_i = 10.2, 12.1$  and  $13.6$  kHz (VLF radio band,  $i = 1, 2, 3$ ). In our previous publications the reflection coefficient module of the first ionosphere ray  $R$  and the effective altitude  $h$  of an electric conductivity layer as functions of time were determined. Here a question about possibility to introduce a third parameter is considered. In this work we considered the frequency dispersion of  $h$ .

For this purpose three VLF inverse problems were solved. For each of them own definition of an effective altitude  $h_i$  was used. Each definition was strictly related to frequency  $f_i$ . In order to answer the above question the self-consistent method of VLF inverse problem solving was used. The method suggests the plenty of data. Due to this, minimization of a functional, which contains the differences between the experimental and calculated values, relative to the values of time functions  $R(t)$  and  $h(t)$  at a fixed moment  $t'$ , was possible. For every of three inverse problems it solved twice: in positive and negative directions of time, i. e. for  $t' = t_0$  and  $t' = t_m$ , respectively. Here  $t_0$  and  $t_m$  are the initial and final time moments for the given disturbance. In the first inverse problem the  $f_1$  и  $f_2$  experimental data were used, in the third inverse problem -  $f_2$  and  $f_3$  were used, and in the second problem the experimental data for all three frequencies were used.

Thus, due to the relative changes of signal amplitudes and variations of signal phases the absolute values of reflection coefficient module for the first ionosphere ray  $R$  and of the effective altitude  $h$  of the electric conductivity layer as functions of time were determined.

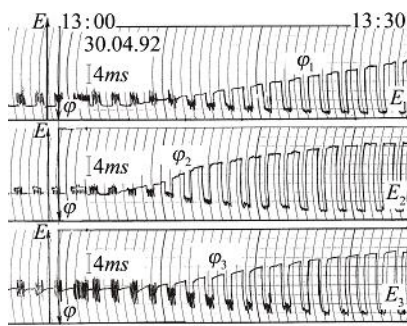


**Fig. 1.** Experimental input data during the ultrarelativistic electron precipitation into polar atmosphere on 30 April 1992

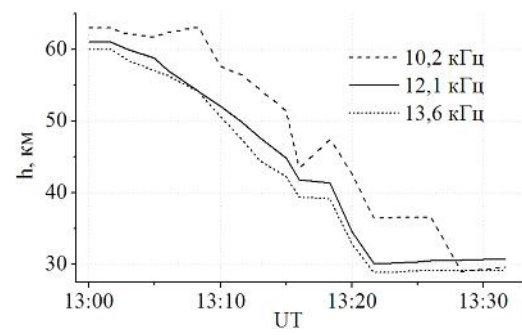


**Fig. 2.** Frequency dispersion (at the radio band 10 – 14 kHz) of the effective altitude, depending on time, during the ultrarelativistic electron precipitation into polar atmosphere on 30 April 1992

## ***Ionosphere and upper atmosphere***

Three curves in Fig. 2 formed a regular sequence as functions of  $h$  without chaotic crossings, which necessary appear when the errors of input data and calculations are too high. Thus, there exists a perspective to solve the inverse problems at nonstationary conditions more accurately than it has been done before, by introducing a third parameter characterizing the electric properties of an ionized atmosphere layer.

## **Equatorial neutral temperature and total mass density minima as effect of the thermosphere-ionosphere coupling**

E.N. Doronina, A.A. Namgaladze (*Murmansk State Technical University, Murmansk, Russia*)

The numerical experiments on the relative role of different thermospheric heat sources in the formation of the equatorial day-time neutral temperature and total mass density minima at the heights of upper thermosphere have been made using the theoretical global Upper Atmosphere Model (UAM). The results have showed that these minima are forming by absorption of the solar ionizing EUV radiation. This radiation is absorbed most effectively at the thermospheric heights of about 150-170 km and heats the neutral gas through the thermosphere-ionosphere coupling by the photons – photoelectrons – thermal electrons – ions collisions. This ionosphere-thermosphere heating by the EUV-radiation and the rotation of the Earth generates the tidal structure with the minimum on the day-side near the equator with maxima on both sides from him.

## **Theoretical investigations of the diurnal variations of the spectral resonance structure parameters in background magnetic noise at high latitudes.**

E.N. Ermakova, D.S. Kotik (*Radiophysical Research Institute, 25 B. Pecherskaya st. Nizhniy Novgorod 603950, Russia*)

The numerical simulations of the magnetic tangential components were fulfilled in frequencies range 0.1-15 Hz for high latitude stations Barentsburg (14.12 E, 78.09 N.) basing on the solution of the problem of the waveguide Earth - ionosphere excitation by ground located source like vertical electric dipole [1,2]. Peculiarities of diurnal variations of the spectral resonance structure (SRS) parameters were investigated. For modeling the ionosphere (International Reference Ionosphere - IRI-2001 and IRI-2007), and ionosphere model based on the EISCAT Svalbard radar data (<http://madrigal.haystack.edu/models/>) were used. Modeling was performed for different seasons suggesting weak geomagnetic activity ( $Ap=15$ ) and minimum solar activity ( $F10.7D=75-85$ ). The results of the calculations showed that ionospheric model based on the EICSA radar data most adequately describes the experimental data. In paper [3] it was shown that occurrence of SRS displays a distinct diurnal variation with minimum at 09 - 12 UT. Our calculations also suggest diurnal variations of the SRS oscillations depth (SRS occurrence) practically for all seasons. Thus, the calculations suggest that solar illumination could be one of the factors affecting the diurnal changes of the SRS parameters at high latitudes under conditions of weak geomagnetic activity.

In addition, results of the SRS modeling using the ground based sources (the ULF waves penetrate into the ionosphere from earth-ionosphere waveguide) were compared with the results of reflection coefficient calculations for low frequency waves incident to the ionosphere from above.

The work was supported by RFBR grant 07-02-01189.

### **References**

1. Sobchakov L.A., S.V. Polyakov and N.L. Astachova: Excitation of the electromagnetic waves in flat wave guide with anisotropic upper wall, *Izvestiya BUZov, Radiofizika*, V.46 N.12, 2003, 1027-1036.
2. Ermakova E.N., Kotik D.S., Polyakov S.V., Research of the peculiarities of resonant structure of ULF spectrum of background noise in view of an inclination of the Earth magnetic field. // *Izv. VUZov, Radiofizika*, 51, N 7 .2008, 575-583.
3. N. V. Semenova and A. G. Yahnnin, Diurnal behaviour of the ionospheric Alfv.en resonator signatures as observed at high latitude observatory Barentsburg (L=15), *Ann. Geophys.*, 26, 2245–2251, 2008

## **On the connection between intensity of atmospheric electric field as measured at ground surface and ionospheric electric field in the Central Antarctica**

A.V. Frank-Kamenetsky<sup>1</sup>, L.N. Makarova<sup>1</sup>, V.N. Morozov<sup>2</sup>, A.V. Shirochkov<sup>1</sup>, G. Burns<sup>3</sup>

<sup>1</sup>*Arctic and Antarctic Research Institute, Saint – Petersburg, 199397, Russia;*

<sup>2</sup>*Main Geophysical Observatory, Saint-Petersburg, 194021, Russia,*

<sup>3</sup>*Australian Antarctic division, Kingston, Australia*

Regular measurements of the atmospheric electric fields performed at Vostok Station ( $\phi = 78.45^\circ$  S;  $\lambda = 106.87^\circ$  E, elevation 3500 m) in Antarctica demonstrated that extremely intense electric fields (1000 – 5000 V/m) can be observed during the snow storms periods (Fig.1). As a result such storms are observed when the wind velocity exceeds 6 m/sec. Usually the measured value of the near ground surface atmospheric electric field at Vostok is about 100 – 250 V/m during the periods with “good weather” conditions. Detailed description of the technical and methodical aspects of these measurements can be found in [Frank-Kamenetsky et al, 2001]. Observed intense electric fields at Vostok station undoubtedly indicate existence of the giant electric charges. The problem is immediately aroused whether these intense electric fields produced by drifting or falling snow can re – distribute electric potential in the ionosphere. The scientific value of this problem is twofold: we could clarify suggestion that strong near ground electric fields produced by the snow storms (or by lithospheric perturbations, such as earthquakes) could influence distribution of electric potential in the ionosphere and vice versa – could external sources, such as the solar wind and IMF, contribute to intensity of the atmosphere electric fields measured near the ground surface. Two different ways to explore this problem were chosen in this paper.

## **Global structure of gravity wave excitation from CHAMP satellite observations and its impact on general circulation of the upper atmosphere**

N.M. Gavrilov (*Saint-Petersburg State University, Atmospheric Physics Department, St. Petersburg, Russia*)

An analysis of variances of the atmospheric refraction index measured with CHAMP satellite receiving radio signals from GPS satellites has been performed. The height-latitude-longitude distributions of the variances up to altitudes 35 km and their annual and inter-annual variations were studied. A simplified parameterization of wave dynamical and thermal impacts for inclusion into general circulation models was developed. A study of sensitivity of the mean general circulation of the middle and upper atmosphere to the horizontal inhomogeneity of IGW sources is made using the COMMA-SPBU numerical model. Taking account of IGW sources inhomogeneity gives a better reverse of the zonal wind near the mesopause. Overall structure of the mean zonal wind distribution is most sensitive to the distribution of wave variance at middle latitudes.

## **The auroral emissions and the electron precipitation under different geomagnetic conditions**

V. Guineva<sup>1</sup>, I. Despirak<sup>2</sup>, R. Werner<sup>1</sup>, E. Trondsen<sup>3</sup>, S. Marple<sup>4</sup>, K. Dahle<sup>5</sup>, P. Stauning<sup>6</sup>

<sup>1</sup>*Solar-Terrestrial Influences Laboratory, Bulgarian Academy of Sciences, Stara Zagora Department, 6000 Stara Zagora, P.O.Box 73, Bulgaria*

<sup>2</sup>*Polar Geophysical Institute, Apatity, Russia*

<sup>3</sup>*University of Oslo, Department of Physics, Norway*

<sup>4</sup>*Lancaster University, Department of Communications Systems, UK*

<sup>5</sup>*Andøya Rocket Range, Andenes, Norway*

<sup>6</sup>*Danish Meteorological Institute, Copenhagen, Denmark*

The opportunity for simultaneous multi-instrument observations by different instruments, as well by sets of instruments of the same kind, nowadays is a precondition for an extensive research of the ionosphere phenomena. For this study, simultaneous ground based observations' data of the OI 5577 Å and 6300 Å emissions, the electron precipitation flux and the terrestrial magnetic field have been used from the following instruments: the All-Sky Imager (ASI), ALOMAR Imaging Riometer for Ionospheric Studies (AIRIS) and the magnetometer, positioned at Andøya Rocket Range (ARR), Andenes ( $69.3^\circ$ N,  $16.03^\circ$ E); ASI, 64-beam Imaging Riometer and the magnetometer at the Auroral Observatory, Longyearbyen, Svalbard ( $78.20^\circ$ N,  $15.83^\circ$ E); IRIS at Kilpisjärvi, Finland ( $69.05^\circ$ N,  $20.79^\circ$ E).

## ***Ionosphere and upper atmosphere***

Several cases are examined under disturbed and quiet geomagnetic conditions: four events were registered during substorm development, on the most disturbed days of November 2005 and January 2006; one event occurred on the quietest day of the measurements in November 2005. The changes of the emissions and the absorption at 38.2 MHz, related to the different geomagnetic conditions have been studied. Estimations of the particle precipitation spectra in the different cases have been obtained. The correlation between the 5577 Å and 6300 Å emissions and the absorption at 38.2 MHz has been examined.

Data access has been provided under the Project “ALOMAR eARI” (RITA-CT-2003-506208), Andenes, Norway. This Project received research funding from the European Community’s 6<sup>th</sup> Framework Program.

## **High-speed spectrograph in visible spectral range for nightglow and aurora observations**

Ya. Ignatovich, S. Chernouss, A. Roldugin (*Polar Geophysical Institute KSC RAS*)

Design of high-speed spectrograph for nightglow and aurora observations is under consideration.

Spectrograph consists of monochromator with transmitting grating coupled with digital EM CCD camera PhotonMAX. Entrance lens field of view can be varied in dependence on scientific task from narrow angle up to fish-eye scales. The device permits to register atmospheric and aurora emissions in free spectral range 450 – 670 nm with temporal resolution smaller than 1 second. Maximal spectral resolution is about 1.2 nm. The special programs “WinView” and “WinSpec” give us a possibility to obtain distribution of emission intensities along selected direction in the camera field of view. Comparison the spectrograph with other devices of this type is under discussion. Primary results of laboratory and field testing of the spectrograph are presented.

## **Singlet and triplet molecular nitrogen in auroral ionosphere**

A.S. Kirillov (*Polar Geophysical Institute, Apatity*)

Molecules of singlet (a', a, w states) and triplet (A, B, W, B', C states) molecular nitrogen play very important role in electronic kinetics of the atmosphere in the aurora, sprites, laboratory discharge and afterglow etc. An application of Landau-Zener and Rosen-Zener approximations allows us to calculate quenching rate coefficients of singlet and triplet molecular nitrogen in collisions with N<sub>2</sub> and O<sub>2</sub> molecules. The calculation has shown the contribution of intramolecular and intermolecular electron energy transfer processes in molecular inelastic collisions. The rate coefficients are applied in the calculation of vibrational populations of singlet and triplet molecular nitrogen in auroral ionosphere. The estimation of relative intensities of ultraviolet Lyman-Birge-Hopfield and Vegard-Kaplan bands show a dependence on the altitude of the atmosphere. We compare the results of our calculations with the data of some rocket measurements.

## **Electronically excited molecular oxygen in the region of the nightglow of the atmosphere**

A.S. Kirillov (*Polar Geophysical Institute, Apatity*)

We analyse the peculiarities of electronic kinetics of O<sub>2</sub> in the region of the nightglow. Special attention is paid to the study of rates of molecular collisional processes. Using quantum-chemical approximations we have calculated quenching rate coefficients for Herzberg states of molecular oxygen. The results of the calculation show good agreement with available in scientific literature laboratory experimental data. The rate coefficients are applied in the calculation of vibrational populations of O<sub>2</sub>(A), O<sub>2</sub>(A'), O<sub>2</sub>(c) in the nightglow. We point out on important role of intramolecular processes in the collisions at the altitudes of 90-110 km. The function of the production of electronically excited molecular oxygen is estimated for the process of atomic oxygen recombination. We compare the calculated populations of Herzberg states with the data of ground-based, rocket and telescope measurements.

## **Numerical modeling of the ionosphere effects of 01 August 2008 solar eclipse**

M.V. Klimenko, and V.V. Klimenko (*West Department of IZMIRAN, Pobedy Av., 41, Kaliningrad, 236017, Russia*)

On August 01, 2008 a total eclipse of the Sun was visible from within a narrow corridor that traversed half of Earth. The path of the Moon’s umbral shadow began in northern Canada and extends across Greenland, the Arctic, central Russia, Mongolia, and China. A partial eclipse was seen within the much broader path of the Moon’s penumbral

shadow, which included northeastern North America, most of Europe, and Asia. The total eclipse lasted for 2 hours, and covered 0.4% of the Earth's surface in a 10200 km long path. This eclipse has caused the special interest that its way passed through area of high latitudes. In this study the numerical calculation results of ionosphere effects of this solar eclipse are presented. Calculations are executed on the basis of Global Self-consistent Model of the Thermosphere, Ionosphere and Protonosphere (GSM TIP), developed in WD IZMIRAN for summer conditions in the minimum of solar activity. The behavior of various parameters of F-region and the lower ionosphere during solar eclipse has been obtained as a result of numerical calculations. The global maps of disturbances of various ionosphere parameters during solar eclipse are built. The calculation results are compared to experimental data.

### **Numerical modeling of the ionospheric precursors of high-latitude earthquakes**

M.V. Klimenko, V.V. Klimenko (*West Department of N.V. Pushkov IZMIRAN, Kaliningrad, Russia, e-mail: maksim.klimenko@mail.ru*)

Recently the number of scientists from different areas of geophysics which on the basis of experimental and theoretical researches try to predict the earthquakes has increased. Not last place in the list of these researches the researchers of ionospheric precursors of the earthquakes are ranked. The earthquake on Alaska in 1964 became the first earthquake on which the researchers of the ionosphere have turned a fixed attention. Intensive searches of the ionospheric precursors of earthquakes are spent within last two decades by numerous groups of researchers. The assumption that observable of some days prior to earthquake the ionospheric effects are caused by the disturbances of the zonal electric field in the near-epicentral area, stated by A.A.Namgaladze, was checked up in numerical calculations with use of the models GSM TIP and UAM, and has found the confirmation. We used this mechanism in numerical experiments for reproduction of observed changes in the ionosphere prior strong high-latitude earthquakes on Alaska in 1964 and 2002 and in Antarctic in 1998. Besides there is a hypothesis of formation of the ionospheric perturbations seismogenic origin owing to propagation and dissipation in the upper atmosphere of the small-scale internal gravity waves (IGW) generated in the epicenter of the future earthquake. It is supposed, that such waves, can be excited in the area of preparation of earthquake, and their vertical propagation provides the localization of the effects dissipation above the epicenter of earthquake. We have simulated the effects of small-scale IGW for the same earthquakes on Alaska and in Antarctic with use of the model GSM TIP. The numerical experiments have shown, that the local perturbations of zonal electric fields and the small-scale internal gravity waves generated in the near-epicentral area allow reproducing the morphology of ionospheric disturbances observed in the periods of seismic activity. Comparison with experimental data has revealed the satisfactory agreement.

### **Numerical modeling of ionospheric parameters during sequence of geomagnetic storms on September, 9-14th, 2005**

M.V. Klimenko, V.V. Klimenko (*West Department of N.V. Pushkov IZMIRAN, Kaliningrad, Russia, e-mail: maksim.klimenko@mail.ru*)

On September, 9th, 2005 the weak geomagnetic storm with the sudden commencement at 14.01 UT was observed. The same day there was a solar flare of class X17. This flare was one of 10 most powerful solar flares registered for all history. Thus there was an emission coronal mass and the arisen shock wave has reached the Earth at 09.30 UT on September, 10th, 2005, having caused a weak geomagnetic storm with the sudden commencement which then was replaced by a strong magnetic storm with the sudden commencement at 01.14 UT on September, 11th, 2005. This storm which proceeded down to September, 15th, 2005, has been caused by the second shock wave from the following solar flare. The storm has caused the strengthening of auroral activity, radio blackout and strong ionospheric storm. In the given study the ionospheric effects of sequence of geomagnetic storms on September, 9-14th, 2005 are considered.

Preliminary results of numerical calculations of ionospheric parameter behavior during sequence of geomagnetic storms with use of the Global Self-consistent Model of the Thermosphere, Ionosphere and Protonosphere (GSM TIP), developed in WD IZMIRAN and added by the new block of calculation of electric fields of magnetosphere and thermosphere origin in the Earth's ionosphere without taking into account of thermospheric tides are presented. Storms have occurred at a mean level of solar activity ( $F10.7 = 95 - 120$ ). Values of a three-hour index of geomagnetic activity  $K_p$  during storms on September, 9th, 10th and 11th, 2005 reached its maximal values 4.3, 5.7 and 7.7 accordingly.

As initial conditions the values of all ionospheric parameters calculated for quiet conditions ( $K_p = 0.7$ ) at 09.00 UT on September, 9th, 2005 have been chosen. During the simulation of quiet behavior of ionospheric parameters between 09.00 UT 09.09.2005 and 24.00 UT 14.09.2005 only the change from day to day of the level of solar

## ***Ionosphere and upper atmosphere***

activity F10.7 was considered. Thus the value of the Kp-index did not vary, remaining equal 0.7. At simulation of the quiet conditions the potential difference through polar caps and field aligned currents of the second region were set as function from Kp. Thus the time delay of variations of the second region field aligned currents, equal of 30 min. relative to the variations of the potential difference through polar caps was considered.

It is analyzed the obtained calculation results for the set of ionospheric stations. The comparison of these results with experimental data obtained at stations Irkutsk (52.2°N, 104.2°E), Yakutsk (62.0°N, 129.4°E) and Millstone Hill (42.6°N, 71.5°W) is lead.

This study is supported by RFBR grant № 08-05-00274.

## **Effectivity of the plasmasphere as a source of the maintenance of the night-time ionospheric F2-layer**

M.A. Knyazeva, A.A. Namgaladze (*Murmansk State Technical University, mariknyazeva@yandex.ru, namgaladzeaa@mstu.edu.ru*)

The processes of the filling and depletion of the plasmasphere were modeled by using the global numerical Upper Atmosphere Model (UAM). The global distributions of the electron density and the geomagnetic field-aligned plasma fluxes were calculated without taking the wind induced and the electromagnetic drift of the plasma. The initial ionosphere and plasmasphere were supposed as fully depleted.

The model calculations show that the  $H^+$  fluxes at the 1000 km directed from the plasmasphere to the ionosphere at the night-time are maximal at the subauroral latitudes ( $\sim 55^\circ$ – $60^\circ$ ) and they form the electron density maxima in the ionospheric F2-layer. These maxima of the electron density do not coincide with the night-time middle-latitude enhanced electron density regions (EEDR's) because the EEDR's are observed at the lower latitudes and they are formed by the wind induced transportation of the ions along the geomagnetic field lines.

The origin of the subauroral maxima of the electron density and the  $H^+$  fluxes has been explained by the peculiarities of the geomagnetic field geometry. The vertical component of the field-aligned plasma pressure gradient decreases because of the inclination of the geomagnetic field decreases by the passage from subauroral to lower latitudes. The high-latitude geomagnetic force tubes are practically depleted due to the volumes of these tubes increase steeply. It results that the effectivity of the plasmasphere as a source of the plasma for the night-time ionospheric F2-layer are maximal at the subauroral latitudes.

## **A model study of the 3D-topology of the enhanced electron density regions in the night-time ionospheric F2-layer**

M.A. Knyazeva, A.A. Namgaladze (*Murmansk State Technical University, mariknyazeva@yandex.ru, namgaladzeaa@mstu.edu.ru*)

The 3D-topology of the enhanced electron density regions (EEDR's) in the night-time middle-latitude ionospheric F2-layer and their manifestations in the plasmasphere have been modeled by using the different versions of the global Upper Atmosphere Model (UAM) and the empirical model of the ionosphere IRI-2001 for various heliogeophysical conditions.

It has been shown that two types of the EEDR's exist in the latitude-longitude distribution of the  $NmF2$ : 1) with the electron density isolines in the form of a “ridge with decreasing altitude” and 2) with the closed isolines in the form of a “hill”. Both types of the EEDR's extend to the plasmasphere along the geomagnetic field lines ( $1.3 \leq L \leq 2.4$ ) as it is seen in the latitude-altitude distributions of the electron density. The EEDR's are reproduced both by the IRI-2001 and by all UAM versions. The physical mechanism of the forming of these regions is based on the joint action of the plasma flows from the plasmasphere and the wind induced transportation of the ionospheric plasma along the geomagnetic field lines. The wind induced vertical ion velocity results in the lowering of the plasma recombination rate due to the plasma transfer to the higher altitudes. The horizontal component of the wind induced velocity causes the equatorward displacement of the EEDR's relatively to the maximum of the wind induced vertical ion velocity. The LT-variation of the EEDR's looks as a displacement of these regions to the higher or lower latitudes by the passage from evening to morning hours. It takes place when the subsolar point is shifted relatively to the geomagnetic equator (depending on the season and UT moment). The season variation of the EEDR's is the following: 1) the first type of the EEDR's is formed in the summer hemisphere, the second type – in the winter one and 2) the asymmetry of these regions relatively to the equator takes place. Electron density in the EEDR's increases with the increasing of the solar activity. The seasonal, UT-, LT- and solar activity effects of the EEDR's are formed by the corresponding variations of the thermospheric wind velocity at the ionospheric F2-layer altitudes.

## **Properties of the low frequency waves in the multi-component ionospheric plasma**

D.S. Kotik (*Radiophysical Research Institute, 603950, Nizhny Novgorod, Russia*)

The refractive index and polarization of electromagnetic waves in frequency band from first Hertz up to several kilohertz were analyzed through all ionosphere thickness from the bottom to the topside. The modeling of refractive index height profiles of the ULF/VLF waves was based on the magneto ionic theory and international standard models of medium parameters: International Reference Ionosphere - IRI-2001, MSIS-E-90 Atmosphere Model and DGRF/IGRF Geomagnetic Field Model 1945 – 2005 (see <http://ccmc.gsfc.nasa.gov/modelweb>).

The main attention was devoted to the ULF part of the band. It was shown that the waves at frequencies 1-20 Hz are circularly polarized and the refractive indexes are frequency depended. The values of refractive indexes of normal waves in the upper ionosphere tend to the values of Alfven and magnetosonic ones only at the limit when the frequency tends to zero. The polarization of normal waves also became linear only at the same limit. In the E region of the ionosphere the refractive index of one of the normal wave rather differs from Alfven wave value and looks like whistler one. The second normal wave in the same region is damped.

The seasonal variations of the refractive indexes profiles during solar cycle were explored. The consequences of above-mentioned variations and several others peculiarities were discussed in respect to the experimentally observed phenomena in the background magnetic noise spectrums. The comparison with new IRI-2007 model was made.

## **GPS deviations dependence on geophysical and atmospheric disturbances**

V. Maklakov<sup>1</sup>, S. Chernouss<sup>1,2</sup>, N. Kalitenkov<sup>2,3</sup>, O. Antonenko<sup>2</sup>, A. Kalitenkov<sup>3</sup>

<sup>1</sup>*Apatity Branch of the Petrozavodsk State University, Apatity*

<sup>2</sup>*Polar Geophysical Institute of the Kola Science Centre RAS, Apatity*

<sup>3</sup>*Murmansk State Technical University, Murmansk*

Experimental studies of deviations in positioning of GPS in high latitudes are under consideration. Two factors influencing on GPS signal propagation are taken into account.

First one is low atmosphere events like cloudiness and precipitation, and second one is ionospheric disturbances associated with aurora. Experiments on continuous registration of GPS signal were carried out in Apatity and Murmansk in 2007-2009. Time series of GPS deviations were compared with simultaneous measurements of auroral and geomagnetic field variations in the network of stations of the Barents Region and weather parameters obtained from local meteorological observations. Simultaneous satellite data from NOAA and DMSP also were under analysis. The distribution of deviations and their amplitudes are shown. Comparison of temporal variations of the GPS deviations and auroral intensity spatial and temporal variations demonstrates a good correlation in case studies. It was found that deviation values depend on precipitations. Physical mechanisms of the GPS accuracy dependence on atmospheric and geophysical factors are discussed.

## **Model simulation of the large-scale mid-latitude F-layer modification by powerful HF waves with different powers in the daytime**

G.I. Mingaleva and V.S. Mingalev (*Polar Geophysical Institute, Apatity, Russia, e-mail: mingalev@pgia.ru*)

The mathematical model of the ionosphere, developed earlier in the Polar Geophysical Institute, is utilized to predict the large-scale F-layer modification by high power, high-frequency radio waves. The utilized model produces the time variations of the electron density, positive ion velocity, and ion and electron temperature profiles within a magnetic field tube over an ionospheric heater. The model is able to take into account the action of powerful HF waves on the ionosphere. The calculations are performed for the point with geographic coordinates of the “Sura” heating facility (Nizhny Novgorod, Russia) for daytime autumn conditions. Simulations are made for different cases, in which the effective absorbed power (EAP) has distinct values belonging to the 5-100 MW range. The results of modeling indicate that conspicuous variations of the electron temperature, positive ion velocity, and electron density profiles can be produced by HF heating during the period of 5 min in the daytime mid-latitude F region, with the maximal amplitudes of variations depending appreciably on the values of the EAP. It turns out that the more the EAP is, the higher values of maximal amplitudes of variations of ionospheric parameters, produced by HF heating, ought to be.

## **Excitation of the artificial magnetic pulsations by SPEAR: a case study**

A.A. Mochalov, A.B. Pashin (*Polar Geophysical Institute, Apatity, Russia*)  
T. Yeoman (*University of Leicester, Leicester, UK*)

A series of heating experiments have been carried out on 2006 at SPEAR heating facility at Svalbard. The experiments on modulated ionosphere heating were mainly aimed on injection of the artificial MHD waves into upper ionosphere. Ground based observations of the artificial magnetic pulsations near heating site provided by Polar Geophysical Institute at Barentsburg show some interesting features. Two events of heating experiments for July 12 and July 15, 2006 are studied. For the both events the ionosphere heating occurred from 05.30 to 06.30 UT, k-index was equal 4. The ionosphere modification took place on neighboring days at the same local time however the differences in the ionosphere response are evident. A spectral density of the magnetic field variations for July 12, 2006 shows the clear artificial emission at the spectrogram of the H-component marks whole one hour interval of the heating. In the D-component an interference of the background emissions and flickering signal at the modulation frequency can be recognized. Power spectra for July 15, 2006 shows a weak narrow banded signal at 3 Hz is seen in the H-component for 10 minutes time interval. Nothing is observed in the D-component.

## **Transient luminous events: challenge for theory and ground-based/space-borne observations**

E.A. Mareev, V.V. Klimenko, S.A. Yashunin (*Institute of Applied Physics, Russian Academy of Sciences, 603950 Nizhny Novgorod, Russia*)

Optical phenomena like sprites and elves in the middle atmosphere and lower ionosphere (often referred as TLEs - transient luminous events) in association with lightning discharges have become a very popular and interesting subject in atmospheric electricity and space physics during the last several years. But it is only recently that sprites have been identified as vertically extensive optical flashes that are initiated near the base of the ionosphere following intense lightning discharges and develop very rapidly downwards and sometimes upwards at a speed which can exceed one tenth of the speed of light.

Recent observations of transient luminous events (TLEs) in the atmosphere encouraged new efforts in the research of intensive lightning discharges, their parent thunderstorm systems and the global atmospheric electric circuit. It is obvious now that all these fields of research are closely related each to others. This paper reports some recent results in the study of TLE electrodynamics. A special attention is paid to the ways for ground-based support of space missions focused on the investigation of TLEs and their parent thunderstorms from space. Possible effects of perturbations of mesospheric composition and chemistry due to sprite generation in the global electric circuit are briefly discussed as well.

Quasi-stationary and fast transient processes connected with powerful lightning discharges and large-scale thunderstorm systems are analyzed. The main physical ideas served as the foundation for sprite and sprite-producing cloud modeling are discussed with rather simple examples.

Approximate solutions of the kinetic equation for electros in weakly ionized plasmas in the electric field are considered. They allows us to describe the main characteristics of the avalanche stage of the discharge, to determine the conditions of further discharge development as well as to find realistic estimations of the parameters needed for the observation planning: discharge current density, electromagnetic emission intensity etc. Features of the fine structure of the discharges in the range of parameters 1-10 m can be also derived.

The role of lightning channel dynamics and especially the M-component mode of charge transfer to ground in lightning discharges in initiating sprites and spite halos turned out to be very important. M-components serve to enhance the electric field at high altitudes and, as a result, may increase the probability of sprite (halo) initiation. It appears that occurrence of an M-component shifts electric field maximum from the axis of the vertical lightning channel and therefore increases the likelihood of initiation of sprites displaced from the channel axis. Since M-components follow return strokes after a time interval of a few milliseconds or more, they may be primary producers of so-called delayed sprites.

## **Preliminary results of ELF amplitude and phase measurements at Apatity and Barentsburg**

S.V. Pilgaev, O.M. Lebed and Yu.V. Fedorenko (*Polar Geophysical Institute, Apatity, Russia*)

In December 2008 at Apatity and Barentsburg we made simultaneous measurements of the vertical electric component of 82 Hz radio signal from Russian ELF transmitter located on the Kola Peninsula. This experiment

aimed to study phase and amplitude variations in the transmission of ELF signals in the Earth-Ionosphere Wave Guide. The receiver phase stability at both sites is achieved by locking data acquisition system clock to the GPS (Global Positioning System) Pulse-Per-Second (PPS) resulting in long-term zero phase drift. The phase and amplitude variations in quiet and disturbed geomagnetic conditions are presented and discussed.

**Condensation of combustion products and optical phenomena in the upper atmosphere, connected with rocket engines operation**

Yu.V. Platov (*Pushkov Institute of Terrestrial Magnetism, Ionosphere and Radiowaves Propagation, RAS, Troitsk, Moscow region, Russia*)

The process of condensation of water and carbon dioxide vapors in a rocket exhaust in the upper atmosphere is examined. The equations of thermal balance and evolution of size condensed particles in the rocket plume are solved for real engine conditions. It is shown that sizes of ice particles can reach  $\sim 100$  Å. The life time of such particles due to sublimation processes is about 2 minutes. The condensed particles are formed “dust” clouds of rocket exhausts with characteristic sizes up to  $\sim 400$  km, which can be observed in scattering sun light. The comparison with results of “rocket” optical phenomena recording is presented.

**“Fock Diffraction Wave” and ultra high relativistic electron precipitations into polar middle atmosphere (Devoted to the 110 birthday anniversary of academician V.A. Fock)**

G.F. Remenets (*Physics Department of St. Petersburg State University*)

At the War II evacuation time Fock V. A. wrote a work “Radio Wave Diffraction Around Earth” [1], which was published as a little book in soft cover in 1946. I hold it in my hands at first in my life more than 40 years ago when I had become an initiating young specialist at the Physics Department of Leningrad State University. At those time I could not imagine that after 30 years of my scientific activity I should return to it in order to prove with a scientist of PGI RAS Beloglazov M. I. an existence of a new geophysical phenomena on the basis of on ground measurements of radio signal amplitudes and phases in an auroral region. The essence of the phenomena is a spontaneous ultrarelativistic (with energy  $\sim 100$  MeV) electron precipitation into polar middle atmosphere. This precipitation generates the X-ray and gamma quantum streams, density of which is enough for middle atmosphere ionization in the 10 – 40 km altitude interval. So a sporadic D layer of atmosphere ionization appears in addition to the regular D layer of ionosphere and an effective altitude of the “ground – layer ionized” wave guide diminishes in two times, id. est. it becomes equal to 30 km instead of 60 km.

The Fock diffraction wave, which is a quite strict consequence of the Maxwell equations for a boundary problem with a sphere of great dimensionless radius and a radio source on it, quantitatively describes the field in the region of half shade and full shade on the sphere surface. After 55 years, after the experimental proof of ionosphere existence due to the fact of first order interference existence between the direct wave and the wave reflected from above, Beloglazov M. I. and I collided with the following experimental fact. Sometimes (very rarely, one – several times a year) at the conditions of a pure “geophysical calm” the amplitudes of radio signals with different frequencies from the most powerful radio source with band of several tens of km diminished at more than ten times at the distance of  $\sim 900$  km. At such distance a receiving on ground point is located in the shadow region relative to an on ground source (the shadow is caused by the spherical Earth surface). The diffraction wave, which is a surface wave, the amplitude of which decreases exponentially as function of altitude, is indifferent relative to the electric properties of the middle atmosphere. The experimental fact that the signal in the pointed conditions disappears in the apparatus with 20 Hz receiving band may mean only one thing, that the Fock diffraction wave is compensated by the wave, which reflects from a sporadic layer of atmosphere electric conductivity with an effective altitude  $\sim 30$  km. This value is gotten by solving an inverse problem relative to the layer parameters, for which full compensation takes place. In normal conditions and in the cases of all other geophysical disturbances, as it follows from the Maxwell equations, the wave, reflected from above, is described by the geometry optic approximation. But in conditions of our abnormal disturbance “the signal from above” achieves the diffraction properties too. So the phase and amplitude conditions for the compensation become qualitatively different from the optics conditions. The stated thought is revealed in the report.

1. Фок В.А. Дифракция радиоволн вокруг земной поверхности. М., Л.: АН СССР, 1946. 54 с.

## **Polarization ellipse variations of Schumann resonance in horizontal and vertical planes according to observations in Barentsburg and Lovozero**

V.C. Roldugin, A.N. Vasiljev (*Polar Geophysical Institute, KSC RAS, Apatity*)

The diurnal variations of all parameters of polarization ellipse of the first Schumann resonance, observed in Barentsburg and Lovozero observatories, are investigated for 1–10 December 2007 data. Therein the near identical measurements of all three magnetic components of ULF emissions in frequency range of 0.1–10 Hz are carried out. The ellipses have been examined in two planes, NS-WE and NS-Z, and usual values of an ellipse are determined: a value of minor semiaxis, a tilting of major axis about W-E and N-S directions, an eccentricity and a rotating sense. The ratio of the vertical amplitude to the total horizontal one is different in both stations: at Barentsburg it is averaged as 0.7–0.9, and in Lovozero it is equal to 0.3–0.5. So, the minor semiaxes in the NS-Z plane are less than in the NS-WE plane at both stations. They have small different diurnal courses. In Barentsburg the major axis is tilted about W-E at 60°, and at 2°–5° about N-S; in Lovozero the values are 70° and 7°–10° correspondingly. The eccentricity in the horizontal plane is equal to 0.80–0.85, and in the vertical planes it is equal to 0.9. It was found also, that the polarization vector rotates mainly clockwise at both stations and in both planes; sometimes duration of clockwise intervals exceeds anticlockwise time interval fifty times over and more. We justify this phenomenon as different influence of the Earth's magnetic field on the SR wave under northward and southward wave propagation.

## **Features of pulsating arcs inferred from ALIS triangulation measurements**

V.V. Safargaleev<sup>1</sup>, D.N. Shibaeva<sup>2</sup>, T. Sergienko<sup>3</sup>, I. Sandahl<sup>3</sup>, U. Brändström<sup>3</sup>

<sup>1</sup>*Polar Geophysical Institute, Apatity, Russia*

<sup>2</sup>*Kola Branch of Petrozavodsk State University, Apatity, Russia*

<sup>3</sup>*Swedish Institute of Space Physics, Kiruna, Sweden*

Pulsating auroras are characterized by repetitive intensity modulation in the auroral luminosity. In contrast to discrete auroras, the properties of pulsating auroras are less investigated, since one needs instruments of high sensitivity as well as rather high temporal and spatial resolution for their study. Over 10 years ago, the Auroral Large Imaging System (ALIS) was designed to handle short-lived small-scale auroral forms of low intensity. We present here results of an investigation of one type of pulsating auroras – pulsating arcs – performed using the capability of ALIS. The observations were performed during the recovery phase of a substorm that is the most typical time for occurrence of pulsating auroras. During the interval, three ALIS digital cameras with fields of view of 57x57 degrees were operating, allowing us to estimate the altitude of the pulsating patterns in the overlap area (60x80 km) with high veracity. It is well known that the altitude of the aurora gives information about the energy of electrons causing the luminosity. The auroras considered looked like a series of thin faint stripes pulsating with a repetition period of a few tens of seconds and drifting slowly equatorward. The triangulation measurements showed that the altitude of the arcs was different for different arcs in a series but did not vary with the intensity variation in each individual arc within one “switch on/off” cycle. This means that the electron precipitation responsible for the arc formation was caused rather by scattering into the loss cone via wave-particle interaction than by field-aligned acceleration in a parallel electric field. In general, the finding is in the agreement with the theory suggested for another type of pulsating auroras – pulsating patches. However, it is not in the consistence with the recent particle measurements by the FAST when it passed above the similar structure (Saito et al., 2002). The possible reason for the generation of the equatorward drifting series of pulsating arcs is discussed.

## **Responses to the earthquakes in the lower high-latitude ionosphere**

N.G. Sergeeva, O.F. Ogloblina, B.E. Vasiljev, S.M. Chernyakov (*Polar Geophysical Institute, Murmansk, Sergnell@mail.ru*)

The experimental data obtained with the partial reflection radar located at the Kola Peninsula (Tumanny observatory, 69.0°N, 35.7°E) during the period from May to August 2006 are analyzed with the aim to reveal the ionospheric responses to earthquakes. During the analyzed period under different geophysical conditions some 40 strong earthquakes with the magnitudes from 5.8 till 7.7 on the Richter scale occurred in the region of island Java. These earthquakes were recorded by seismic stations located at the Kola Peninsula and the Northern Scandinavia. The earthquakes which occurred under very quiet geomagnetic conditions and weak solar flares were chosen to find

the responses to earthquakes in the lower ionosphere. Thus, 10 strong earthquakes were selected. For these earthquakes general behavior of the lower ionosphere parameters was found.

On days of earthquakes, the internal gravity waves with the periods of 3-6 hours were observed in the daily spectra of the ordinary component of a partly- reflected signal along with the tidal atmospheric waves with the periods of 24, 12, 10 hours.

We have been analyzed the amplitudes spectra of the ordinary component of the partially reflected signal on other days under the same geomagnetic conditions, but without the earthquakes. There were only two such days during the interval under consideration. Only the tidal atmospheric waves with periods of 18, 12, 8 hours were observed.

Thus, we may conclude that the amplitude fluctuations of the ordinary component of the partially reflected signal of few hours period are connected with the internal gravity waves related to the earthquakes.

This study was supported by Russian Foundation for Basic Research (grant № 07-05-00012).

### **On the problem of correct collocation of ground based (optical) and high-altitude satellite measurements**

D.N. Shibaeva<sup>1</sup>, V.V. Safargaleev<sup>2</sup>, T.I. Sergienko<sup>3</sup>, I.A. Kornilov<sup>2</sup>

<sup>1</sup>*Kola Branch of Petrozavodsk State University, Apatity, Russia*

<sup>2</sup>*Polar Geophysical Institute, Apatity, Russia*

<sup>3</sup>*Swedish Institute of Space Research (IRF), Kiruna, Sweden*

The data of multi-spacecraft projects such as CLUSTER and THEMIS, when compared correctly with the ionospheric measurements in the conjugated area, could provide insight into nature of the number of magnetospheric processes. In our study we concentrate on the problem of satellite-auroras conjugation. This is the two-step process that includes (1) the mapping of auroras and (2) satellite projection to the ionosphere. The event considered is the passage of CLUSTER quaternion through the Lovozero all-sky camera conjugated area ( $L \sim 4.5$ ) during the interval of pulsating auroras. For aurora mapping we used the package of procedures developed for the Auroral Large Imaging System (ALIS). The package Orbit Visualization Tool (OVT) provided the coordinates of satellite footprint for different models of geomagnetic field. Our study shows that the largest discrepancy (300 km) is between dipole+T96 and IGRF+T96 models, so in different models the satellite was probing quite different auroral situations. The IGRF+T96 and IGRF+T89 models gave the difference in satellite projection of about 100 km. This led to the association of the satellite measurements with different auroral structures. The smallest discrepancy in projection (few kilometers) was for IGRF+T02 and IGRF+T96 models. But even in this case, there was a doubt whether the satellite is inside or outside the auroral structure. We should note that Lovozero is on the closed magnetic field lines, the shape of which is often regarded as a "dipole-like". The situation with detail association of the auroras with satellite measurements seems to be more dramatic if the satellite is in the distant magnetotail or in the lobes.

### **Nightglow observations of short-period global atmospheric waves**

G.M. Shved<sup>1</sup>, N.V. Karpova<sup>1</sup>, P.P. Ammosov<sup>2</sup>, and G.A. Gavril'yeva<sup>2</sup>

<sup>1</sup>*St. Petersburg State University, St. Petersburg-Petrodvorets, Russia*

<sup>2</sup>*Institute of Cosmophysical Research and Aeronomy, Yakutsk, Russia*

From 12 November of 2007 to 14 February of 2008 the nighttime emissions of hydroxyl (6-2 band) and oxygen (Atmospheric system, 1-0 band) were measured at the Maimaga station ( $63^{\circ}\text{N}$ ,  $129.5^{\circ}\text{E}$ ). The measurements have resulted in the series of rotational temperature near the altitudes of 87 and 94 km, respectively, for 67 nights with sampling time of 10 min. The spectral analysis with the Lomb-Scargle method for unevenly spaced data has been applied to the series of several days duration. The steady-frequency harmonics in the  $\sim 2\text{-}10$  h period range have been detected. The high subharmonics of solar tide with numbers up to  $m = 10$  (2.4 h period) and a harmonic at the 9-10 h period, which may be associated with normal atmospheric modes, have been revealed in the spectra. (The study was supported by the Russian Foundation for Basic Research, the project 07-05-00475.)

## **Thomson scattering of electromagnetic waves in the polar mesosphere containing the charged dust**

V.D. Tereshchenko (*Polar Geophysical Institute, Murmansk, 183010, Russia; E-mail: vladter@pgi.ru*)

Now in number of methods of research polar mesosphere included strongly has come Thomson (or incoherent) scattering. For determination of medium parameters by this method it is necessary to know character of influence of the charged particles of sorts which are taking place in mesospheric plasma, on a spectrum and total power of scattered radiation. In work formulas for differential and total scattering cross sections of radio waves in plasma with a magnetic field, containing the charged dust are received. It is made by solving the kinetic equations with the BGK model collision integral. Calculations show that presence in mesosphere the charged dust results to the widest spectrum and increase of intensity of scattered radiation. The widest spectrum will be for negative dust particles. Thus total power of scattered radiation will be approximately twice more, than in absence of the charged dust. The study was supported by the RFBR grant № 07-05-00012 and the Federal target program (the state contract 4/ГФ/Н-08 from September, 09, 2008).

## **About behavior of the polar lower ionosphere during a solar eclipse on August, 1, 2008**

V.D. Tereshchenko, E.B. Vasiljev, V.A. Tereshchenko, O.F. Ogleblina, S.M. Chernyakov (*Polar Geophysical Institute, Murmansk, 183010, E-mail: vladter@pgi.ru*)

The ionospheric effects of solar eclipses are studied for a long time. However till now there is no full clearness in understanding of the phenomena occurring in the ionosphere. Besides, reaction of the polar ionosphere to solar eclipses was investigated rather seldom. The solar eclipse on August, 1, 2008 in Murmansk began at 08:46 UT. The maximal phase of the eclipse has made 0.81, which took place at 09:51 UT. The end of the eclipse was at 10:56 UT. In work results of observations of this solar eclipse, received on installations of partial reflections and vertical sounding of the ionosphere near to Murmansk are submitted. Good conformity between the data, received by two methods is established. It is shown, that the maximal phase of the eclipse of electronic concentration at heights of 75-85 km in 2-3 times become lower, than prior to the beginning of the eclipse. Thus the minimal frequency of the reflection measured with the help of the ionospheric sounding station, decreases in 1.4 times, and the total electronic contents at heights from 55 up to 110 km – in 2.5 times. The effect of the eclipse is shown and in similar quasi-periodical fluctuations of considered parameters. The behavior of regions F1 and F2 the polar ionosphere during the eclipse qualitatively corresponds to earlier carried out researches.

The study was supported by the RFBR grant № 07-05-00012 and the Federal target program (the state contract 4/ГФ/Н-08 from September, 09, 2008).

## **Backscatter volume cross sections and amplitudes of electrostatic electrojet fluctuations inferred from joint STARE and EISCAT measurements**

M.V. Uspensky<sup>1</sup>, A.V., Koustov<sup>2</sup> and P. Janhunen<sup>1</sup>

<sup>1</sup>*Finnish Meteorological Institute, Helsinki, Finland*

<sup>2</sup>*University of Saskatchewan, ISAS, Saskatoon, Canada*

STARE Norway and Finland radar data for the afternoon-evening were combined with EISCAT CP1 measurements of the electron density and electron drift velocity vector to investigate variations of the volume cross section (VCS) of auroral backscatter with electric field, electron density and flow angle of observations. Our statistics consists of ~6000 points for flow angles of 40-85°, electron drifts between 500-2000 m/s, effective electron densities of (0.3-1.5) 10<sup>11</sup> m<sup>-3</sup> and the height thickness of the backscatter volume between 12 and 17 km. It is shown that the flow angle variations of VCS is significantly weaker than reported in the past (~5 dB within the range of available flow angles) and it is not symmetric with respect to the direction of the electron drift. By adopting a semiempirical equation for normalized spatial power spectrum of auroral E-region irregularities, the relative amplitudes of electrostatic electrojet density fluctuations  $\langle (\delta N / N)^2 \rangle^{1/2}$  were estimated. The obtained values of several (up to 10) per cent are consistent with reported *in situ* rocket measurements. The VCS values are shown to depend almost linearly on product of the square of the electron drift velocity and the square of the effective electron density magnitude.

In our observations we found existence of backscatter irregularities of close intensity in condition with the

backscatter aspect angle of  $\sim 1^\circ$  and in the band of the large (e.g.  $>60^\circ$ ) flow angles, where linear fluid and kinetic plasma theories invariably predict negative growth rates. The observations can be reasonably explained by efficient nonlinear wave-wave coupling similar as it described by Kudeki and Farley (1989) and Lu et al. (2008) for the equatorial electrojet.

### **Impact of the ionospheric perturbations on the radio occultation meteorological sounding of the Arctic atmosphere**

V.I. Zakharov, V.E. Kunitsyn, Ya.A. Ilyushin (*Moscow State University, Moscow, Russia*)

Radio occultation refractometry of the atmosphere is an effective technique of the meteorological monitoring. Inversion of signal phase yields the vertical profile of atmospheric refractivity, which is determined by the meteorological parameters. These techniques are ultimately required in the Arctic region, where meteorological observations with the traditional instruments are especially difficult.

An original approach for correction of CHAMP GPS occultation data, incorporating radiosondes profiles and high resolution regional prognostic model, has been proposed in [1]. It has been tested on the real occultation data from the Arctic region, using the climatic model HIRHAM4 (AWI, Potsdam) and the radiosondes data from the WMO network for the period 2001-2007.

Tests shows that the proposed approach in fact improves the profiles in more than 65% situations. However, high solar activity ( $K_p > 4 \dots 5$ ) and geomagnetic variations ( $|Dst| > 60$ ) reduce the correction efficiency. This is due to the polar ionospheric perturbations which are ignored in the correction technique.

For these reasons, numerical simulations of the GPS occultation experiments [2] accounting for the ionospheric perturbations have been performed. Phase and amplitude fluctuations of the signals due to ionospheric perturbations have been investigated. Possible approaches to the reconstruction of the global ionospheric structure in the vicinity of the auroral oval from the tangentially propagating navigational satellite signals are also discussed [3].

#### References

1. V. Kunitsyn et al. // *Phys.Chem.Earth* 29 (2004) 277-286
2. Ya.A. Ilyushin // *J. Atm. and Solar-Terr. Phys.* 70 (2008) 1863–1869.
3. Захаров В.И., Куницын В.Е. // Эл.-магн. волны и эл. сист. 2008. Т.13. N.2-3. с.82-89.

### **Numerical simulations of the ionospheric TEC disturbances associated with the New Zealand earthquake of Nov. 22, 2004**

O.V. Zolotov, A.A. Namgaladze, O.V. Martynenko, B.E. Prokhorov (*Murmansk State Technical University, Murmansk, Russia; ZolotovO@gmail.com*)

The paper presents the results of the investigation of the anomalous ionospheric TEC (total electron content) variations as pre-earthquake signatures for the strong seismic event of Nov. 22, 2004, 20.26UT (07.26LT), New Zealand (46.69 S; 164.78 E), M 7.1.

The ionospheric TEC variations have been estimated using GPS (Global Positioning System) observational data of the IGS stations (Australian and New Zealand) and ionosonde measurements as well. We also have built and analyzed differential TEC maps for a few days before and after the seismic event basing on the global TEC maps provided by IGS community. The observed anomaly looks like local TEC reduction at the near-epicenter area (about  $\sim 40$  degrees in longitude and  $\sim 25$  degrees in latitude) and reaches values up to -43% relative to the non-disturbed level during a day before the earthquake.

The numerical model simulations have been based on a previously set hypothesis that the vertical drift of the F2-layer ionospheric plasma under influence of the zonal electric field of presumably seismic origin is the main reason for the observed disturbances in the TEC. To check the hypothesis for the case of the New Zealand earthquake we have carried out numerical calculations by means of the global time-dependent 3D self-consistent Upper Atmosphere Model (UAM). The seismic electric fields have been modeled by setting different additional electric potentials at the boundaries of the forthcoming strong shock event near-epicenter area with negative charges at the west and positive charges at the eastern boundary.

Model results reproduce well the observed TEC behaviour at the southern hemisphere. Corresponding TEC disturbances at the magnetically conjugated northern region are weaker both in the model case and GPS-observational data.

The work was partially supported by grant No. 08-05-98830 of the Russian Foundation for Basic Research.

## **Sensitivity of the Upper Atmosphere Model results to the input parameters specification for geomagnetic storms modelling**

Yu.V. Zubova, A.A. Namgaladze (*Murmansk State Technical University, Murmansk, Russia*)

The global numerical models are used as a powerful tool for investigation and prediction of the upper atmosphere behaviour under different geomagnetic conditions. Numerical modelling of geomagnetic storms has great difficulties related to the specification of the input parameters such as the characteristics of the field-aligned currents system, precipitating electron fluxes, the O<sup>+</sup> with N<sub>2</sub> reaction rate, the neutral atmosphere and thermospheric circulation parameters. We have performed numerical experiments in order to estimate the sensitivity of the Upper Atmosphere Model results to these input parameters. The theoretically calculated electron density, ion and electron temperatures were compared with the data of the incoherent scatter radars observed the ionospheric E and F region variations during the March 2001 and April 2002 magnetic storms. The comparison has showed that the method of the neutral composition and temperature calculation has the most significant influence on the global model results. The vibrationally excited molecular nitrogen taken into account by geomagnetic storm modeling improves the agreement of the theoretical results and the observed ionospheric parameters. The method of the precipitating fluxes specification influences on the electron density theoretically calculated for not only the high-latitude E region, but also the high-latitude and subauroral F region. The method of the thermospheric wind calculation plays the important role for the modeled middle-latitude electron density. The theoretically calculated night-time subauroral electron density is highly sensitive to the specification of the field-aligned currents particularly to the amplitude and location of the second zone currents.

## **Экспериментальные исследования спектральных структур в фоновом низкочастотном шуме методом разнесенного приема.**

Е.Н. Ермакова, С.В.Поляков, Ю. В. Шлюгаев, А.В. Щенников (*Научно-исследовательский радиофизический институт, Н. Новгород, Россия*)

В работе исследованы данные двухпунктовой регистрации компонент фонового шума при разных базах: 50 км - «Новая Жизнь» 56 N, 45,45 E и мобильный приемный пункт; 400км - «Новая Жизнь» и «Борок» 58,07 N 38,23.

На примере разнесенного приема с базой в 50 км и регистрации сильных спорадических эмиссий в диапазоне Pc-1, приходящих в пункты приема («Новая жизнь» и мобильный пункт) с севера, выполнено экспериментальное исследование возможности одновременного распространения низкочастотных полей в волноводе земля-ионосфера и ионосферном МГД-волноводе. Исследование проводилось на основе корреляционного анализа и построения спектров разностного сигнала.

По наблюдениям в пунктах «Борок» и «Новая Жизнь» исследованы и выявлены разные свойства спектральной резонансной структуры СРС на этих пунктах. Были обработаны и проанализированы весенне-осенние периоды, когда резонансная структура наиболее ярко выражена на средних широтах. Разные свойства СРС чаще регистрировались в вечерние часы после захода солнца. Двухпунктовая схема регистрации полей и использование специальной программы для обработки данных позволили выявить различия в глубине резонансных осцилляций и основных частот на станциях, разнесенных на расстояние порядка 400 км. Смещение основных частот СРС приводило к кажущемуся смещению частот первого Шумановского резонанса на приемных пунктах из-за большой глубины модуляции и большого диапазона частот, в котором наблюдалась СРС. При измерениях на базе в 50 км было обнаружено, что свойства СРС идентичны.

Работа выполнена при финансовой поддержке РФФИ, грант № 07-02-01189.

## **GPS позиционирование и авроральные возмущения**

Н. Калитёнков<sup>1,2</sup>, С. Черноус<sup>2</sup>, А. Калитёнков<sup>1</sup>

<sup>1</sup>*Мурманский государственный технический университет, Мурманск*

<sup>2</sup>*Полярный геофизический институт КНЦ РАН, Мурманск*

Представлены результаты двух серий экспериментальных исследований изменения точности GPS позиционирования во время развития авроральных возмущений. В первой серии экспериментов

навигационный приемник работал в режиме полного обзора неба и принимал навигационную информацию от достаточно большого (избыточного) количества (как правило, от двенадцати) навигационных спутников, что давало возможность выбирать для обработки их оптимальное созвездие. Во второй серии экспериментов искусственно блокировалась радиовидимость южной части небосвода, и навигационный приемник работал с сигналами ограниченного, но достаточного для навигационных целей количества спутников, находившихся в зоне его видимости, то есть со спутниками северной части небосвода. Радиосигналы этих спутников распространяются через ионосферу авроральной зоны и полярной шапки, которая практически постоянно возмущена и меняется лишь степень ее возмущенности. За время экспериментов были отмечены относительно спокойные периоды, а также регистрировались резкие и глубокие вариации горизонтальной компоненты напряженности геомагнитного поля и изменения положения и интенсивности форм полярных сияний на сети обсерваторий Баренцрегиона. Из анализа временных вариаций погрешности GPS, авроральных и геомагнитных вариаций следует, что значительные выбросы погрешностей позиционирования регистрируются одновременно со значительными по величине вариациями Н-компоненты геомагнитного поля и вариациями пространственно-временной структуры полярных сияний. По результатам второй серии экспериментов сделан вывод, что радиосигналы со спутников проходя через области ионосферы, где регистрируются дискретные формы полярных сияний, теряют информационную способность, это приводят к так называемому нарушению целостности системы и ухудшению точности позиционирования либо полному сбою работы навигационной системы.

## **Полярные сияния как индикатор возмущенности среды распространения навигационных радиосигналов**

Н. Калитёнков<sup>1,2</sup>, С. Черноус<sup>2</sup> А. Калитёнков<sup>1</sup>, О. Антоненко<sup>2</sup>, М. Иванюгин<sup>1</sup>

<sup>1</sup>*Мурманский государственный технический университет, Мурманск*

<sup>2</sup>*Полярный геофизический институт КНЦ РАН, Апатиты*

Для определения географических районов, в которых возможны нарушения работы GPS (сбои, уменьшение точности позиционирования), а также времени суток, когда такие нарушения будут отмечаться, предлагается использовать «синоптические» карты овала полярных сияний для различных геофизических условий и разных моментов мирового (UT) времени. Рассматриваются несколько возможных способов реализации диагностики авроральной активности: наземные оптические измерения с помощью ПЗС камеры с полем зрения, совпадающим с диаграммой направленности GPS приемника; спутниковые оптические измерения с высокоапогейных и низкоорбитальных ИСЗ; измерения потоков частиц, возбуждающих полярные сияния, с ИСЗ DMSP. В докладе представлена программа определения положения и интенсивности авроральных высыпаний по данным ИСЗ DMSP в поле зрения, соответствующем диаграмме направленности антенны GPS приемника, с помощью средств визуального программирования «Borland Delphi 7 Studio». Обсуждаются косвенные методы определения изменений параметров аврорального овала по геомагнитным данным на сети станций. Показывается, что использование геомагнитных индексов на различных временных масштабах (от 15 минут и выше) позволяет определять как параметры и динамику аврорального овала, так и положение проекций возмущенных областей ионосферы на земную поверхность. Проведена оценка возможности практического использования существующих моделей прогноза положения аврорального овала на примере данных Аляскинского геофизического института.

На конкретных ситуациях показано, что «синоптические» карты удобны для различного рода сопоставлений при решении навигационных задач и задач динамического позиционирования, поскольку позволяют для конкретных моментов времени и конкретных величин геомагнитного возмущения привязать области среды распространения информационно-навигационных радиосигналов, пораженные неоднородностями электронной плотности к маршруту плавания или месту проведения специальных работ, что, в свою очередь, позволяет спланировать упреждающие действия по дублированию систем радиосвязи и радионавигации.

## **Ионосферные антенны КВ диапазона**

Н.В. Калитёнков, А.Н. Калитёнков, В.И. Милкин, А.В. Гурин, А.Н. Кучура (*Мурманский Государственный Технический Университет, Мурманск*)

Представлены результаты исследования одной из особенностей ионосферного распространения радиоволн коротковолнового диапазона, наблюдаемой на высокоширотных радиотрассах при излучении в направлениях юг-север, запад-восток, восток-запад. Радиоволны при таком распространении на нисходящем участке траектории проходят через области ионосферы, пораженные неоднородностями электронной плотности, ориентированными вдоль направления геомагнитного поля.

Ориентированные вдоль направления геомагнитного поля неоднородности электронной концентрации имеют достаточно широкий спектр масштабов и распределены, как правило, по всей толще ионосферы. Во время авроральных суббурь их количество существенно возрастает на высотах  $E$ -слоя. Плотность неоднородностей электронной концентрации определяется степенью магнитной активности, а их локализация тесно связана с локализацией форм полярных сияний. Максимально резкие неоднородности с перепадом электронной концентрации, достигающей 100 %, наблюдаются в местах локализации наиболее интенсивных дискретных форм полярных сияний.

Приводятся результаты расчета диаграмм направленности переизлучения таких областей для различных сочетаний: частота распространяющейся радиоволны, плотность ионосферных неоднородностей, плотность фоновой плазмы, длина неоднородности вдоль направления геомагнитного поля. Обсуждается возможное приложение полученных результатов к случаю трансионосферного распространения КВ радиоволн.

## **F-рассеяние в дневной ионосфере средних широт, связанное с крупномасштабными неоднородностями концентрации ионосферной плазмы, выделенным по данным Интеркосмос-19**

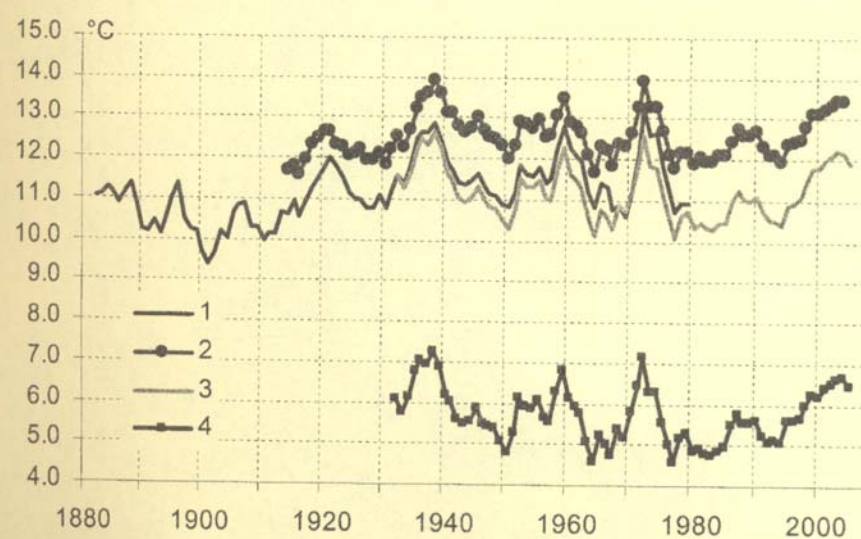
Ю.А. Суковатов<sup>1</sup>, А.Т. Карпачев<sup>2</sup>, В.А. Телегин<sup>2</sup>

<sup>1</sup>*Алтайский государственный университет, sukovatovy@mail.ru*

<sup>2</sup>*ИЗМИРАН, Троицк, telegin@izmiran.ru*

В работе рассмотрены два случая локализованных неоднородностей концентрации ионосферной среднеширотной плазмы, приводящие к появлению внешнего F-рассеяния в момент прохождения спутника над ними. Первый случай соответствует максимуму концентрации, второй – минимуму. Для теоретической интерпретации указанных случаев внешнего F-рассеяния мы используем градиентно-дрейфовую неустойчивость плазмы внешней ионосферы. С этой целью из уравнений квазигидродинамики ионосферной плазмы для физических условий, соответствующих наблюдениям, получено выражение для инкремента градиентно-дрейфовой неустойчивости и декремента диффузационного затухания дрейфовых волн. С учетом выбранной нами геометрии, наблюдаемых градиентов концентрации и параметров плазмы внешней ионосферы получен достаточный критерий возникновения градиентно-дрейфовой неустойчивости. Оказалось, что наблюдаемые градиенты достаточны для выполнения критерия развития неустойчивости в обоих рассматриваемых случаях. При развитии неустойчивости происходит генерация дрейфовых волн с длинами волн, много меньшими размеров наблюдаемых неоднородностей, в ионосфере образуется тонкая структура, которая и приводит к появлению F-рассеяния.

*Low Atmosphere, Ozone*





## **Features of cosmic rays influence on ionization in a troposphere of high latitudes**

O.I. Akhmetov (*Polar Geophysical Institute RAS, Apatity, Murmansk region, Russia*)

The investigation of cosmic rays influence on electrical characteristics of the atmospheric ground layer in high latitudes is presented. The analysis of the experimental measurements of an atmospheric current, vertical component of electric field, cosmic rays intensity and the calculation specific conductivity of atmosphere in 2006-2006 are shown for all kind of seasons. The daily average variations for each season and conductivity estimation biased on balloon born measurements of the cosmic rays intensity are discussed.

It is shown that the atmospheric specific conductivity in a ground layer depend on the cosmic rays intensity during winter and spring seasons in the atmosphere of high latitudes. Seasonal dependence of the cosmic rays intensity influence on the average specific conductivity is disclosed and its magnitude is estimated.

The value of specific conductivity calculated by the atmospheric current density and the vertical component of electric field data is in agreement with the value calculated from balloon born of the cosmic rays intensity measurements.

The work was supported by the RSA DPS program “Atmosphere electrodynamics, radiophysical methods of atmospheric process researches” (project 4.5).

## **Spectral characteristics of an atmospheric current density and atmospheric pressure in high latitude atmosphere**

O.I. Akhmetov (*Polar Geophysical Institute RAS, Apatity, Murmansk region, Russia*)

The investigation of an atmospheric current and atmospheric pressure noise characteristics in summer 2008 is presented, the problem of possible source of observed self-similarity in measured signal is discussed.

The multifractal analysis of the atmospheric current and atmospheric pressure micro pulsations is carried out by Abry's method based on hypothesis of self-similarity in observed signal [1-3]. Spectral indices of the atmospheric current and atmospheric pressure micro pulsations are estimated by global wavelet transform.

It is shown that the atmospheric current signals with a power spectrum probably caused by turbulent aerodynamic processes under a disturbed atmosphere. Spectral index values of such signals are in the range from 2 to 3,7. The atmospheric current signals have not power spectrum under an undisturbed atmosphere condition. That may be caused by dominating contribution a global current to observed signal.

The pressure micro pulsations have a power spectrum with value of spectral indices about 2 under an undisturbed atmosphere condition while spectrum of pulsations in a disturbed atmosphere is not a power spectrum.

1. Abry P., Goncalves P., Flandrin P. Wavelets, spectrum analysis and 1/f processes. *Wavelets and Statistics*. Edited by Antoniadi A. and Oppenheim G. Springer-Verlag. 1995. p.15.
2. Abry P., Flandrin P., Taqqu M.S., Veitch D. Self-Similarity and Long-Range Dependence through the Wavelet Lens, Invited chapter for: *Theory and Applications of Long Range Dependence*, edited by Doukhan P., Oppenheim G., Taqqu M.S., Birkhauser, Boston, 2002.
3. Lashermes B., Roux S.G., Abry P., Jaffard S. Comprehensive multifractal analysis of turbulent velocity using the wavelet leaders// *European Physical Journal B*, 2008, vol.61, No.2, p.201.

## **Global thunderstorm activity during 2001 and 2007 according to observations of the Schumann resonance intensity in the Arctic**

M.I. Beloglazov, O.I. Akhmetov and A.N. Vasiljev (*Polar Geophysical Institute, Apatity, Russia*)

Study of relationship between electric, aerosol, chemical and thermobaric components of atmosphere peculiar importance demands analysis of global electric circuit's (GEC) role in solar-terrestrial relationships system and climate fluctuation. The central place in GEC is taken by problem of the global atmospheric current generator. It could be considered as a global thunderstorm generator that is operated by lightning activity and atmospheric ionization.

One of the basic ionization sources in troposphere and stratosphere is galactic cosmic rays (GCR). Probably, GCR intensity variation should result in to changes of lightning formation processes. Atmospheric noise electromagnetic field (ANEMF) intensity in frequencies of Schumann Resonances (SR) can be an indicator of global thunderstorm activity in this case. Therefore it is possible to expect, that there is certain dependence SR intensity on the Sun activity state. However, this problem is studied till now insufficiently.

## **Low atmosphere, ozone**

Diurnal and seasonal variations of intensity ANEMF in the first SR frequency (about 8 Hz, SR-1), measured in Polar geophysical institute of Russian Sciences Academy "Lovozer" station ( $67,97^{\circ}\text{N}$ ,  $35,02^{\circ}\text{E}$ , Kola peninsula), during 2001 and 2007 are viewed below. According to observation in Apatity (Kola peninsula, <http://pgia.ru/CosmicRay/Default.htm>) neutron component of the GCR intensity at the ground level in 2007 (year of the quiet Sun) was about 15 % higher than in 2001 (year of high solar activity). The initial data for every days were separated into 20 minutes intervals with overlap of 50 % for calculation of diurnal variations of amplitude SR-1. Power spectrums for each of them were made by modified Welch's periodograms method.

The analysis indicates, that ANEMF intensity variations measured in the SR-1 frequency on Kola peninsula are representing overall picture of space-time variations basic regularities of global thunderstorm activity, namely: maximum of thunderstorm activity nearly  $16\div18\text{LT}$  and increase of thunderstorms number during summer time in northern hemisphere. According to the existent basic knowledge about behavior regularity of global thunderstorm activity, SR-1 power variations allow to reveal some specific space-time singularities of thunderstorms intensity variations too. In particular, about 06UT the evidently expressed maximum of the SR-1 power is found out. The most probable reason of that can be presence of the thunderstorm center in the west side of central part of the Pacific ocean with an activity maximum in the interval  $21\div22\text{LT}$ . The power of this center some times is less than each of three basic world thunderstorm centers. It's shown, that increase of the solar activity level (the reduction of galactic cosmic rays intensity) causes to increase of SR-1 power, that demonstrates increasing of global thunderstorm activity in this period.

This work was supported by the Fundamental Research Program of RAS Physical Science Department (Project 4.5).

## **Optical quantum amplifiers simple realization**

V.V. Bertsev, L.A. Petrunkin, D.N Glebovsky (*St.- Petersburg State University Center for Social Assistance Scientifically-Productive Division, Chemistry and Physics Section Interference Spectroscopy Laboratory*)

The report concerns to methods of observation of weak atmospheric and auroral emission at acceptable level of signal/noise ratio. A possibility to realize a quantum amplifier to register low light level intensity by laser amplifier is under discussion. The main idea is that including of negative feedback into a quantum generator leads to its transformation in quantum amplifier.

In our experiment He-Ne optical quantum generator (laser) LGN-105 has been used. The feedback was realized by special addition mirror in the LGN-105. In this situation we had no induced radiation at laser working wavelength (632.8 mm), i.e. negative feedback is 100% at this frequency (472.3 THz). After that we have closed additional mirror (by hand, glass, black paper, metal). In this case negative feedback would be 0%; consequently we have seen laser radiation at wavelength 632.8 mm (the case of isolated laser). Thus we have realized optical quantum amplifier at 472.3 THz. Energy amplification of this type amplifier is more than  $10^{12}$ .

If we close additional mirror by fluoroplastic (teflon) than visible generation is absent (full transparency at  $3.39\mu$ , 100% negative feedback). If we pass methane between laser and additional mirror, visible generation appears (absorption at  $3.39\mu$  is present, negative feedback is attenuated). Thus realization of the quantum amplifier may be simple and high sensitivity methods for auroral and nightglow emissions registration. Comparison of the traditional methods used devices with photo-cathode and CCD sensors is done. Possibility of detection the low-level methane concentration is proposed. This kind of measurements could be useful in atmospheric research.

## **Altitude distribution of air temperature in the Khibiny massif and mesoclimate zoning**

V.I. Demin (*Polar Geophysical Institute, Apatity, Russia*)

Meteorological observation data in the Khibiny massif were corrected to common period. Typification of station locations was carried out for estimation of data representativeness. The found functions of the altitude distribution of the air temperature explain more than 95% of the spatial variability of temperature in the region. The results were used for mesoclimatic zoning of the Khibiny. The mesoclimatic zone map was created using GIS based software.

## **Air temperature dynamics in the Kola Peninsula and determination of optimal time period for calculation of climatic parameters**

V.I. Demin (*Polar Geophysical Institute, Apatity, Russia*)

Dynamics of the air temperature in the Kola Peninsula were studied. The difference between the mean monthly temperatures of the previous and following decades can reach to 1-3°C. The increase of the calculation period up to 30 years does not allow finding more stable statistical characteristics too. There is necessity of prolonged periods (50-80 years). However the long-term climate changes come into particular prominence during these prolonged periods. Temperature variations cause the nonstationarity of series and its difference from the Markov process because of the long-term tendency to the warming. This fact gives rise to problem for determination of optimal time period which is necessary for calculation of the stable mean climatic features that use in the economic activity.

## **Surface ozone variations during snowstorm and drifting snow**

V.I. Demin, M.I. Beloglazov (*Polar Geophysical Institute, Apatity, Russia*)

The relation between the ozone concentration and the wind snow removal was studied on the assumption that the corona discharge is possible close to snowflake during snowstorm because of the strong local electrical field amplification at the end of dendritic crystals.

The data of ozone and the horizontal snow transfer measurements at the Lovchorr Mountain during snowstorm and drifting snow were used. The effect of this possible process of ozone generation in the surface layer has not been detected.

## **Mountain and valley circulation in the Khibiny mountains**

V.I. Demin, M.I. Beloglazov (*Polar Geophysical Institute, Apatity, Russia*)

The conditions for appearance of the mountain-valley circulation in the Khibiny Mountains are unfavorable as a whole because of geographical location. However the question on its presence in the literature remains open. First and foremost it is caused by deficient sensitivity of the standard techniques of the wind data processing.

The wind observations at the top of Lovchorr Mountain were analyzed for the detection of the mountain-valley circulation in the Khibiny. The index of periodicity of wind was calculated for every season as sum of difference of deviations from norm of wind recurrences of opposite directions. Some grouping of main wind directions during day was detected that reveals the weak mount-valley circulation. The presence of the mount-valley circulations in summer detected by ozone variations at the Lovchorr Mountain too. However the contribution of the mountain and valley circulation to the ozone variations is less than 1.5 ppb.

## **Ozone and turbulence in the tropo-stratosphere from simultaneous radar and ozonesonde measurements in Japan and Indonesia**

N.M. Gavrilov<sup>1</sup>, S. Fukao<sup>2</sup>, M. Fujiwara<sup>3</sup>, H. Hashiguchi<sup>2</sup>, T. Koide<sup>4</sup>, Mamoru Yamamoto<sup>2</sup> and Masayuki Yamamoto<sup>2</sup>

<sup>1</sup>*Saint-Petersburg State University, Atmospheric Physics Dept., St. Petersburg, Russia*

<sup>2</sup>*Kyoto University, Research Institute for Sustainable Humanosphere, Kyoto, Japan*

<sup>3</sup>*Hokkaido University, Graduate School of Environmental Earth Science, Sapporo, Japan*

<sup>4</sup>*Japanese Meteorological Agency, GEMD, Ozone Layer Monitoring Office, Tokyo, Japan*

Results are presented of the analysis of simultaneous observations of atmospheric mesoscale dynamics with MST radars in Shigaraki, Japan (35°N, 136°E) and of ozone in the tropo-stratosphere with ozonesondes in Tsukuba, Japan (36°N, 140°E), also in West Sumatra, Indonesia (0.2 S, 100.3 E). From the World Ozone Data Centre we selected 236 ozonesonde profiles measured in Tsukuba at approximately same latitude as that of Shigaraki at the days of MU radar observations during years 1986 - 2007. The ozonesondes give information about vertical profiles of ozone and temperature at altitudes up to 30 km. Simultaneous measurements are used to study height structure and temporal variations of tropospheric and stratospheric ozone and their relations to variations of dynamical characteristics of the atmosphere during the experiment. Particular attention is given to clarification of the role of turbulent diffusion and

## **Low atmosphere, ozone**

mesoscale dynamics in the tropo-stratospheric ozone exchange. A broad region around the tropopause was dynamically active. Maxima of turbulent diffusivity were observed at 8 - 14 km altitude. Such maxima may produce vertical turbulent ozone fluxes across the tropopause with magnitudes comparable to those required for the global ozone budget. There are some differences in turbulent transport of ozone in the tropo-stratosphere at middle and low latitudes.

## **High resolution spectroscopic measurements and theoretical absorption spectra of the O<sub>2</sub> atmospheric system**

V. Guineva<sup>1</sup>, R. Werner<sup>1</sup>, I. Vince<sup>2</sup>

<sup>1</sup>*Solar-Terrestrial Influences Laboratory, Bulgarian Academy of Sciences, Stara Zagora Department, Bulgaria*

<sup>2</sup>*Astronomical Observatory, Belgrade, Serbia*

The rotational absorption lines from the P branch of the molecular oxygen atmospheric system (1,0) band (687 nm - 697 nm) have been used for the effective temperature evaluation. Ground based spectroscopic observations have been performed during June/July 2006 at the solar telescope of Belgrade Astronomical Observatory. A spectral resolution of about  $10^5$  has been achieved. The linear dispersion is 20.8 mm/nm (about 900 pixels/nm) at  $\lambda \approx 690$  nm. The CCD camera's chip covers about 0.4 nm of the spectrum and one doublet can be observed at a time. A set of observations, consisting of 20 measurement days, were performed. Every observational set consists of the CCD spectrograms centered at the wavelengths of the chosen 13 line doublets with rotational quantum numbers from 1 to 25. The signal to noise ratio has been estimated about 400. A synthetic spectrum of the (1,0) band has been created based on line-by-line calculations. Typical summer temperature profiles have been used. The theoretical equivalent widths have been computed. The theoretical and measured line profiles and their equivalent widths have been compared. A good agreement has been obtained in all cases taking into account the presence of water vapour lines. The dependence of the equivalent widths on the rotational quantum number has been worked out assuming strong absorption. It allows the evaluation of the effective atmosphere temperature. The possible contaminations in some cases are discussed. The theoretical estimates and the measurement results have been examined.

## **Millimeter-wave measurements of the variability of the mesospheric ozone in polar latitudes**

A.A. Krasilnikov, L.M. Kukin, Y.Y. Kulikov, V.G. Ryskin (*Institute of Applied Physics, Russian Academy of Sciences, Nizhny Novgorod, Russia*)

The observations were made with a ground-based millimeter wave instrument – mobile ozonometer [1] at Apatity (67°N, 35°E), measuring the thermal emission line in the pure rotational spectrum  $6_{1,5} - 6_{0,6}$  transition of ozone at the resonance frequency 110836.04 MHz. The measurements of spectra of atmospheric emission were carried out by the method of its calibration on hot and cold reference loads. Measurements of ozone vertical profiles (altitudes 22-60 km) from 20 to 28 April, 2007 were going on. The irregularity of diurnal variations mesospheric ozone is found out. Our data on behaviour O<sub>3</sub> at height of 60 km are compared to measurements of a German microwave spectrometer which is installed on Ny Alesund, Svalbard (79°N, 11°E). For an explanation of an irregularity of a daily course the information about the charged particles precipitation in the upper atmosphere is involved.

The study was supported by the grants 06-05-64734, 07-05-10042 of Russian Foundation for Basic Research.

1. Y.Y. Kulikov, A.A. Krasilnikov, A.M. Shchitov, New mobile ground-based microwave instrument for research of stratospheric ozone (some results of observation), The Sixth International Kharkov Symposium on Physics and Engineering of Microwaves, Millimeter, and Submillimeter Waves (MSMW'07) Proceedings, Kharkov, Ukraine, June 25-30, 2007. V.1, P. 62-66, 2007.

## The response of the ozone and dioxide of nitrogen of the middle atmosphere to the solar irradiance variability during total eclipse August 1, 2008 in Siberia (mountain Altai)

Y.Y. Kulikov<sup>1</sup>, M.B. Emelyanov<sup>1</sup>, A.A. Krasilnikov<sup>1</sup>, L.M. Kukin<sup>1</sup>, L.V. Lubyako<sup>1</sup>, A.V. Poberovskiy<sup>2</sup>

<sup>1</sup>*Institute of Applied Physics, Russian Academy of Sciences, Nizhny Novgorod, Russia*

<sup>2</sup>*Institute of Physics, University of St.-Peterburg, St.-Peterburg, Russia*

The microwave observations were used portable ozonometer (observation frequency 110.8 GHz, single-sideband noise temperature 2500 K) and heterodyne receiver at frequency 93 GHz with double-sideband noise temperature 1000 K to for definition of tropospheric attenuation.

The measuring procedure of atmospheric transparency on thermal emission was method of a variation of zenith distance. Besides in the program of observation of a solar eclipse small-sized spectrometer Ocean Optics HR4000 for measurement of dioxide of nitrogen ( $\text{NO}_2$ ) was involved.

It is the diffracted spectrometer with the spectral resolution 0.6  $\text{nm}$  in the region of a spectrum 398-607  $\text{nm}$ . Technique of definition of  $\text{NO}_2$  total content is measurements of atmospheric scattering of sunlight coming of zenith. Time of registration of one spectrum there is from 15 ms up to 60 s depending on intensity of a light stream. Duration of measuring campaign was from July, 26 on August, 6, 2008. Microwave ozonometer was located in settlement Jodro (50.4°N, 87.0°E) at Chuisky trakt, height above sea level 800 m. The receiver on frequency 93 GHz and the infrared spectrophotometer were at height of 2200 m on distance about 6 km from Jodro. As a result of observations the data on variations mesospheric ozone and  $\text{NO}_2$  total content up to, in time and after a total solar eclipse are received. In particular, to fix increasing of the  $\text{NO}_2$  total content during an eclipse. The unique data about variations of a transparency of the lower atmosphere are received during an eclipse in a millimeter wave band.

The study was supported by the grants 06-05-64734, 08-05-10047 of Russian Foundation for Basic Research.

## Peculiarity of behavior of temperature in St.-Petersburg during last 25 years

A.A. Lubchich (*Polar Geophysical Institute, Apatity, Russia*)

The monthly average temperature of air in St.-Petersburg since 1775 is studied. It is shown that over last 25 years the pace of warming increases in all months with the exception of November. The temperature during a winter period grows rather fast in comparison with a summer (e.g., over 250 years the temperature of air increased by 4.5 degrees in January in comparison with 0.8 degrees in August). Over 20 century, the correlation of temperature and its spectra in St.-Petersburg, Petrozavodsk, Kandalaksha, and Murmansk is analyzed (see Figures 4-5 on the poster). The possible dependence of temperature changes from variations of the solar and magnetic activity is discussed. The behavior of daily average temperature of January in St.-Petersburg over last 100 years is also analyzed. The daily temperature of January averaged over 100 years monotonously decreases, varying from  $-6.4$  to  $-8.2^\circ\text{C}$ . Any significant peculiarities in its behavior (e.g., so-called Christmas frosts or Epiphany frosts) are not found. However, extremely cold days with daily mean temperature below  $-30^\circ\text{C}$  are on January, 9-17<sup>th</sup>.

## Recent progress in the global electric circuit research

E.A. Mareev (*Institute of Applied Physics, Russian Academy of Sciences, 603950 Nizhny Novgorod, Russia*)

The global atmospheric electric circuit, i.e. the quasi-stationary current contour supported by the operation of different (primarily thunderstorm) generators over the globe, being an inherent part of the Earth's environment, occupies a unique place at the interface between the lithosphere and ionizing gaseous envelopes – ionosphere and magnetosphere. It forms due to continuous operation of ionization sources providing the exponential growth of conductivity in the lower atmosphere, from one hand, and to continuous operation of thunderstorm generators providing a high rate of electrical energy generation and dissipation in the troposphere. Therefore, the global circuit is upon the influence of both geophysical and meteorological factors, and can serve as a convenient framework for the analysis of possible inter-connections between the atmospheric electric phenomena, climatic processes and solar-terrestrial coupling. Recent experimental and theoretical studies allow deeper understanding of global electric circuit operation. This talk summarizes some recent results and outstanding problems in this field.

The progress in the global circuit operation is connected first of all with the better description of the electric sources in the circuit and their contribution to the current and energy balance. One of the most interesting problems is the role of mesoscale convective systems (MCS). It was shown recently that MCS stratiform regions make an especially large current contribution to the global circuit. On the other hand, stratiform regions of MCS are characterized by

## **Low atmosphere, ozone**

enhanced rate of powerful positive flashes, which are known to correlate with sprites. The generation of extensive layers of positive charge in thunderstorms, meteorological conditions for their formation and their abundance on the globe are intriguing problems of atmospheric electricity.

The lifetime of electric energy in the atmosphere is introduced and investigated as the total electric energy of the atmosphere related to the total mean rate of electric energy dissipation. This lifetime, as determined from general estimations and convenient analytical expressions, turns out to be very small – from about 10 to about 100 seconds, depending on the assumptions on the control parameters of principal sources in the global electric circuit. In particular the energy lifetime is less than the relaxation time of the “global condenser” and field relaxation time near the ground surface.

A series of new numerical models has been elaborated allowing the description of nonstationary and electromagnetic processes in the global circuit. We have examined in particular the way in which different types of lightning flashes, both cloud-to-ground (CG) and intracloud (IC) flashes, drive current in the global circuit. A numerical model of the transient electric field due to CG and IC lightning flashes and their Maxwell relaxation (slow transients) is developed. The electric field ( $E$ ) and current distributions, the decay time of  $E$ , and the total charge transferred to the ionosphere and the ground are calculated. Because of the slow transients, only a portion of the charge neutralized by a flash contributes to the global circuit, with the efficiency depending on the altitudes of the lightning charges. Typical CG flashes have efficiencies of 55-75%, and typical IC flashes have 5-15%. Total current estimations of the combined CG and IC slow transient processes in the global electric circuit range from 50-400 A.

A problem of distinguishing between the global and local variations of the electric field and current in the global atmospheric electric circuit is a long-term fundamental problem of atmospheric electricity. Synchronous changes of the aeroelectric field at widely spaced stations could serve as a direct manifestation of the global operation of the circuit. Synchronous observations of the electric field have been performed in summer periods of 2005 - 2008 at three stations, spaced at the distances 100 to 370 km each from another. Demonstrating an occasional presence of the diurnal variation over the land, these results show clearly the coupling of electrodynamic perturbations with the regional atmospheric dynamics, operation of convective generators and electro-aerodynamical turbulence of the lower atmosphere.

## **A simulation study of the transformation of circumpolar vortex flows of the lower and middle atmosphere during the period from January to June**

I.V. Mingalev, K.G. Orlov, and V.S. Mingalev (*Polar Geophysical Institute, Apatity, Russia, e-mail: mingalev@pgia.ru*)

The mathematical model of the global neutral wind system of the atmosphere, developed earlier in the Polar Geophysical Institute, is utilized to investigate the transformation of the planetary circulation of the lower and middle atmosphere during the period from January to June. The utilized model produces three-dimensional global distributions of the zonal, meridional, and vertical components of the neutral wind velocity and neutral gas density at the levels of the troposphere, stratosphere, mesosphere, and lower thermosphere. The characteristic feature of the model is that the vertical component of the neutral wind velocity, as well as horizontal components of the neutral wind, are obtained by means of a numerical solution of the appropriate momentum equation for a viscous gas without any simplifications of this equation, with the hydrostatic equation being not used. Moreover, the model does not include the internal energy equation for the neutral gas. Instead, the global temperature field is assumed to be a given distribution obtained from the NRLMSISE-00 empirical model. In the model calculations, global distributions of the atmospheric parameters were computed for conditions corresponding to six dates, which belong to six different months beginning from January. The results of modeling indicate that the horizontal non-uniformity of the neutral gas temperature, which is distinct in different months, influences essentially on the transformation of circumpolar vortex flow of the lower and middle atmosphere during the period from January to June.

This work was partly supported by the Basic Research Program No.16 of the Presidium of the Russian Academy of Sciences and by the RFBR grant 08-01-91304-Ind.

## The ionization of the Earth's atmosphere and ozone layer's variations after solar proton events during January 2005

I.N. Myagkova<sup>1</sup>, A.V. Kukoleva<sup>2</sup>, A.A. Krivolutsky<sup>2</sup>, T.Yu. Vyushkova<sup>2</sup>, A.A. Kuminov<sup>2</sup>

<sup>1</sup>*Scobeltsyn Institute of Nuclear Physics, MSU, Moscow, Russia*

<sup>2</sup>*Central Aerological Observatory Dolgoprudny, Russia*

Results of calculations of ionization and ozone response variations polar regions of atmosphere of the Earth at altitudes from zero to 120 km caused by solar protons, generated in the flares occurring on the Sun in second half of January, 2005 are presented. Differential spectra of solar protons were calculated according to GOES-10 and CORONAS-F satellites data.

Solar flares produce the intensive fluxes of high-energy protons and strongly influence on the near-Earth environment and Earth's atmosphere. Solar protons penetrating into high latitudes in the Earth's atmosphere cause its ionization and transform its chemical compound. The response of an ozone layer on additional NO<sub>x</sub> and HO<sub>x</sub> manufacture the middle atmosphere depends not only on solar protons intensity, but also on solar particle spectrum, and modeling of the processes in atmosphere of the Earth, based on experimental data about flux and spectra of solar particles is an actual problem.

It was shown that solar proton events of January, 2005 have strongly influenced a condition of high-altitude atmosphere of the Earth. The obtained results of the modeling based on the polar low-altitude satellite CORONAS-F data (which was during the considered period at altitude about 400 km) are significantly differ in comparing with ones based on the data of geostationary satellite GOES-10. It is probably caused by distinction of observable fluxes and spectra of protons (in particular with 1-5 MeV energy) at the geostationary orbit and at low (400-500 km) altitudes.

This work was partly supported by RFBR foundation grants 07-02-92004-HHC\_a.

## Study of Q-type ELF bursts in the Shuman resonance frequency range.

V.V. Pchelkin, M.I. Beloglazov, A.N. Vasiljev, A.I. Voronin (*Polar Geophysical Institute RAS, Apatity, Murmansk region, Russia*)

Q-type ELF bursts are studied by using the data of ELF range magnetometer of the observatory Lovozero. The selection of the bursts has been performed with a specially designed program of intellectual search. For the selected cases, the estimates of the Earth-ionosphere resonator quality, as well as of the first resonator mode, have been made. They are compared with the analytical estimates and with the results of Fourier analysis. The directions of signal propagation have been determined for all cases, and their distribution function was constructed.

## Vertical profiles of NO<sub>x</sub> in the middle atmosphere at high latitudes during quiet period and solar proton events

A.B. Ponomarev<sup>1</sup>, L.I. Miroshnichenko<sup>2</sup>, A.S. Kirillov<sup>1</sup>

<sup>1</sup>*Polar Geophysical Institute, Apatity, Murmansk Region, Russia*

<sup>2</sup>*IZMIRAN, Troitsk, Moscow Region, Russia*

A one-dimensional time-dependent model of the middle atmosphere is applied in the calculation of vertical profiles of NO<sub>x</sub> at high latitudes. The results of the calculation are compared with the data of satellite and balloon-borne measurements. Also we investigate periods of enhanced production of NO<sub>x</sub> in the middle atmosphere during very intensive solar proton events (SPE), especially due to invasion of intensive fluxes of high-energy solar cosmic rays (SCR). Our study is based on the model of upper limit spectrum (ULS) for SCR. Energy distribution of solar cosmic rays is suggested to be a power-law function with a changing spectral index up to maximum expected energies of 100 GeV. Model calculations of enhanced NO<sub>x</sub> concentrations in the middle atmosphere are made for different periods of time in the course of the events for three energy intervals: 10 MeV- 100 MeV, 100 MeV - 1 GeV, 1 GeV - 10 GeV.

## **Low atmosphere, ozone**

### **Response of the atmosphere-ocean system to solar activity variations of different time scales**

O.M. Raspopov<sup>1,3</sup>, V.A. Dergachev<sup>2</sup>

<sup>1</sup>*St. Petersburg Filial of Pushkov Institute of Terrestrial Magnetism, Ionosphere and Radiowave Propagation of RAS, St. Petersburg Russia, oleg@or6074.spb.edu*

<sup>2</sup>*Ioffe Physical-Technical Institute of RAS, St. Petersburg, Russia*

<sup>3</sup>*Polar Geophysical Institute of Kola Scientific Center of RAS, Murmansk, Russia*

Analysis of the influence of solar activity variations on the lower atmosphere involves consideration of atmospheric effects of either short-term solar activity variations (hours or days) or long-term solar cyclicity (tens and hundreds of years). Differences in development of the physical processes in the atmosphere associated with solar activity (SA) variations of different time scales are often ignored when the data are treated. However, it is important to bear in mind, for example, that in the processes caused by long-term SA variations a significant role is played by atmospheric circulation leading to regional responses of atmospheric parameters to global solar forcing. In the case of decadal variations (11- and 22-year solar cycles) the solar signal can interact with inherent noises in the atmosphere-ocean system of the same frequency range. Experimental data show that this interaction can result in a 2-3-fold solar signal amplification.

### **Effects of solar activity and cosmic rays on the lower atmosphere (on memory and the 75th anniversary of PGI seminar founder prof. M.I. Pudovkin)**

O.M. Raspopov<sup>1,3</sup>, S.V. Veretenenko<sup>2</sup>

<sup>1</sup>*St. Petersburg Filial of Pushkov Institute of Terrestrial Magnetism, Ionosphere and Radiowave Propagation of RAS, St. Petersburg Russia, oleg@or6074.spb.edu*

<sup>2</sup>*Ioffe Physical-Technical Institute of RAS, St. Petersburg, Russia*

<sup>3</sup>*Polar Geophysical Institute of Kola Scientific Center of RAS, Murmansk, Russia*

A review of the data obtained by M.I.Pudovkin, his co-workers and followers on the problem of the influence of solar activity on atmospheric processes and climate change are presented. Later research activities in this field are mentioned. Attention is drawn to the necessity to include into consideration the atmospheric circulation when analyzing the formation of the global pattern of the atmosphere-ocean system response to solar forcing.

### **Peculiarities of connection between space-time variations of precipitation and geomagnetic activity**

O.A. Rubtsova, V.A. Kovalenko, S.I. Molodykh (*Institute of Solar-Terrestrial Physics SB RAS olga@iszf.irk.ru*)

Currently mechanisms of solar activity effects on weather and climate have been discussed. In [1,2], authors proposed a physical mechanism of solar activity effects on climatic characteristics and the atmospheric circulation through the atmospheric electricity. A model of the solar activity effect on climatic characteristics of the Earth's troposphere was elaborated on the basis of the mechanism under consideration. The model key concept is the heliogeophysical disturbance effect on the Earth climatic system's parameters, which influence energy flux going from the Earth to space in high-latitude areas. When the solar activity increases, radiation cooling of high-latitude regions decreases, thermobaric field restructures, average meridian gradient of temperature between polar and equatorial regions decreases, defining the atmospheric circulation. Precipitation is a quantitative and the most sensitive indicator of the atmospheric circulation change.

NCEP/NCAR Reanalysis and CMAP data were used to analyze particularities and regularities of long-term variations in amount of precipitation in 1950-2007. Global decrease in amount of precipitation was found to dominate till late 1990s. It started increasing only 10 years ago. Peculiarities of distribution and long-term variations in amount of precipitation in different latitudes and longitudes were also considered.

Correlation analysis of connection between the amount of precipitation and the geomagnetic activity and atmospheric circulation was carried out. Peculiarities of the space-time distribution of correlation coefficients were studied. The connection was found out to depend on a season. Cold periods in the northern hemisphere were characterized by a direct relationship between the geomagnetic activity and amount of precipitation in high latitudes, whereas a negative relationship was observed in subequatorial latitudes.

One of the main statements of our model is corroborated by the results obtained from the analysis of changes in the geomagnetic activity, troposphere's thermobaric characteristics and precipitation.

1. Rubtsova O.A., Kovalenko V.A., Molodykh S.I. Isolated heliogeophysical disturbances in the high-latitude troposphere // Optika Atmosfery i Okeana, 2008. V. 21, No. 6, P. 532-535.
2. Zherebtsov G.A., Kovalenko V.A., Molodykh S.I., Rubtsova O.A., and Vasil'eva L.A. Impact of helio-and geophysical disturbances on thermobaric and climatic characteristics of the Earth's troposphere // Cosmic Research, 2008. V. 46, No. 4, P. 358-366.

### **Solar wind influence on atmosphere processes in winter Antarctica**

O. Troshichev, L.V. Egorova, A.S. Janzhura and V.Ya. Vovk (*Arctic and Antarctic Research Institute, St.Petersburg, 199397, Russia*)

Galactic cosmic rays altered by the solar wind are traditionally regarded as the most plausible agent of the solar activity influence on the Earth's atmosphere. Meanwhile, it is well known that severe reductions in the galactic cosmic rays flux, known as Forbush decrease (FD), are caused by the solar wind of high speed and density, which sweeps the galactic cosmic rays on its way. Since the FD beginnings are registered at the Earth's orbit simultaneously with dramatic disturbances in the solar wind, the atmospheric effects, assigned to Forbush decreases, can be, in reality, result of the solar wind influence on the atmospheric processes. The paper presents the summary of the experimental results demonstrating the strong influence of the interplanetary electric field on atmospheric processes in the central Antarctica, where the large-scale system of vertical circulation is formed during the winter seasons. The influence is realized through acceleration of the air masses, descending into the lower atmosphere from troposphere, and formation of cloudiness above the Antarctic Ridge, where the descending air masses income into the surface layer. The acceleration is followed by sharp increase of the atmospheric pressure in the near-pole region, which gives rise to the katabatic wind strengthening above the entire Antarctica. The cloudiness formation is resulted in the sudden warmings in the surface atmosphere, since the cloud layer efficiently backscatters the long wavelength radiation going from the ice sheet, but does not affect the adiabatic warming process of the descending tropospheric air masses. When drainage flow strong strengthening the circumpolar vortex about the periphery of the Antarctic continent decays, the surface easterlies typical of the coast stations during the winter season are replaced by southerlies and the cold Antarctic air masses rush in the Southern ocean.

### **Polarization detection of dust and aerosol in the middle and upper atmosphere**

O.S. Ugolnikov, I.A. Maslov (*Space Research Institute, Moscow, Russia*)

The work is based on the twilight method of atmosphere sounding. During the different stages of twilight the sky background is formed by the scattering of solar emission at different altitudes in the atmosphere and it helps to investigate the atmosphere layers separately. Polarization measurements allow to reduce the large contribution of multiple scattering and to expand the information on the scattering properties. Polarization of the twilight sky is sensitive to the dust and aerosol in the different layers of the atmosphere. Usually they decrease the value of polarization during the corresponding stage of twilight.

The level of stratospheric aerosol is quite low in the most part of time. It increases, in particularly, after the strong volcanic eruptions. Sufficient contribution of aerosol scattering in the stratosphere was detected above the observation point (Crimea, Ukraine) in December, 2006. The comparative analysis of a number of twilights allowed to estimate the aerosol to molecular scattering ratio (0.1-0.2) and the polarization of aerosol scattering by the angle 90° (0.28). Stratospheric aerosol is possibly related with Rabaul volcano eruption in October, 2006.

The dust scattering is seen in the mesosphere after the maxima of major meteor showers. Polarization analysis helped to detect the Leonids dust inflow in November, 2002, at the altitude above 90 km and its slow shift downwards during the following days.

### **Lunar eclipses optical profiles: Aerosol, water vapor and ozone relations**

O.S. Ugolnikov, I.A. Maslov (*Space Research Institute, Moscow, Russia*)

The work contains the review of 5 lunar eclipses observations in 2004-2008. Holding the surface photometric measurements of the Moon in the umbra, penumbra and outside the penumbra, the optical map of the umbra is built. This map is reflecting the optical conditions of the limb atmosphere regions where the solar emission is refracting to the shadow regions. The geometry of the eclipse gives the possibility to investigate the different atmosphere layers

## Low atmosphere, ozone

above the limb locations analogous to the space limb measurements. Here the role of spacecraft is played by the Moon.

The measurements in the near-IR range outside the atmosphere gases absorption bands show the umbra inhomogeneity and difference with the results of gaseous model calculations. This difference is related with the aerosol extinction that can be retrieved from the data. Results show the increase of the aerosol amount in the upper troposphere above the equatorial continental locations for the eclipses of May, 04, 2004 and March, 03, 2007. Equatorial maritime locations contain less aerosol, as it was seen during the eclipses of February, 21 and August, 16, 2008. The correlation of aerosol and cloud clusters is clearly seen worldwide. The regions of high aerosol concentration in the southern polar hemisphere also coincide with the minima of total ozone amount. In the northern polar atmosphere this relation is unseen. The fact can be related with the different polar stratospheric vortex activity in two hemispheres.

The measurements in the water vapor absorption band conducted during the eclipse of March, 03, 2007, show the good correlation of results with the space measurements of total water vapor amount. This relation allowed to determine the scale of water vapor vertical distribution, that is close to 1.3 km, slightly varying with the latitude.

## Near tropopause inter-annual ozone variation at European high latitudes

R.Werner<sup>1</sup>, K. Stebel<sup>2</sup>, H.G. Hansen<sup>3</sup>, U.-P. Hoppe<sup>4</sup>, M. Gausa<sup>5</sup>, R. Kivi<sup>6</sup>, P. von der Gathen<sup>7</sup>, Y. Orsolini<sup>2</sup>, N. Kilifarska<sup>8</sup>

<sup>1</sup>*Solar-Terrestrial Influences Laboratory, Bulgarian Academy of Sciences, Stara Zagora Department, Stara Zagora, Bulgaria*

<sup>2</sup>*Norwegian Institute for Air Research (NILU), Kjeller, Norway*

<sup>3</sup>*Norwegian Institute for Air Research (NILU), The Polar Environmental Centre, Polarmiljøsenteret, Tromsø, Norway*

<sup>4</sup>*Norwegian Defence Research Establishment (FFI), Kjeller, Norway*

<sup>5</sup>*Andoya Rocket Range, ALOMAR, Andenes, Norway*

<sup>6</sup>*Arctic Research Centre, Finnish Meteorological Institute, Sodankylä, Finland*

<sup>7</sup>*Alfred Wegener Institute for Polar and Marine Research (AWI), Potsdam, Germany*

<sup>8</sup>*Geophysical Institute, Bulgarian Academy of Sciences, Sofia, Bulgaria*

The geographic area at high latitudes beyond the polar circle is characterized by long darkness during the winter (polar night) and by a long summertime insolation (polar day). In consequence the polar vortex is formed and the surrounding it strong polar jet is characterized by a strong potential vorticity gradient representing a horizontal transport barrier. The ozone dynamic at the lower and middle stratosphere is controlled by both chemical destruction processes and transport processes.

To study the inter-annual ozone variation at high latitudes ozone vertical distributions are examined, gathered from the Arctic Lidar Observatory for Middle Atmosphere Research (ALOMAR) (69.3°N, 16.0°E,) station at Andenes and of ozone soundings of the stations at Sodankylä (67.4°N, 26.6°E) and at Ny-Alesund (78.9°N, 11.9°E). The data sets cover the time period from 1994 up to 2004. We find a second ozone maximum near 13 -15 km, between the tropopause and the absolute ozone maximum near 17- 20 km. The maximum is built up by the combination of air mass transport and chemical ozone destruction, mainly caused by the NO<sub>x</sub> catalytic cycle, which begins after the polar night and intensifies with the increasing day length. The formation of a troposphere inversion layer is observed. The inversion layer is thicker and reaches higher altitudes in winter than in summer. However the temperature inversion during summer is stronger. The formation of an enhanced ozone number density is observed during the spring-summer period. The ozone is accumulated or become poor by synoptic weather patterns just above the tropopause from spring to summer. In seasonal average an ozone enhancement above the tropopause is obtained.

The stronger temperature inversion during the summer period inhibits the vertical stratosphere-troposphere exchange. The horizontal advection in the upper troposphere and lower stratosphere is enforced during the summer. The combination of these mechanisms generates a layer with a very low ozone number density above the troposphere inversion layer subsisting from June/July up to the late autumn.

## **Total ozone variability over the Russian territory during the period 1973-2008**

A.M. Zvyagintsev<sup>1</sup>, L.B. Ananiev<sup>2</sup>, and A.A. Artamonova<sup>2</sup>

<sup>1</sup>*Central Aerological Observatory, Dolgoprudny, Russia*

<sup>2</sup>*Hydrometeorological Research Center of Russia, Moscow, Russia*

Based on the data from the ground M-124 ozonometer network and TOMS/SBUV satellite-borne observations, total ozone (TO) variability over Russia during 1973-2008 is analyzed. TO time variations are well enough described by a regression model including a piecewise linear trend and the affecting factors such as solar activity, Quasi-Biennial Oscillation (QBO) of the zonal equatorial wind and Arctic Oscillation (AO). During the period 1979-1995, a negative TO trend was observed all over the Russian territory, while during 1996-2007, a positive trend was observed, which was close to the former in absolute value. The determination coefficient of the regression model of the mean-monthly TO anomalies within the zonal belts and separate cells in the mid latitudes of the Northern Hemisphere is 35-80 %. The influence of QBO and AO on TO is essentially different in different seasons, being the most pronounced at the end of the cold season and the slightest at the end of the warm one. The mean December-March AO index considerably determines TO values almost throughout the following months of the current year, especially in the high latitudes of the Northern Hemisphere. The AO may cause TO deficit over the northern areas of Sakha-Yakutia in early spring to reach 40-50 D.U. or more, while the influence of QBO is 1.5 times weaker. The mean annual TO value in 2008 is largely determined by the corresponding AO and QBO values.

## **Surface ozone variations in Moscow and Kyiv**

A.M. Zvyagintsev<sup>1</sup>, I.N. Kuznetsova<sup>2</sup>, E.A. Lezina<sup>3</sup>, Ya.O. Romaniuk<sup>4</sup>, and M.G. Sosonkin<sup>4</sup>

<sup>1</sup>*Central Aerological Observatory, Dolgoprudny, Russia*

<sup>2</sup>*Hydrometeorological Research Center of Russia, Moscow, Russia*

<sup>3</sup>*Moscow Service of Ecology Monitoring (Mosecomonitoring), Moscow, Russia*

<sup>4</sup>*Main Astronomical Observatory of the NAS of Ukraine, Kyiv, Ukraine*

Surface ozone measurements in two megacities, namely Moscow (56 N, 38 E, 190 m a.s.l.) and Kyiv (51 N, 31 E, 120 m a.s.l.), are compared. Seasonal-diurnal variations of ozone and temperature are presented. Ozone temporal series in both cities are similar and according our classification may be referred to ones for semi-polluted non-elevated sites. There are two maximums (in spring and summer) in ozone seasonal variations and only one maximum (in summer) in temperature variations at both sites. The mean ozone concentrations for any time and any day as well as temperatures in Kyiv are higher than appropriate ones in Moscow. The summer ozone maximum can be attributed to photochemical processes. The spring ozone maximum is more likely caused by dynamical/transport processes than by photochemistry. In both cities ozone episodes appear for some adverse meteorological situations which are dangerous for human health. They often are observed in July-August period; their number in Kyiv is higher than in Moscow. A statistical models of ozone concentrations for both cities are created; ozone concentration is presented as regressive function of temperature, relative humidity, wind speed and its direction in planetary boundary layer. Such models can be used for ozone concentration forecasting.

## **Детектирование планетарного числа молний на основе статистического анализа характеристик электромагнитного шума в диапазоне шумановских резонансов**

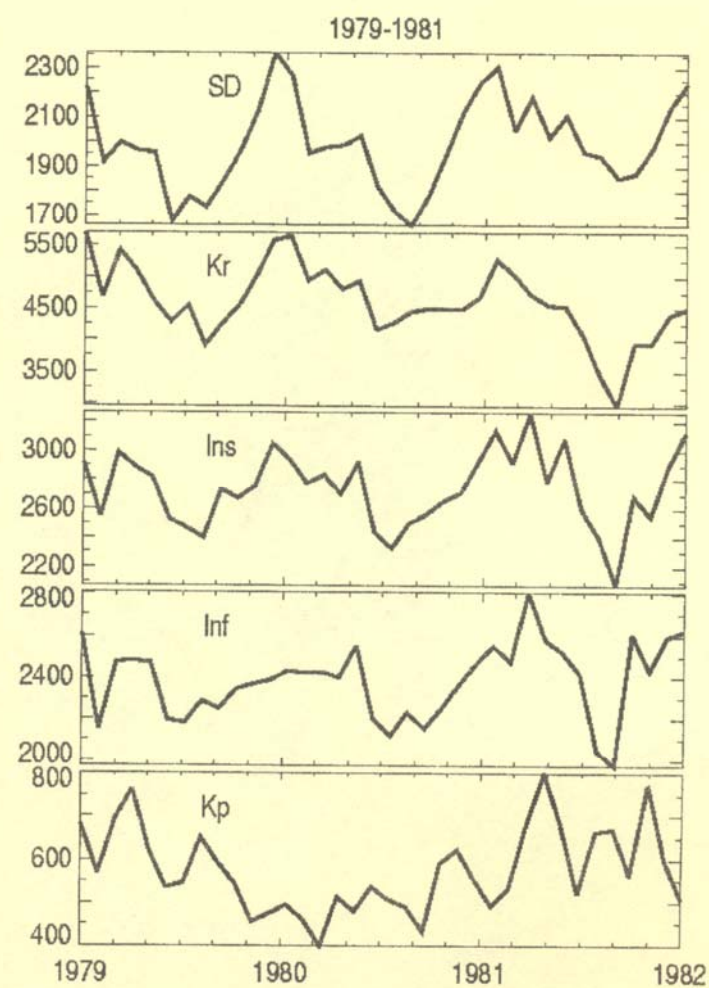
В.Г. Вяткин, В.В. Клименко, Ю.В. Шлюгаев (*Институт прикладной физики РАН, г. Нижний Новгород*)

Число молний в единицу времени в мировых грозовых очагах является важным параметром, характеризующим ЭДС глобальной электрической цепи, а также мощность генератора электромагнитного шума в полости Земля-ионосфера. Обычно подсчет молний производится с борта ИСЗ по числу оптических вспышек. Оптическими вспышками сопровождаются все разряды, включая внутриоблачные и междуоблачные, тогда как основными генераторами ЭДС и шума являются разряды облако-Земля. В данной работе предложен и опробован метод детектирования числа молний в мировых грозовых центрах по статистическим характеристикам э.м. шума, наблюдаемого в полосе 1-30 Гц. Исходя из вида эмпирической функции распределения мгновенных значений шума, имеющей медленно спадающие крылья, задается двухкомпонентная модель источника шума в виде суммы нормального шума и импульсного шума,

### *Low atmosphere, ozone*

состоящего из потока экспоненциально затухающих радиоимпульсов. В рамках заданной модели аналитически вычисляется плотность вероятности мгновенных значений шума. Затем с помощью процедуры минимизации невязки между эмпирическим и расчетным распределениями оптимизируются параметры модели, в числе которых и плотность импульсов в единицу времени. Плотности импульсов, полученные в результате обработки экспериментальных данных ( $\sim 10\text{--}30 \text{ c}^{-1}$ ), с разумной точностью согласуются с числом оптических вспышек детектируемых на ИСЗ.

## *Heliosphere*





## Functional state of human organism depends on intensity of cosmic rays modulated by solar cyclic activity

N. K. Belisheva (*Polar-Alpine Botanical Garden Institute, KSC RAS, Apatity, Russia*)

Composition of peripheral blood and functional state of cardio-vascular system of the healthy examinees were compared in the years with high (1991) and low (2008) Solar cyclic activity (SCA) and, correspondently, high and low geomagnetic activity (GMA), low and high intensity of Cosmic rays (CR). The quantity of stick neutrophils, monocytes, eosinophils, leucocytes in peripheral blood of examinees have been  $0,65 \pm 0,09$ ;  $5,04 \pm 0,36$ ;  $1,70 \pm 0,32$ ;  $5,66 \pm 0,09$ , ( $p < 0,01$ ), correspondently, in the year with high SCA (1991). The means of these indices have increased in the year with low SCA (2008) up to  $3,58 \pm 0,19$ ;  $10,57 \pm 0,20$ ;  $3,78 \pm 0,16$ ;  $6,14 \pm 0,11$  ( $p < 0,01$ ), correspondently. The number of segmented neutrophils, lymphocytes, in opposite, have increased in the years with high SCA ( $50,80 \pm 0,72$ ;  $41,72 \pm 0,75$  correspondently,  $p < 0,001$ ) and decreased in the years with low SCA ( $44,59 \pm 0,75$ ;  $36,51 \pm 0,64$  correspondently,  $p < 0,001$ ). The differences were also found between correlations of cardio-vascular state indices, variations of geomagnetic field and CR in the years with high and low SCA. In result of experimental research we found, that functional state of organism are modulated by "dose" ratio of geomagnetic field (GMF) variations and the secondary component of Cosmic rays (CR). We revealed the possible mechanisms for modulation of organism functional state: 1) Alterative regulation by GMF variations and neutron intensity near the Earth's surface, when the one in a two component has maximum value and other – minimum value. 2) Complementary (additional) regulation, when the values of the GMF variations and neutron intensity near the Earth's surface reciprocally supplement each other. 3) Prevalent regulation by GMF variations or neutron intensity near the Earth's surface, when the one in a two component has predominant significance over other. By comparison of functional state of human blood in the years with high (1991) and low (1996, 2008) SCA we found that the decrease of geomagnetic activity and the increase of intensity of CR impact on composition of peripheral blood. An increase of 20 percent of CR intensity near the Earth space produces the increase of leucocytes, monocytes, eosinophils, stab neutrophils (immature forms of blood cells), the decrease of lymphocytes, segmented neutrophils. Moreover, in the years with high intensity of Cosmic rays on the minimum of SCA, multiple phenomenon, associated with abnormal growth, appearance of nanuses (dwarfs), gigants, morphosis on plant were observed. Similarity effects exposure of plant to ionizing radiation in the result of Chernobyl catastrophe have been discovered on pine, betula, oak in 1987 years. Analogical morphosis have been observed on new born children in result of exposure of Iraq inhabitants to depleted uranium. Because effectiveness of ionizing radiation has not threshold, similar biological effects can be induced by high, low, weak and hyperweak doses of radiation, including the impact of Cosmic Rays. The probability of appearance of different deviations from normal development of organism increases on the minimum of SCA associated with the increase of CR intensity.

## Comparison studies exposure of human organism to cosmic rays in control group and under chronic irradiation by natural radio nuclides

N.K. Belisheva<sup>1</sup>, N.A. Melnik<sup>2</sup>, S.A. Chernouss<sup>3</sup>, O.V. Antonenko<sup>3</sup>, E.V. Perminova<sup>3</sup>, A.L. Kosova<sup>3</sup>, A.N. Vinogradov<sup>4</sup>, T.B. Novikova<sup>5</sup>

<sup>1</sup>*Polar-Alpine Botanical Garden-Institute KSC RAS, Apatity, Russia*

<sup>2</sup>*Institute of Chemistry and Technology of Scarce Elements and Mineral Source, Apatity*

<sup>3</sup>*Polar Geophysical Institute, Apatity, Russia*

<sup>4</sup>*Regional Seismic Centre, Apatity, Russia*

<sup>5</sup>*Hospital with Polyclinic attached to Kola Science Centre RAS, Apatity, Russia*

The aim of investigation was that estimate exposure of human organism to natural ionizing radiation sources, including the secondary component of cosmic rays (CR) near the Earth surface and natural radio nuclides. Research was carried out on the control group of examinees and persons has been exposed to natural radio nuclides. In the course of this study, some morpho-functional characteristics of peripheral blood and indices of cardio-vascular system state were assessed on daily basis through one month on the control group. The assessment exposure of human organism to natural radio nuclides was carried out on medical examination of persons at Institute of Chemistry and Technology of Scarce Elements and Mineral Source. The long time (1976-2008 years) these persons contacted with samples of minerals incorporating natural radio nuclides. Dynamics of functional state of human organism was compared with associated variations of CR, geomagnetic field and atmospheric pressure. The significance correlations were found between CR variations and indices of functional state of peripheral blood in control group and among persons have been irradiated by natural radio nuclides. We found that the number of significance correlations of indices of functional state of peripheral blood with CR were more in control group than

in one of irradiated persons. Average indices of blood functional state of irradiated persons were similar with one manifesting under increase of intensity of CR in control group. Moreover, chronic ionising irradiation transforms the organism sensitivity to external impact and cause a realignment of the blood components with respect to one another. The features of such changes depend on accumulated doses of irradiation and person's organism functional state. Lymphocyte, segmented neutrophiles, stick neutrophils have manifested the most sensitivity to variations of CR intensity in control group, whereas hemoglobin, erythrocytes and thrombocytes were more sensitive in irradiated persons. In addition the correlation between frequencies of heat rhythm, arterial pressure and functional state of peripheral blood as well modulation of cardio-vascular state by the complex of physical agents, including the CR, were shown in control group. The similarity exposure of effects to weak doses of natural radio nuclides and of secondary component of CR near the Earth's surface are discussed.

### **Зависимость состояния лесов Мурманского региона от вариаций гелиогеофизических агентов**

А.А. Алхимчиков<sup>1</sup>, Н.К. Белишева<sup>2</sup>, И.В. Калашникова<sup>2</sup>

<sup>1</sup>Комитет по лесному хозяйству Мурманской области, Мурманск, Россия

<sup>2</sup>Полярно-Альпийский Ботанический Сад-Институт КНЦ РАН, Апатиты, Россия

В работе использовали статистические данные Мурманского комитета по лесному хозяйству о состоянии лесов Мурманской области с 1958 по 2005 г.г. Эти данные включали среднегодовое число лесных пожаров и площади возгорания, а также заболеваемость леса, оцененное по числу очагов поражения болезнями леса. Динамика показателей состояния леса была сопоставлена со среднегодовыми числами Вольфа, интенсивностью нейтронной компоненты космических лучей (КЛ) у поверхности Земли, детектируемой нейтронным монитором (Апатиты, Полярный геофизический институт КНЦ РАН), числом случаев возрастания нейтронной компоненты у поверхности Земли в результате солнечных протонных событий (ground level enhancement –GLE) и интенсивностью GLE, оцененной по количеству станций, зарегистрировавших эти события. Следует отметить, что на качество статистических данных по оценке состояния лесов повлияли события перестройки, поэтому данные 90-х годов и далее имеют значительные погрешности. Тем не менее, сопоставление среднегодовых значений количества и площадей пожаров с 1958 по 2005 г.г. с показателями солнечной активности (СА) и интенсивностью нейтронной компоненты у поверхности Земли выявило между ними значимые корреляции. Оказалось, что число пожаров имеет выраженную периодичность, причем число пожаров возрастает через 5 лет после минимума СА и максимальной интенсивности КЛ на минимуме СА. Коэффициент корреляции с интенсивностью нейтронной компоненты со сдвигом в 5 лет составляет 0,4 ( $p<0,05$ ). Более того, сопоставление числа пожаров с GLE выявило между солнечными протонными событиями, числом и площадью возгораний определенные связи. Так, максимальное число пожаров и площадей возгорания отмечено в 60-е, 70-е годы и 80-е годы, а также тренд возрастания после 90-го года. В 1960 г. было зарегистрировано 5 случаев GLE на 237 станциях, с 1971 по 1973 – 5 случаев GLE, в 1981-1982 г.г. зарегистрировано 5 случаев GLE, а в 1989 г. – 7 случаев GLE. Однако, несмотря на явную сопряженность явлений возгорания леса и солнечных протонных событий, следует думать, что причиной, способствующей лесным пожарам, могли бы служить метеорологические агенты, вариации которых, в свою очередь, обусловлены СА.. Исследование заболеваемости леса и вариаций гелиогеофизических агентов выявило существенные связи между количеством очагов поражения леса определенными болезнями (ржавчина хвои, рак серянка, снежное шютте, сосновая губка, еловая губка, корневая губка) и СА. Оказалось, что максимум заболеваемости приходится на минимум СА при возрастании интенсивности нейтронной компоненты КЛ у поверхности Земли. Так, при среднем числе очагов поражения леса  $3990 \pm 448.4$ , в 1996 г. на минимуме СА число очагов поражения возросло до 176409, что в 44 раза превысило средний уровень заболеваемости леса по Мурманскому региону. Коэффициент корреляции между числом очагов поражения леса и СА составил -0.88 ( $p<0,01$ ), а с показателем интенсивности нейтронной компоненты 0.48 ( $p<0,05$ ). Таким образом, нами выявлена определенная связь между состоянием лесов в Мурманской области и вариациями гелиогеофизических агентов. Однако для выяснения причинно-следственной связи между СА и состоянием лесов требуются дополнительные исследования.

## **Влияние гравитационных возмущений на аномальное поведение человека и высших животных**

В.М. Воробейчиков<sup>1</sup>, О.А. Трошичев<sup>1</sup>, Э.С. Горшков<sup>2</sup>, В. В. Степанов<sup>1</sup>

<sup>1</sup>*Государственное учреждение "Арктический и антарктический научно-исследовательский институт", Санкт-Петербург, Россия*

<sup>2</sup>*Санкт-Петербургский Филиал Института земного магнетизма, ионосферы и распространения радиоволн РАН, Санкт-Петербург, Россия*

К настоящему времени накоплен значительный материал о влиянии Луны на физиологическое состояние организма человека, в зависимости от лунных фаз. В частности, выявлено влияние Луны на течение острых психотических состояний человека, показана связь с различными психическими заболеваниями, эпилепсией, сомнамбулизмом, с суицидными проявлениями, обнаружено влияние лунных фаз на поведенческие реакции здоровых людей, в том числе на асоциальное поведение человека, отмечено влияние Луны на поведение высших животных. Несмотря на то, что исследователи давно обратили внимание на геофизические и погодные факторы, сопровождающие влияние Луны состояние людей, доказать непосредственное влияние Луны на поведение человека и животных представляется сложно задачей. В наших исследованиях впервые доказано существование нового механизма воздействия космических факторов на биологические системы, благодаря чему установлен неизвестный ранее феномен, объясняющий влияние Луны на аномальное поведение человека и животных. Указанный механизм проявляется в том, что в период новолуния и полнолуния под воздействием Луны ускоряется процесс размножения кишечной палочки (*E.coli*) в толстом кишечнике человека и животных, активность которого, в свою очередь, регулируется внешними условиями. В результате этого процесса, в *E.coli* происходит интенсификация метаболизма и, соответственно, скорость поступления ее метаболитов в кровь хозяина, что приводит к нарушениям или сбоям работы жизненно важных систем человека и животных. При этом, процесс метаболизма и поступления метаболитов в кровь происходит в полнолуние значительно интенсивнее, чем в новолуние. Экспериментальные наблюдения за изменениями продолжительности лаг-фазы (*L*) *E.coli* в зависимости от фазы Луны проводились в период с 2002 по 2006 г.г. Предпочтение отдавалось новолуниям и полнолуниям, сопряженным, соответственно, с солнечными и лунными затмениями. Как показали результаты наблюдений, для всех этих событий характерны общие признаки: существенное уменьшение продолжительности *L* с последующим ее восстановлением (полным или частичным); изменение продолжительности *L*, как правило, за несколько часов до наступления наблюдаемой фазы Луны (что исключает связь изменений времени *L* с «экранированием» Солнца); привязанность минимальных значений продолжительности *L* к моментам максимумов событий. Мы показали, что для всех упомянутых событий характерно существенное уменьшение продолжительности *L* с последующим, после прохождения Луной зенита, ее восстановлением. Когда Луна пересекает линию Земля–Солнце позади Земли (полнолуние), *L* сокращается до 1 часа (во время лунного затмения – до 0,5 часа), при этом период уменьшения и последующего восстановления *L* до невозмущенного уровня (*L* ~ 3,5 часа) занимает около 10 часов. Когда Луна пересекает линию Земля–Солнце перед Землей (новолуние), *L* уменьшается до 1,5 часа, но длительность этого уменьшения составляет всего лишь ~ 0,5 часа. Во время солнечного затмения *L* падает до нуля, а период сокращенной *L* длится более 10 часов. Закономерным следствием наблюдаемого сокращения *L* является ускоренное размножение бактерий в экспоненциальной фазе их роста. Резкое сокращение *L* приводит к возрастанию скорости синтеза и выделения метаболитов бактериями, в результате чего возрастает поступление продуктов их жизнедеятельности в организм за счет всасывающей функции кишечника. Наши исследования показали, что для жизнедеятельности бактерий большее значение имеет положение Солнца и Луны относительно Земли, а не открытость или закрытость Солнца (дня, ночи, затмения). Описанные явления позволяют предполагать, что фактор, действующий на исследуемые процессы, имеет гравитационную природу. Полученные результаты позволяют уточнить существующие представления о механизме влияния гравитационных сил, связанных с взаимным расположением Солнца, Земли и Луны и привязанном к моментам наступления определенных фаз Луны на поведение человека и высших животных, согласно которым указанное влияние осуществляется приливными процессами. В настоящей работе показано, что такое влияние на аномальное поведение человека и высших животных вызывается активным поступлением в кровь метаболитов кишечной палочки, обусловленным ее ускоренным размножением под действием гравитационных сил связанных с взаимным расположением Солнца, Земли и Луны и привязанных к моментам наступления определенных фаз Луны.

## **О восприятии времени в экстремальных условиях Арктики и Антарктики**

В.В.Иванов<sup>1</sup>, Э.С.Горшков<sup>1</sup>, Н.К.Белишева<sup>2</sup>, В.В.Мещеряков<sup>1</sup>

<sup>1</sup>*Санкт-петербургский Филиал Института земного магнетизма, ионосферы и распространения радиоволн РАН, Санкт-Петербург, Россия*

<sup>2</sup>*Полярно-Альпийский Ботанический Сад-Институт КНЦ РАН, Анатиты, Мурманской обл., Россия*

Проблема восприятия времени привлекает неослабевающее внимание исследователей, причем индивидуальная оценка течения времени связывается с функцией “биологических часов”.

Каждый организм живет по своим собственным индивидуальным часам. На основе многолетних работ хронобиологов установлено, что темпы времени особым образом сказываются на функциональном состоянии человеческого организма. Естественно, что условия среды обитания также влияют на ход “биологических часов”.

В связи с этим особый интерес вызывает оценка влияния на динамику индивидуального хода времени экстремальных условий высоких широт.

В данной работе приведены результаты исследований, выполненных в разное время в Арктике (январь-февраль 1995 г.) и Антарктике (январь 2001 - январь 2002 гг., в составе 46 РАЭ).

В 1995 г. проведена регистрация длительности индивидуальной минуты (ДИМ) у 8-ми испытуемых – сотрудников магнитно-ионосферной станции “Колба” (о. Диксон). Наблюдения проводились по стандартной методике три раза в день в одно и то же время. В анализе использованы среднесуточные значения ДИМ.

Результаты. Каждый испытуемый имел свой индивидуальный диапазон изменения ДИМ из общего интервала от 35 до 150 с. Период наблюдений пришелся на момент перехода от полярной ночи к полярному дню. Характерно, что с приближением полярного дня у части испытуемых наблюдался заметный спад уровня ДИМ с дальнейшей его стабилизацией в период полярного дня. При этом перепад значений (особенно у двух испытуемых) оказался значительным: 35 с (45 %) и 15 с (20 %). Следует отметить, что у двух испытуемых ДИМ оставался достаточно стабильным ( $40 \pm 5$  с и  $60 \pm 6$  с) в течение всего периода наблюдений.

В Антарктике наблюдения на станции Восток выполнены одним испытуемым из той же группы, который отличался высокой стабильностью ДИМ при работе в Арктике, сопоставимым с ходом физического времени (60 с). Регистрация ДИМ проводилась в среднем 7-8 раз в сутки. В анализе использованы среднесуточные значения.

Результаты. С приближением полярной ночи в течение 15-20 дней наблюдалось возрастание уровня ДИМ с 47 до 57 с с последующим спадом до 52 с. В течение полярной ночи (~ 4 месяца) уровень ДИМ был относительно стабилен ( $54 \pm 1.5$  с). С приближением полярного дня наблюдалось монотонное (в течение ~ 25 дней) возрастание ДИМ с 54 до 59 с с последующим спадом уровня до 55 с при установлении полярного дня.

Таким образом, в обоих экспериментах проявилась явная связь динамики ДИМ с сезонными событиями (переход от ночи ко дню и наоборот). Наличие этой связи и индивидуальных особенностей в динамике ДИМ свидетельствует об информативном значении этого показателя для жизнедеятельности человека.

## **К вопросу о сравнительной адаптации сердечно-сосудистой системы и дыхания при смене климатографического района и остром инфекционном заболевании**

Т.Г. Кузнецова<sup>1</sup>, В.В. Иванов<sup>2</sup>, Э.С. Горшков<sup>2</sup>

<sup>1</sup>*Институт физиологии им. И.П.Павлова РАН, Санкт-Петербург, Россия*

<sup>2</sup>*Санкт-петербургский Филиал Института земного магнетизма, ионосферы и распространения радиоволн РАН, Санкт-Петербург, Россия*

Исследование проведено на одном и том же испытуемом в ситуациях развития острого инфекционного заболевания и перестройки гомеостаза при изменении климатогеографического фактора – экспедиции из Санкт-Петербурга на о. Диксон и обратно, длившейся два полярных месяца. Для оценки функционального состояния организма использовали отношение (К) частоты пульса (ЧП) к частоте дыхания (ЧД) - К = ЧП/ЧД, аттракторная оценка сердечного ритма и корреляционная зависимость ЧП и ЧД в этих ситуациях.

Анализ полученных фактов позволил прийти к заключению, что оба процесса имеют сходную картину.

Перемещение на запад (по сравнению с перемещением на восток) сопровождалось более быстрой перестройкой биоритмов организма и более выраженным синдромом адаптации – десинхронозом, т.е.

интенсивность воздействия возрастала. В условиях высоких северных широт процесс адаптации проходил более плавно, чем после возвращения в Санкт-Петербург, когда был зафиксирован срыв адаптации, что можно связать с перестройкой циркадных ритмов физиологических функций из-за “выпадения” в период полярной ночи фотопериодизма из общего комплекса синхронизаторов.

В период развития заболевания этот процесс происходил более резко с большим напряжением механизмов регуляции сердечного ритма.

Корреляционный анализ ЧП и ЧД выявил “провалы” в корреляционной зависимости длительностью в один месяц как в период развития заболевания, так и в период пребывания испытуемого в Санкт-Петербурге после возвращения из заполярной зоны.

В целом же процесс возвращения к “нормальному”, характерному для данного испытуемого, уровню коэффициента корреляции для первого и второго случаев составил 4 и 7 месяцев, соответственно.

Использование аттракторного анализа частоты пульса для оценки напряженности механизмов регуляции сердечного ритма показало, что состояние болезни и резкое изменение климатогеографического фактора соответствовал максимальным по модулю уровням показателей аритмической напряженности (-0.42 и -0.6, соответственно). При этом состояние предболезни характеризовалось вариабельной напряженностью сердечной деятельности (0.53). Процесс адаптации к условиям Заполярья сопровождался падением показателя напряженности от практически нулевого уровня (при нахождении испытуемого в Санкт-Петербурге) до (-0.6). В дальнейшем оба показателя напряженности резко изменили свои уровни и знаки, достигнув максимальных значений 0.68 и 0.62, характеризующих вариабельную напряженность. Процесс достижения “нормального” уровня показателя напряженности ( $\pm 0.25$ ) для первого и второго случаев составил 9 и 8 месяцев, соответственно.

Дополнительный анализ динамики показателей - ЧП, ЧД и К - в процессе адаптации к воздействию климатогеографического фактора выявил наличие двух адекватных срывов адаптации, приуроченных к “первому” появлению Солнца и к “первым” дням в Санкт-Петербурге после возвращения с Диксона. При этом первый “срыв” соответствует такому же уровню показателя аритмической напряженности, как и второй (-0.6). Проявленная реакция организма испытуемого на “первое” появление диска Солнца над горизонтом связано с влиянием солнечной активности на организм человека, впервые обнаруженным А.Л.Чижевским при исследовании заболеваемости и смертности.

Таким образом, можно предположить общие закономерности в динамике функционального состояния организма, обеспечивающей его гомеостаз в период болезни и при резком изменении климатогеографического фактора. Однако при развитии острого заболевания процессы перестройки функционального состояния протекают более “остро”, а при смене климатогеографического фактора более плавно, с меньшей, но выраженной нагрузкой на сердечно-сосудистую и дыхательную системы.

### **Экспериментальные исследования ослабления биологически активного солнечного излучения по измерениям в Апатитах**

С.А. Черноус, В.А. Шишаев, О.В. Антоненко, М.И. Белоглазов (*Полярный геофизический институт КНЦ РАН, Апатиты*)

Спектральные измерения интенсивности биологически активного ультрафиолетового (УФ) излучения, как в Арктике, так и в Антарктике показывают, что облака могут существенно ослабить это излучение, как на масштабах суток, так и на масштабах часов или даже десятков минут. Это создает проблему не только для исследования долговременных трендов собственно интенсивности УФ излучения, но и для мониторинга вариаций общего содержания озона (ОСО), расчеты которого базируются на измерениях интенсивности УФ радиации. Ошибки такого рода трудно обнаружить при стандартных схемах измерения с низким временным разрешением, например, озонометром M-124 или измерителем Робертсона-Бергера. Измерения, проводимые с более высоким временным разрешением, позволят идентифицировать возможные ошибки и учесть их.

Экспериментальная база наблюдений основана на регулярных непрерывных измерениях интенсивности солнечной ультрафиолетовой радиации в диапазонах спектра UV-A (315-400 нм) и UV-B (280 – 315 нм), а также на измерениях фотосинтетически активной радиации PAR в видимой области спектра с помощью калиброванного в абсолютных единицах прибора ELDONET на стратосферном полигоне ПГИ в Апатитах с 2006 года по настоящее время. Исследования влияния облачности и поглощения озоном на изменения интенсивности солнечного ультрафиолетового излучения в приземном слое атмосферы показали, что ослабление солнечного излучения облачностью слабо зависит от спектрального диапазона наблюдений. Построена гистограмма, характеризующая количественно вклад облачности в общее ослабление УФ излучения. Показано, что непрерывные записи излучения в UV-A и UV-B диапазонах могут быть использованы при оценке точности измерений ОСО стандартными сетевыми приборами.



## AUTHOR INDEX

### A

Akhmetov O.I. .... 19, 71  
Alhimichkov A.A. .... 86  
Ammosov P.P. .... 63  
Ananiev L.B. .... 81  
Angelopoulos V. .... 27, 29  
Antonenko O.V. .... 59, 67, 85, 89  
Antonova E.E. .... 15, 27, 30  
Apatenkov S. .... 29  
Artamonova A.A. .... 81  
Avdeeva E.G. .... 26

### B

Balabin Yu.V. .... 43, 44  
Barkhatov N.A. .... 45, 51  
Barkhatova O.M. .... 15, 51  
Bashinov A.V. .... 36  
Belakhovsky V.B. .... 31, 35  
Belisheva N.K. .... 85, 86, 88  
Beloglazov M.I. .... 52, 53, 71, 73, 77, 89  
Bertsev V.V. .... 72  
Bespalov A.A. .... 36  
Bespalov P.A. .... 15  
Bogomolov A.V. .... 46  
Bonnell J. .... 29  
Borovkov L.P. .... 16  
Boroyev R.N. .... 20  
Bösinger T. .... 51  
Brändström U. .... 62  
Burns G. .... 55

### C

Chernouss S.A. .... 56, 59, 66, 67, 85, 89  
Chernyakov S.M. .... 62, 64  
Chugunova O. .... 37

### D

Dahle K. .... 55  
Danilin A.N. .... 20  
Dashkevich Zh. V. .... 43  
DeJong A. .... 16  
Demekhov A.G. .... 36, 51  
Demin V.I. .... 72, 73  
Dergachev V.A. .... 78  
Despirak I.V. .... 16, 31, 43, 48, 55  
Dmitrieva N.P. .... 45  
Doronina E.N. .... 54  
Dremukhina L.A. .... 19, 25, 26

### E

Egorova L.V. .... 79  
Emelyanov M.B. .... 75

Engebretson M. .... 37  
Ermakova E.N. .... 54, 66

### F

Fedorenko Yu.V. .... 60  
Feldstein Ya.I. .... 21, 25  
Fillingim M. .... 29  
Foerster M. .... 25  
Frank-Kamenetsky A.V. .... 55  
Frey H.U. .... 38, 39  
Fujiwara M. .... 73  
Fukao S. .... 73

### G

Gausa M. .... 80  
Gavrilov N.M. .... 55, 73  
Gavrilyeva G.A. .... 63  
Germanenko A.V. .... 44  
Glebovsky D.N. .... 72  
Glotova N.A. .... 44  
Golovchanskaya I.V. .... 25  
Gordeev E. .... 16  
Gorshkov E.S. .... 87, 88  
Grigor'ev G.I. .... 51  
Grigorenko E.E. .... 25  
Gromova L.I. .... 19, 25, 26  
Guineva V. .... 16, 31, 43, 55, 74  
Gurin A.V. .... 68  
Gvozdevsky B.B. .... 43, 44, 45

### H

Haaland S.E. .... 25  
Haldoupis C. .... 51  
Hansen H.G. .... 80  
Hashiguchi H. .... 73  
Hoppe U.-P. .... 80  
Hoshino M. .... 25

### I

Ignatovich Ya. .... 56  
Ilyushin Ya.A. .... 65  
Ivanov V.V. .... 88  
Ivanova I.M. .... 45  
Ivanyugin M. .... 67

### J

Janhunen P. .... 64  
Janzhura A.S. .... 21, 79

## K

Kalashnikova I.V. ....	86
Kalinin M.S. ....	48
Kalinina E.A. ....	45
Kalitenkov A.N. ....	59, 66, 67, 68
Kalitenkov N.V. ....	59, 66, 67, 68
Karpachev A.T. ....	68
Karpova N.V. ....	63
Katkalov Yu.V. ....	17, 20, 45
Kilifarska N. ....	80
Kirillov A.S. ....	56, 77
Kirpichev I.P. ....	15
Kivi R. ....	80
Kleimenova N.G. ....	17, 19, 27
Klimenko M.V. ....	17, 56, 57
Klimenko V.V. ....	39, 60, 81
Klimenko V.V. ....	17, 56, 57
Knyazeva M.A. ....	58
Koide T. ....	73
Kopytenko Yu.A. ....	28
Kornilov I.A. ....	18, 29, 63
Kornilova T.A. ....	18, 29
Kosova A.L. ....	85
Kotik D.S. ....	54, 59
Koustov A.V. ....	64
Kovalenko V.A. ....	78
Kozelov B.V. ....	26, 32
Kozelova T.V. ....	26
Kozyreva O.V. ....	17, 19, 27
Krainev M.B. ....	48
Krasilnikov A.A. ....	74, 75
Krivolutsky A.A. ....	77
Kuchura A.N. ....	68
Kudryashova N.V. ....	20
Kukin L.M. ....	74, 75
Kukoleva A.V. ....	77
Kukovyakin M.V. ....	53
Kulikov Y.Y. ....	74, 75
Kuminov A.A. ....	77
Kunitsyn V.E. ....	65
Kuznetsova I.N. ....	81
Kuznetsova T.G. ....	88

## L

Larson D. ....	29
Lazutin L.L. ....	26
Lebed O.M. ....	60
Levitin A.E. ....	15, 19, 25, 26, 45
Lezina E.A. ....	81
Lubchich A.A. ....	16, 48, 75
Lubyako L.V. ....	75

## M

Makarova L.N. ....	55
Maklakov V. ....	59
Malova Ch.V. ....	32
Manninen J. ....	37, 39
Mareev E.A. ....	60, 75

Marjin B. V. ....	27
Marple S. ....	55
Martynenko O.V. ....	65
Maslov I.A. ....	79
McFadden J. ....	29
Melnik N.A. ....	85
Mescheryakov V.V. ....	88
Milkin V.I. ....	68
Mingalev I.V. ....	32, 76
Mingalev O.V. ....	32
Mingalev V.S. ....	59, 76
Mingaleva G.I. ....	59
Miroshnichenko L.I. ....	77
Mochalov A.A. ....	60
Moiseyev A.V. ....	20, 37
Molodykh S.I. ....	78
Morozov V.N. ....	55
Mullayarov V.A. ....	37
Myagkova I.N. ....	27, 46, 77

## N

Namgaladze A.A. ....	54, 58, 65, 66
Nikolaev A. ....	27
Novikova T.B. ....	85

## O

Ogloblina O.F. ....	62, 64
Orlov K.G. ....	76
Orlova K.G. ....	15
Orsolini Y. ....	80
Ostafiychuk R.M. ....	20
Ostapenko A.A. ....	37
Ovchinnikov I.L. ....	15

## P

Parkhomov V.A. ....	40
Pashin A.B. ....	60
Pchelkin V.V. ....	19, 46, 77
Perminova E.V. ....	85
Petlenko A.V. ....	28
Petrukovich A.A. ....	28
Petrunkin L.A. ....	72
Pilgaev S.V. ....	60
Pilipenko V.A. ....	35, 37, 39
Platov Yu.V. ....	61
Poberovskiy A.V. ....	75
Podgorny A.I. ....	43, 46, 47
Podgorny I.M. ....	43, 47
Polyakov S.V. ....	66
Ponomarev A.B. ....	77
Popova T.A. ....	38, 40
Prokhorov B.E. ....	65
Ptitsyna N.G. ....	19
Pulinets S.S. ....	15

## R

Rajta T. .... 37  
Raspopov O.M. .... 78  
Remenets G.F. .... 52, 53, 61  
Riazantseva M.O. .... 27  
Roldugin A.V. .... 38, 56  
Roldugin V.C. .... 28, 38, 62  
Romaniuk Ya.O. .... 81  
Rossolenko S.S. .... 15  
Rubtsova O.A. .... 78  
Ryazanceva M.O. .... 40  
Ryskin V.G. .... 74

## S

Safargaleev V.V. .... 62, 63  
Sakharov Ya.A. .... 17, 20  
Samsonov A.A. .... 28, 29  
Samsonov S.N. .... 37  
Sandahl I. .... 62  
Saranskiy S.N. .... 20  
Sauvaud J.-A. .... 25  
Schennikov A.V. .... 66  
Schur L.I. .... 44  
Selivanov V.N. .... 20  
Sergeev V. .... 16, 27, 29  
Sergeeva N.G. .... 62  
Sergienko T.I. .... 62, 63  
Shibaeva D.N. .... 62, 63  
Shilimov V.A. .... 31  
Shirochkov A.V. .... 55  
Shishaev V.A. .... 89  
Shlugaev Yu.V. .... 66, 81  
Shukhtina M.A. .... 16, 44  
Shved G.M. .... 63  
Sibeck D.G. .... 29  
Singer H. .... 27  
Solovyev S.I. .... 20, 37  
Sosonkin M.G. .... 81  
Stauning P. .... 55  
Stebel K. .... 80  
Stepanov V.V. .... 87  
Stepanova M.V. .... 15  
Sugak T. .... 29  
Sukovatov Yu.A. .... 68

## T

Telegin V.A. .... 68  
Tereshchenko V.A. .... 64  
Tereshchenko V.D. .... 64  
Titova E.E. .... 37  
Trakhtengerts V.Yu. .... 36  
Trondsen E. .... 55

Troshichev O. .... 21, 79, 87  
Tsegmed B. .... 40  
Turunen T. .... 37

## U

Ugolnikov O.S. .... 79  
Uspensky M.V. .... 64

## V

Val'chuk T.E. .... 47  
Vashenyuk E.V. .... 43, 44, 45  
Vasiljev A.N. .... 62, 71, 77  
Vasiljev B.E. .... 62  
Vasiljev E.B. .... 64  
Vellante M. .... 37  
Veretenenko S.V. .... 78  
Vince I. .... 74  
Vinogradov A.N. .... 85  
Volkov M.A. .... 21  
von der Gathen P. .... 80  
Vorobeichikov V.M. .... 87  
Vorobjev V.G. .... 21, 29, 30, 31  
Voronin A.I. .... 77  
Vovchenko V.V. .... 15, 30  
Vovk V.Ya. .... 79  
Vyatkin V.G. .... 81  
Vyushkova T.Yu. .... 77

## W

Werner R. .... 55, 74, 80

## Y

Yagodkina O.I. .... 29, 30, 31  
Yagova N.V. .... 39  
Yahnin A.G. .... 38, 39  
Yahnina T.A. .... 39  
Yamamoto Mamoru. .... 73  
Yamamoto Masayuki. .... 73  
Yashunin S.A. .... 60  
Yeoman T. .... 37, 60

## Z

Zaitsev A.N. .... 31  
Zakharov V.I. .... 65  
Zastenker G.N. .... 40  
Zelenyi L.M. .... 25, 32  
Zolotov O.V. .... 65  
Zubova Yu.V. .... 66  
Zverev V.L. .... 21, 30  
Zvyagintsev A.M. .... 81